OPTIMIZATION OF CORE-FLOODING DESIGN FOR SURFACTANT-POLYMER EOR

BY

MOHAMED ELMUZAFAR AHMED ELTAHIR AHMED

A Thesis Presented to the
DEANSHIP OF GRADUATE STUDIES

KING FAHD UNIVERSITY OF PETROLEUM & MINERALS

DHAHRAN, SAUDI ARABIA

In Partial Fulfillment of the
Requirements for the Degree of

MASTER OF SCIENCE

In

PETROLEUM ENGINEERING

December 2017

KING FAHD UNIVERSITY OF PETROLEUM & MINERALS

DHAHRAN- 31261, SAUDI ARABIA

DEANSHIP OF GRADUATE STUDIES

This thesis, written by **Mohamed Elmuzafar Ahmed Eltahir Ahmed** under the direction of his thesis advisor and approved by his thesis committee, has been presented and accepted by the Dean of Graduate Studies, in partial fulfillment of the requirements for the degree of **MASTER OF SCIENCE IN PETROLEUM ENGINEERING.**

Dr. Abdullah Sultan
(Advisor)

Dr. Dhafer A. Al Shehri
Department Chairman

Dr. Hasan S. A Al-Hashim
(Member)

Dr. Salam A. Zummo
Dean of Graduate Studies

Dr. Abdulkarim M. Sofi
(Member)

10/11/18
Date

To my mother Suad Osman may Allah give her health and joy, my father, brothers and sisters for their prayers and for my wife who suffered the hard times with me during this work, my aunts and uncles.

To my friend with whom I was able to make it up to this point.

ACKNOWLEDGMENTS

All praise and thanks to Allah almighty who gave me the power and the will to do this work and facilitation he did throughout my life up to this level and forever.

I would like to pass my sincere gratitude to KFUPM and the Ministry of Education for granting me this scholarship to complete my master degree, I am very thankful and grateful to my thesis advisor Dr. Abdullah Sultan, from whom I have learnt the value of hard work, for giving me this spectacular opportunity to be a member of his research group and his patience to my ignorance and his will to encourage me and give me the enthusiasm to complete this degree, besides his continues support, help, guidance and valuable comments.

I would like to extend my gratitude to my thesis committee Dr. Hassan Al Hashim and Dr. Abdulkarim Al-Sofi for their precious comments and valuable contribution throughout this work and for the time they have spent to review, point out the gaps and the relevance of the results.

Special thanks to the college of Petroleum & Geosciences and the department of Petroleum Engineering for granting me permission to use the equipment's and resources in the labs, all thanks are extended to the faculty and staff that I have learnt from them a lot.

I cannot forget the technical support that I have found from; Mr. Abdulrahim Muhammadain, Assad Barri, Ahmed Abdulazeem and Lionel Talley in the core-flooding, Ahmed Mahboob in the contact angle, Abdulsamed Iddris and Mobeen Murtaza for their help, Abdulrahman Y. Al Ghamdi, Mushabbab Q. Al Raqdi and Wasef Nofal, Dr. Kamal Shahzad and DR. Abdulrauf for their assistance Eassa Abdullah for his guidance in the

dean stark and air permeability, Zaid Zaffar, Sayed Hussaini and Hani Salman in the micro-CT and image processing, Dr. Jimoh Adewole, Dr. Mazin and Ahmad Adewunmi in the HPLC, Abdelmlik Elsnona and Abbas in rock properties, Tajudeen Adeyinka in the IC and UV-Vis and I am very thankful to any help and support I get from any one that I couldn't mention his name in this window.

I appreciate the support provided by Saudi ARAMCO for funding this project through the research institute, Center for Integrated Petroleum Research (CIPR) and the technical support by EXPEC ARC specially Dr. Taha Okasha, Mustafa Hakimuddin and Essam al-Kully for giving the opportunity to use the centrifuge instrument.

I can't find a sufficient expression to thank my family specially my mother and wife for their prayer and patience over the years and my brother Osman Ahmed, not to forget my friends in KFUPM who act like a second family their presence beside me made it easy and I cannot imagine how hard the life would be without them.

TABLE OF CONTENTS

LIST OF TABLES

LIST OF FIGURES

LIST OF ABBREVIATIONS

CEOR	:	Chemical-Enhanced-Oil-Recovery
SP	:	Surfactant-Polymer
ASP	:	Alkali-Surfactant-Polymer
HTHS	:	high temperature high salinity
IFT	:	interfacial tension
$\mathbf{N_M}$	:	Mobility Number
$\boldsymbol{\lambda_o}$	:	Oil mobility
$\boldsymbol{\lambda_w}$	:	Water mobility
$\mathbf{K_{ro}}$	:	Oil relative permeability
$\boldsymbol{\mu_o}$	:	Oil viscosity
$\mathbf{Kr_w}$	:	Water relative permeability
$\boldsymbol{\mu_w}$	:	Oil viscosity
$\mathbf{N_{ca}}$	:	Capillary number
$\boldsymbol{\Delta P_{vis}}$	:	viscous forces
$\boldsymbol{\Delta P_{cap}}$	:	Capillary forces
v	:	velocity
$\boldsymbol{\sigma}$	:	interfacial tension
$\mathbf{N_B}$	:	Bond number
$\boldsymbol{\Delta P_{grav}}$	:	gravitational forces
$\boldsymbol{\rho}$	:	density (g/cc)
g	:	gravitational acceleration = 9.8 m/s^2
k	:	Permeability (md)
$\mathbf{N_T}$	:	Trapping number

PO	:	Propoxylated alkyl sulfates
EO	:	Ethoxilated alkyl sulfates
PEG	:	Polyethylene glycol
LTPF	:	Low-tension polymer flooding
AMPS	:	2-acrylamido-2methyl propane sulfonate and acrylamide
HPAM	:	Hydrolyzed polyacrylamide
OOIP	:	Original Oil In Place
OIIP	:	Oil Initially In Place
TVP	:	Thermoviscosifying polymer
CMC	:	Critical Micelle Concentration
PASF	:	Polymer Assisted Surfactant flood
HPLC	:	High performance liquid chromatography
S_{wi}	:	Initial water saturation
ROS	:	Residual oil saturation
TDS	:	Total dissolved solids
API	:	American petroleum institute
SARA	:	Saturates Aromatic Resin Asphaltene
ATBS/ AM	:	Acrylamido tertiary butyl sulfonate/ acrylamide
DHR	:	Discovery Hybrid Rheometer
DI	:	Deionized water
IC	:	Ion Chromatography
CT	:	Computed Tomography
XRM	:	X-ray microscopy
PV	:	Pore Volume

ABSTRACT

Full Name : Mohamed Elmuzafar Ahmed Eltahir Ahmed

Thesis Title : OPTIMIZATION OF CORE-FLOODING DESIGN FOR SURFACTANT-POLYMER EOR

Major Field : Petroleum Engineering

Date of Degree : December 2017

Chemical-Enhanced-Oil-Recovery (CEOR) processes are mean of increasing the recoveries from the oil fields after the primary recovery phase. There are many types of chemical EOR, such as Polymer (P), Surfactant (S), Surfactant-Polymer (SP) and Alkali-Surfactant-Polymer (ASP) flooding. In harsh reservoir conditions (high salinity and high temperature) many CEOR methods wouldn't be effective. This issue raises the challenge to design optimum recipes that resist these harsh conditions and hence attain maximum hydrocarbon recovery at minimum possible cost. Designing an optimum SP system is vital since the materials to be used are expensive and must be used wisely. The ultimate tool is a set of experiments that can be used later for upscaling and optimization of the CEOR process.

This thesis evaluates the effectiveness of (SP) in mobilizing the oil and increase sweep efficiency in carbonate rocks. This was done by performing extensive core-flooding tests supported by pore scale imaging. In addition, contact angle and rheology measurement were performed.

The polymers used are a Thermo-Viscosifying Polymer (TVP) and an Acrylamido Tertiary Butyl Sulfonate (ATBS)/acrylamide (AM) copolymer. The surfactants are different grades of amphoteric carboxybetain. These potential chemicals were selected through a rigorous evaluation process based on previous work on KFUPM including long-term thermal

stability, fluid rheology, Interfacial Tension(IFT), adsorption and microfluidic studies. The contact angles were measured at high pressure and high temperature using a captive drop analyzer. Slug size and injection sequence optimization were investigated using core-flooding experiments conducted using long composite cores of about 12 inch in length and 1.5-inch diameter. The samples were aged for two weeks. The experiments were conducted at 90^{o}C. The sea water (SW) used in the injection had salinity of 57,000 ppm.

The results demonstrated the role of surfactant-polymer interaction and their effects on wettability and fluid rheology. The optimum chemical combination was found to be carboxybetaine (0.05% wt.) and ATBS/AM (0.25% wt.). Observed that the recoveries were directly proportional to the slug-size. Chemical injection sequence had significant impact on the ultimate recovery. SW–SP–SW showed higher recovery than the other sequences (SW-P-S-SW, SW-S-SW-P-SW and SW-P-SW-S-SW). This is postulated to be due to advantageous synergies between the chemicals.

In the low shear range (0.001 to 3) s^{-1} the dynamic viscosity of mixtures containing ATBs/AM exhibit small variation with or without the surfactant. However, TVP works better with surfactant SS-880 than surfactant SS-885.

The contact angle experiments suggested two weeks thermal aging is enough to restore the original wettability for calcite rock discs while one week was too short. However, the micro-CT scan results indicated a water-wet in-situ wettability for the two weeks aged rock. Accordingly, further aging is needed to achieve native state wettability.

Based on ion concentration analyses, calcium dissolution was noticed in most of the cases. To the exception was the polymer injection where no dissolution has been noticed. In addition, in the presence of polymer, there was an apparent adsorption of sodium and

magnesium ions. The surfactant to the contrary had no effect on sodium and magnesium adsorption.

The core-flooding experiments support the importance of optimizing the design of CEOR processes taking into consideration the type of chemicals, concentrations, slug sizes, and flooding sequence of the different combination of sea water (SW), surfactant (S) and polymer (P).

For future work the dynamic adsorption for the surfactant and polymer should be investigated. In addition, for the micro-CT imaging, it is better to do the experiment in-situ by using a core-flooding system coupled with the micro-CT scanner to be able to take images at more steps.

ملخص الرسالة

الاسم الكامل: محمد المظفر أحمد الطاهر أحمد

عنوان الرسالة: تحسين تصميم أسلوب الغمر الفيضي لمزيج عناصر السطح الفعالة مع البوليمر بغرض تعزيز إستخلاص النفط

التخصص: هندسة البترول

تاريخ الدرجة العلمية: ديسمبر 2017

وتعتبر عمليات الإستخلاص الكيميائي المعزز للنفط وسيلة لزيادة الإنتاج من حقول النفط في المرحلة الثالثة من الإستخلاص. هناك العديد من الطرق المستخدمة في الإستخلاص الكيميائي المعزز للنفط, مثل الحقن المفرد للبوليمر، و الحقن المفرد لعناصر السطح الفعالة، الحقن الآني لمزيج عناصرالسطح الفعالة مع البوليمر و أخيرا الحقن الآني لخليط القلويات عناصرالسطح الفعالة و البوليمر. في الظروف القاسية لخزان النفط متمثلة في الملوحة العالية / درجة الحرارة العالية، فإن العديد من أساليب الإستخلاص لا تكون فعالة بالصورة المطلوبة. هذه المسألة تثير التحدي لتصميم الوصفة الأمثل لمقاومة هذه الظروف الصعبة في نفس الوقت لتحسين انتاج المواد الهيدروكربونية إلى أقصى حد ممكن مع مراعاة أقل تكلفة ممكنة.

تقدم هذه الرسالة نتائج تجارب مكثفة بأسلوب الغمر الفيضاني للعينة الصخرية مدعومة بتجارب زاوية الإلتماس لمعرفة نوع البلل في الشرائح الصخرية و دراسة الخواص الإنسايبية للمحلول الكيميائي المستخدم بهدف تقييم مقدرة أسلوب الحقن الآني لمزيج عناصرالسطح الفعالة مع البوليمر في تغيير البلل و زيادة كفاءة الإستخلاص في العينات الصخرية الكربونية.بالإضافة إلى إلى التصوير الدقيق للمسامات الصخرية لتقييم التغير في البلل في داخل المسام وفهم آلية الاستخلاص إما عن طريق أساليب الحقن الفردية أو توليفاتها المزدوجة.

البوليمرات المستخدمة هي البوليمر الذي تزيد لزوجته بالحرارة و الثاني هو سلفونات الأكريل أميد ثلاثي البيوتيل مع أكريل أميد كبوليمر مرافق. على الجانب الآخر فإن عناصر السطح الفعالة المستخدمة هي أنواع مختلفة من الكاروكسي

بيتايين مزدوج الشحنة. آخذين بعين الإعتبار أن الإختيار الأولي لهذه المواد الكيميائية الفعالة كان من خلال عملية تقييم صارمة تحتوى على إختبارات الاستقرار الحراري على المدى الطويل، إنسيابيةالسوائل، قوى التوتر السطحي، الامتزاز دراسات الدقيقة على مقياس الميكروميتر للسوائل. تم قياس زوايا الإلتماس في ظروف ارتفاع الضغط وارتفاع في درجة الحرارة باستخدام محلل القطرة على الشرائح الصخرية. تمت دراسة تحسين حجم الكمية المحقونة و التسلسل في الحقن للمواد الكيميائية المستخدمة باستخدام تجارب الغمر الفيضي باستخدام عينة صخرية مركبة طويلة طولها حوالي 12 بوصة وقطرها 1.5 بوصة. وكانت العينات قد وضحت تحت ظروف الخزان لمدة أسبوعين وأجريت التجارب في حرارة 90 درجة مئوية مع ملوحة مياه قدرها 57،000 جزء في المليون.

وأظهرت النتائج دور تفاعل عناصر السطح مع البوليمر وتأثيرها على التبلل و إنسيابية السوائل. وجد أن المزيج الكيميائي الأمثل الذي يمكن أن يتحمل الظروف القاسية مثل الملوحة ودرجة الحرارة العالية، وفي الوقت نفسه يحصل على أفضل إنتاج ممكن يتكون من كاربوكسي بيتايين و سلفونات الأكريل أميد ثلاثي البيوتيل مع أكريل أميد كبوليمر مرافق, ولوحظ أن الانتاج يتناسب طرديا مع حجم البكمية المحقونة بينما التسلسل الكيميائي هو أكثر أهمية على الانتاج الأكبر. حق مزييج عناصر السطح مع البوليمر مسبوقا و متبوعا بحقن المياه المالحة يظهر أعلى إنتاج بالمقارنة مع التسلسلات الأخرى من خلال الاستفادة من تأثير التآزر للمواد الكيميائية.

نتائج تجارب الغمر الفيضي وضحت فهم متقدم لأهمية تصميم عملية الإستخلاص الكيميائي المعزز للنفط مع الأخذ بعين الاعتبار نوع المواد الكيميائية، وتركيزاتها والأحجام المحقونة، وتسلسل المواد الكيميائية لمختلف التوليفات المستخدمة.

ومن الواضح أن عملية تصميم نظام الحقن الأمثل أمر حيوي لأن المواد التي سيتم استخدامها مكلفة. وبالتالي، يجب أن تستخدم بحكمة. والهدف النهائي هو إعداد مجموعة من التجارب التي يمكن استخدامها في وقت لاحق كمعيار أساسي يستند إلى المحاكاة والاستفادة المثلى من عملية حقن مزيج عناصر السطح مع البوليمر لتعزيز استخلاص النفط.

CHAPTER 1

INTRODUCTION

1.1 Research motivation

The harsh conditions Middle Eastern resources resembled mainly in high temperature and high salinity (HTHS) represent a great challenge to chemical EOR (CEOR) because those conditions affect the chemical stability and rheological properties. This is beside the precipitation problem. However, the increasing maturity of Middle East reservoirs will eventually raise the need to use those techniques. Hence a complete screening for harsh condition endurance and potential recovery evaluation for any chemical to be used in such conditions is inevitable.

1.2 Background

Chemical EOR technologies have been used for decades and its development is increasing rapidly due to the massive need of hydrocarbons in the world and because most of the reservoirs have reached tertiary recovery phase. The main reason for using surfactant is to lower the interfacial tension (IFT) between water and oil. While the use of polymer generally linked with surfactant for mobility control to ensure the best sweep efficiency.

The early studies of CEOR flooding focused mainly on sandstone reservoirs [1]–[3]. However, recently its attention shifted towards carbonate reservoirs due to the increasing number of maturing carbonate fields [4]–[8].

SP flooding is more feasible than individual flooding of surfactant or polymer and ASP flooding by combining the benefits of IFT reduction and mobility control and by avoiding operational and precipitation problems associated with ASP flooding [9].

The amount of chemicals used in CEOR is of great importance which lead to the need of concentration and slug size optimization; the optimum slug we are looking for is the slug that gives the highest possible recovery with the lowest cost.

The rock wettability affects the EOR process by influencing the oil recovery, even though oil wet rock will enhance the film drainage [8]. The highest overall oil recovery will be achieved under water wet conditions [14]. Therefore, it is very important to restore the original wettability before starting a core-flooding experiment to avoid optimistic recovery.

The problems that face CEOR in gulf area were the high salinity and high temperature. High salinity causes chemical precipitation due to the presence of divalent cations such as Ca^{++} and Mg^{++} [15], [16] as well as decreasing the polymer viscosity and elasticity [17]. On the other hand high temperature affects the chemical stability and lead the polymer to degrade and act inefficiently [5], [7]. To solve this problem a comprehensive study of the chemical was done which include thermal stability, fluid rheology, micro-emulsion stability and IFT at these harsh condition [18]–[21]. Then the best candidates should be tested by core-flooding to choose the one that gives the highest recovery. Besides, the occurrence of monovalent cations such as Na^{+} will decrease the pH of the solution due to the ion exchange with the H^{+} in the rock surface. Therefore the pH drop below the isoelectric point [22] which will result in higher adsorption of chemical on carbonate rock specially anionic surfactants [10], [22]–[24].

Studying the flooding sequence is important to identify the best sequence that minimize the fingering and maximize the recovery. The literature reported many sequences such as:

polymer pre-flush to minimize the surfactant adsorption [6] and SP co-injection followed by polymer injection [25] and other sequences.

To our best knowledge and based on the literature surveyed, there is no systematic optimization process that combine all these effects in one study. Despite the fact that some of the effect have been studied individually or scattered inside one of a bigger project and highlighted slightly. That gave us the motivation to do such a job and cover the research gab in that area.

When chemicals pass through reservoir rock, adsorption on the surface of the rock can affect the feasibility of the process. Therefore, it is an important element to be considering during the design to select chemicals that are economical and technically achieve the goal. Also there is hydrodynamic dispersion which results from mixing a fluid in another miscible one while flowing through permeable formation, basically the dispersion dilutes the slugs and decreases its effectiveness. We have to consider another important factor that happens when low viscosity fluid is displacing higher viscosity fluid which called viscous fingering. Due to the difference in molecular weight, polymers in SP-EOR process might move slowly in the pore system and cause chromatographic separation. Adsorption and chromatographic separation can be investigated and evaluated using core flood experiments in the lab before scaling the process to field and avoid any major failure.

Polymer flooding (P) EOR is widely used process that improves the sweep efficiency through reducing the mobility ratio of the displaced and displacing fluid but polymer has no effect on the residual oil which need high capillary force to mobilize, hence the addition of the surfactant helps in lowering the oil/water IFT and increasing the ratio between the viscous forces to capillary forces (capillary number) and took the term SP flooding.

The challenges that are still facing the CEOR process in carbonate reservoir (especially in the Middle East) are high salinity, high temperature and reservoir heterogeneity which affect the recovery and efficiency. For example, polymer cannot resist high temperature because of hydrolysis and at the same time surfactant may precipitate in the high salinity medium which complicate the screening process for the best chemical to be used even more. Furthermore, the carbonate reservoir known with low permeability and containing fracture that have high permeability which results in channeling and decreasing the sweep efficiency.

EOR used to recover residual oil in porous media held up by capillary and viscous forces, hence, we can express this relationship by using dimensionless numbers like Mobility number, capillary number, Bond number and Trapping number.

Mobility number is the ratio between the mobility of displacing phase to the mobility of displaced phase which is oil so to have lower mobility number, either we increase the viscosity of the displacing phase like using polymer or decreasing the oil viscosity using heat.

$$N_M = \frac{\lambda_w}{\lambda_o} = \frac{\left[\frac{K_{rw}}{\mu_w}\right]}{\left[\frac{Kr_o}{\mu_o}\right]}$$

Capillary number (N_{ca}) is the ratio of viscous force to capillary force acting on the displaced fluid, we can increase it by decreasing the IFT using surfactant.

$$N_{ca} = \frac{\Delta \mathrm{P_{vis}}}{\Delta P_{cap}} = \frac{\mu v}{\sigma}$$

Bond number (N_B)is the ratio between hydrostatic forces and capillary forces. so in SP we can only increase Bond number by decreasing the IFT through surfactant because the increment by increasing density is negligible.

$$N_B = \frac{\Delta P_{grav}}{\Delta P_{cap}} = \frac{\Delta \rho g \left(\frac{k}{\phi}\right)}{\sigma}$$

[26] found that at constant Bond number, hydrocarbon recovery increases with the increase of Capillary number up to a specific limit and then decreases dramatically because of the higher viscous forces and the flow stability.

Trapping number is a combination of Bond number and Capillary number in a way that can sufficiently address the combined effect of capillary, viscous, and buoyancy forces in three dimensions.

$$N_T = \sqrt{N_{ca}^2 + 2N_{ca}N_B sin\alpha + N_B^2}$$

For horizontal flow α = 0°, for vertical flow = 90°.

1.3 Thesis Objectives

The objective of this thesis is to enable a robust optimization of the SP process for the previously screened chemicals. The following challenges will be addressed:

1- To identify the best chemical combinations.

2- To determine the optimum slug size.

3- To optimize the injection sequence.

4- To investigate the recovery mechanism and wettability at the pore-scale level.

1.4 Chapters Description

This thesis consists of five chapters: Chapter 1 introduces the subject and the objectives of the thesis to answer the question what are we doing? Chapter 2 is a literature review identifying the research gabs. Chapter 3 presents the methodology and describes the materials being used in order to explain how are we going to do it. Chapter 4 presents and discusses the obtained results. Finally, chapter 5 summarizes the conclusions and recommendations.

CHAPTER 2

LITERATURE REVIEW

The surfactant chemistry has developed so fast recently providing us with good knowledge of the chemical properties and structure to be able to use it in the specific conditions in terms of temperature and salinity, like the large hydrophobe (24 carbon number and above) surfactants are very stable in high temperature. In this literature survey we will review the core-flooding based work over the years.

2.1 Potential Chemicals and screening

Osterloh & Jante investigated the efficiency of using polyethylene glycols, PEGs, to reduce the adsorption of propoxylated alkyl sulfates (PO) as well as ethoxilated alkyl sulfates (EO) surfactants, onto clay. They found that the addition 1000 ppm of PEGs to PO/EO surfactants decreased the static adsorption on the kaolinite to a level that is very hard to detect based on their experiment which was done on Berea sandstone core. They also concluded that oil recovery was increased so much when PEG-1000 was added to the microemulsion of PO/PE surfactant as a result of the reduction in the surfactant adsorption. To maximize the cost-effectiveness; the oil recovery should be high by injecting the sufficient amount of PEG-1000 to meet the requirement of the core then you can inject the lowest possible amount of the surfactant required to produce high oil recovery [3].

Al-Hashim et al., studied the feasibility of many chemicals for CEOR application in carbonate reservoirs in gulf areas which featured with high salinity and temperature and found that ethoxylated sulfonate surfactant can tolerate high temperature (90^{o}C) and also suitable for high salinity of (57,000 ppm), but Triton X-100 is not recommended for high

temperature because it seperates at (84^{o}C). in the other hand FLOCON 4800C polymer found to degrade at (90^{o}C) aging if the oxygen was not removed [8].

Wang et al. did a thorough investigation about the SP flooding in heterogeneous formations using more than 40 core-flooding experiments with different combinations of SP formulations at 30^{o}C, flow rate of 0.2 cc/min, slug size of SP was 0.3 PV, core length of 5 cm, diameter of 2.5 cm sand pack for Two-layer without crossflow model and three parallel core each one has length of 30 cm, width of 4.5 cm and thickness of 1.5 cm for Three-layer model with crossflow.

They found the critical IFT and the best or optimized viscosity in heterogeneous model, a maximum recovery can be obtained at the critical values, however, the critical IFT greater than the lowest one and the best viscosity lower than the maximum viscosity (Figure 1). He also realized that the optimized SP with the optimized values for IFT and viscosity improves the oil recovery more than that SP with the lowest value of IFT (Figure 2). The main reason for the existence of the critical values is the emulsification and the problems related to it (Wang et al. 2010).

Solairaj conducted his work with an attempt to simplify the process of choosing the best surfactant structure for surfactant-polymer flooding. He developed a new correlation that relates the optimum structure for the surfactant to the affecting parameters such as salinity, temperature and the number of equivalent-alkane-carbon but he didn't include hydrophobe branching, divalent cations and co-solvent.

$$N_c = a_1 E_o + a_2 N_{po} + a_3 N_{EO} + a_4 (T - T_{ref}) + a_5 \log(S^*) + C$$

Where:

a_1, a_2, a_3, a_4 and a_5 : the regression coefficieints.

C: The intercept.

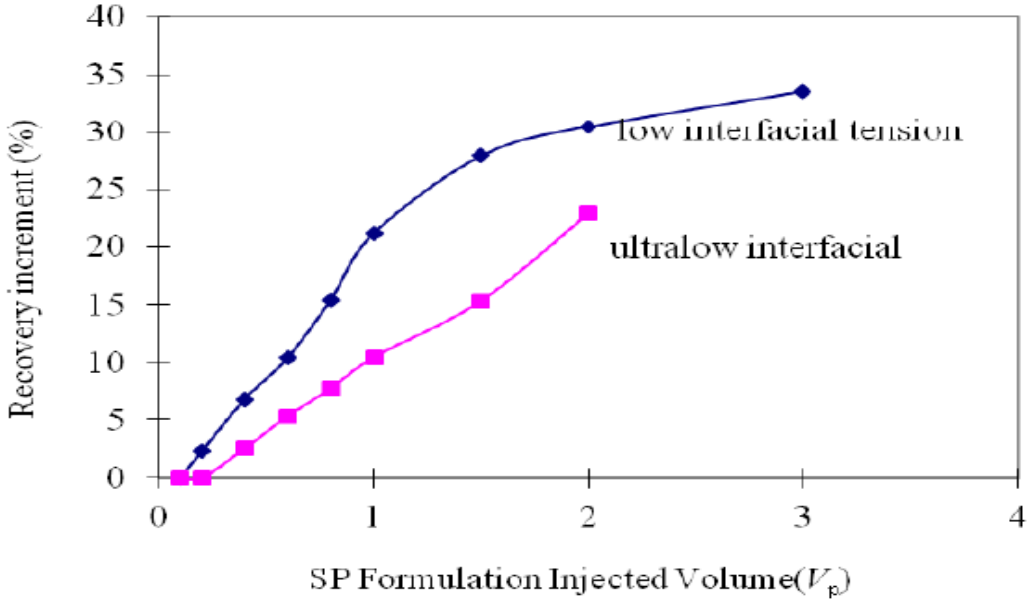

Figure 1: Oil recovery increment for different SP formulations [27]

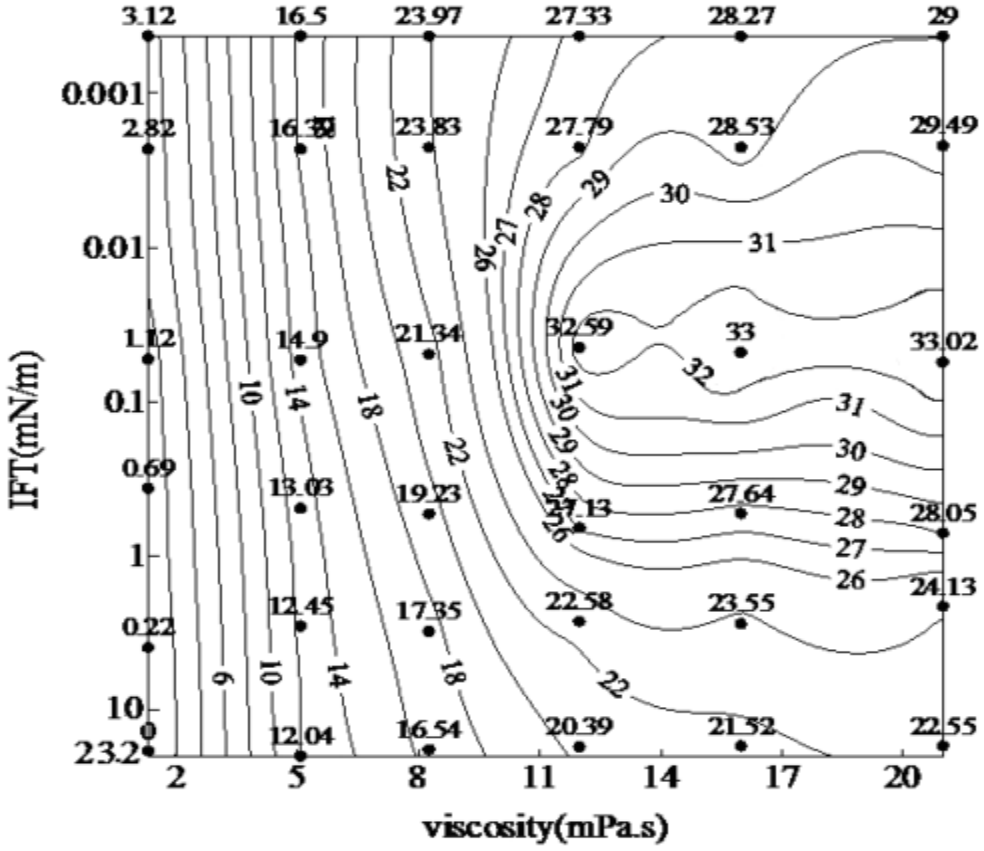

Figure 2: Oil recovery diagram for SP (Wang et al. 2010)

N_c: The mole weighted average carbon number in the surfactant mixture hydrophobe.

E_o: Oil Equivalent alkane carbon number.

N_{PO}: The mole weighted average of propylene oxide number (PO)in the surfactant mixture.

N_{EO}: The mole weighted average of ethylene oxide number (EO)in the surfactant mixure.

T: Is the temperatur of interest T_{ref} is 21°C.

S^*: The optimum salinity in ppm.

He correlated the formulation variables by multi-variable regression. The correlation coefficient values are in the following table:

Table 1: Standard deviation and regression coefficient summary

R-squared				
Standard Error: 1.4742				
	Coefficients	Standard Error	Normalized Standard Error	T Stat
Intercept, C	65.60251	7.543203	0.114983454	8.696903
EACN, a_1	0.47556	0.102007	0.214499497	4.662016
PO, a_2	-1.2971	0.115217	0.088827158	-11.2578
EO, a_3	-0.59155	0.122456	0.207010608	-4.83067
dT, a_4	0.030726	0.010537	0.342921504	2.916119
Log sal, a_5	-10.7535	1.586312	0.147516179	-6.77892

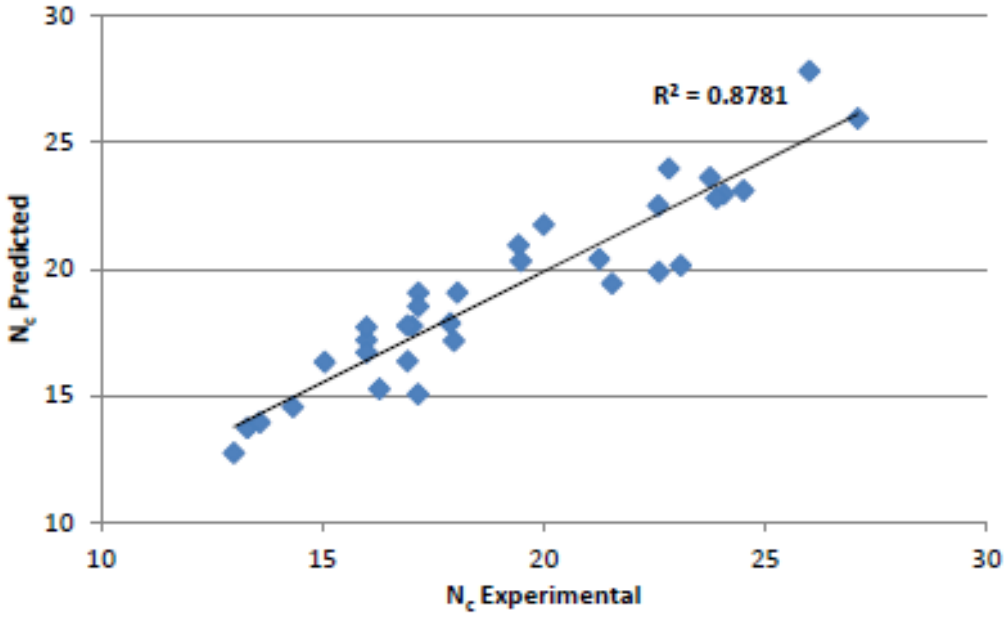

Figure 3: Predicted vs. experimental N_c [28]

And the predicted N_c versus the experimental N_c are in the following figure. The R-square was 0.87 [28].

Bataweel et al. made their study to evaluate the low-tension polymer flooding, (LTPF) which means the surfactant concentration is low (0.25 – 1 wt.%) in harsh environment in terms of salinity and temperature. They used amphoteric and anionic surfactants in Berea sandstone cores and found that amphoteric surfactants paired with the HPAM and AMPS which reduce the activity of the surface till the concentration of the polymer free aggregate was achieved. As the polymer concentration increases the surfactant concentration needed to achieve the polymer free aggregate concentration also increases. They also concluded that anionic surfactants demonstrated less retention because of the surface charge in the core which is negative when using this kind of surfactant. The most important conclusion that they had reached is reducing the IFT alone doesn't increase the recovery unless mobility controlling agent is used like polymers [29].

Feng et al. studied the use of Betaine surfactant with adding alkali lignin as a sacrificial additive to decrease the adsorption in SP systems to enhance heavy oil reservoir recoveries. They evaluated four experimentally self-made surfactants; SBET-12, SBET-16, CBET-12 and CBET-16. The results demonstrated that at a range of concentration of 0.01wt%~0.1wt% of betaine the IFT decreased to 0.001 mN/m or less than that without alkali, achieving the requirement of surfactant-polymer flooding. Besides, He found that using a mass-ratio of alkali lignin to betaine of 1 to 7.5 can reduce the adsorption approximately to 40% (Figure 4), in addition to that the polymer added to the system accelerated the IFT reduction between water and oil. He accomplished a recovery of 13%~20% after the end of water-flooding [30].

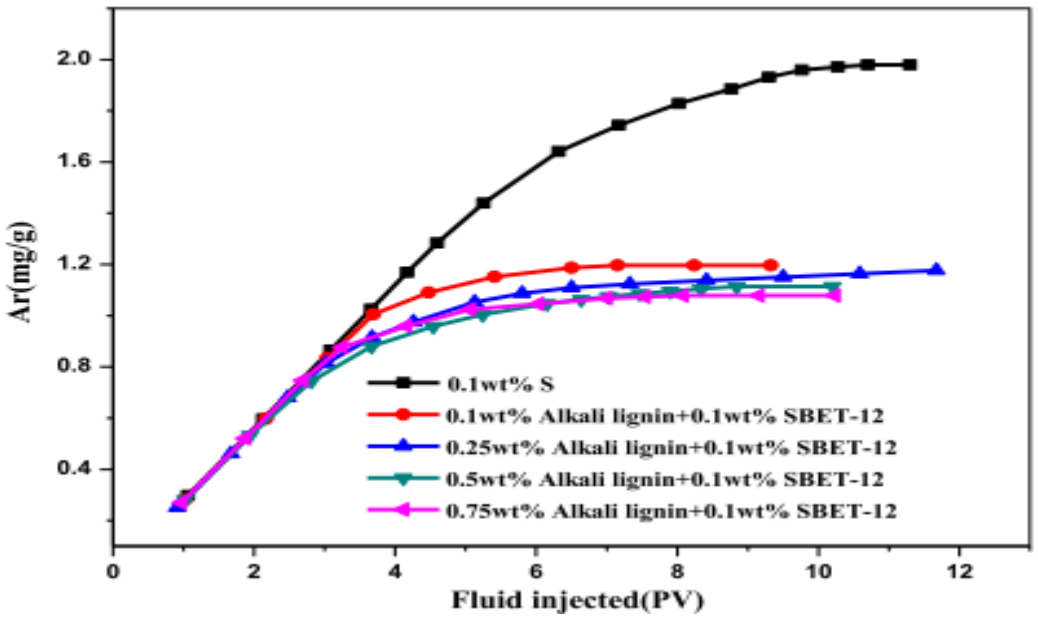

Figure 4: The effect of alkali lignin to surfactant adsorption [30]

Kamal et al. studied the effect of aging to the structural changes of non-ionic ethoxylated fluorocarbon surfactant and its thermal stability as well as the effect of temperature, surfactant concentration, Polymer concentration on the surfactant-polymer rheological properties at high pressure. They found that the viscosity at low temperature slightly increased at the beginning of adding surfactant, after the concentration of surfactant increased the viscosity decreased. However, at high temperatures the viscosity wasn't observed to increase with the addition of surfactant. Also the presence of salt in the sea water brine decreases the polymer viscosity as a result of so-called charge shielding effect, on the other hand the thermal stability of the surfactant on the presence of salt was observed [18].

Zhu et al. conducted a research to screen and evaluate suitable chemicals for ASP/SP EOR for Huabei field and found that salt resistant polymer KYPAM and FP6040 showed a good properties and the surfactants Petroleum sulfonate were the best among the other seven surfactants included in the test and the combination of the selected chemicals showed a 20-23 % recovery out of OOIP over the water flood recovery [31].

Alanis, Alsofi, Wang, & Han evaluated bio based surfactant comprehensively for SP application starting from the compatibility test, critical micelle concentration, long term stability, IFT reduction to finally core-flooding evaluation and found that bio surfactant (S-021206) was potential and recovered 6.5 % of OOIP [32].

Kamal et al. performed a comprehensive evaluation for TVP rheological properties and its interaction with carboxy betaine based surfactant SS-885, it showed thermos-thickening behavior (Figure 5) and its IFT with SS-885 is low and suitable for EOR, it's given in (Figure 6) [20].

Kamal et al. evaluated carboxybetaine-based amphoteric and propoxylated anionic surfactants for CEOR use. The anionic surfactant exhibits lower IFT in comparison to the other one. Thermal aging for 10 days at 90 °C has been done to the surfactants where the amphoteric was stable in term of IFT but the IFT for the anionic has increased a lot (Figure 7). Further evaluation for the surfactant showed that the Critical Micelle Concentration CMC is 0.025% wt. (Figure 8). CMC is defined as the lowest concentration at which the surfactant molecules starts to form aggregates or micelles inn other words it the lowest IFT when plotting the IFT against surfactant concentration [19].

Wu et al. investigated the effect of polymer interaction in SP systems, he studied two betaine-type amphoteric surfactant and two sulfonated partially hydrolyzed polyacrylamide and found that the IFT is affected by the surfactant aggregation resulted from the presence of the polymer and varied at different temperatures [33].

Magzymov et al. studied the effect of surfactant mixtures on the phase behavior of the micro emulsion and found that the composition of the surfactant mixtures and the pure surfactant individual properties are the depending factors that govern the micro emulsion phase behavior. Besides oil recovery is strongly affected when the composition of surfactant mixture is altered by selective retention, adsorption or degradation [34].

Adkins et al. introduced new process to manufacture low cost anionic surfactants using Guerbet alcohol. They can be produced by adding propylene oxide and/or ethelyne oxide to Guerbet alcohol. Those surfactants have high performance and can be stabilized with alkali at high temperature [11].

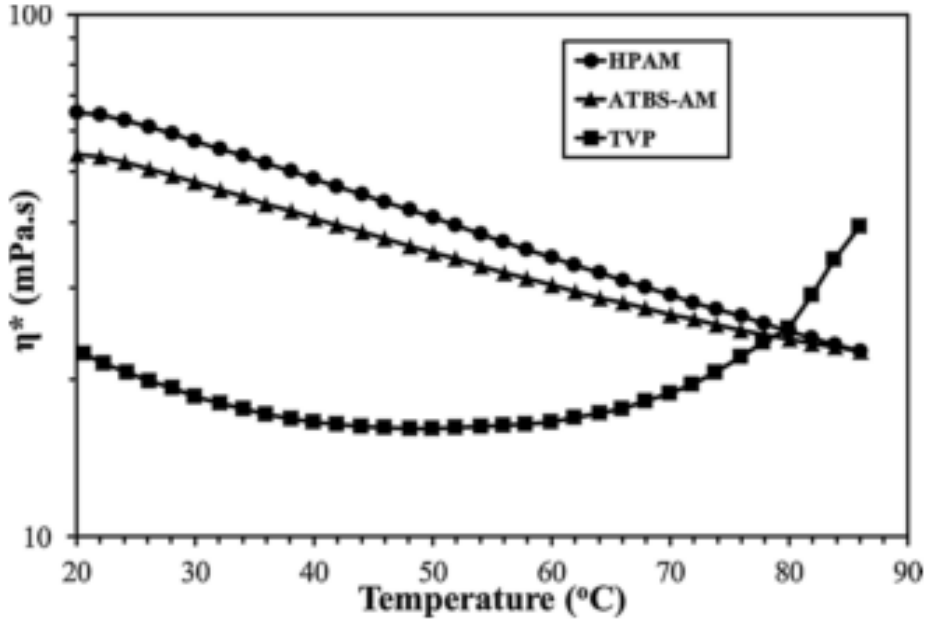

Figure 5: Thermo-thickening behavior of TVP [20]

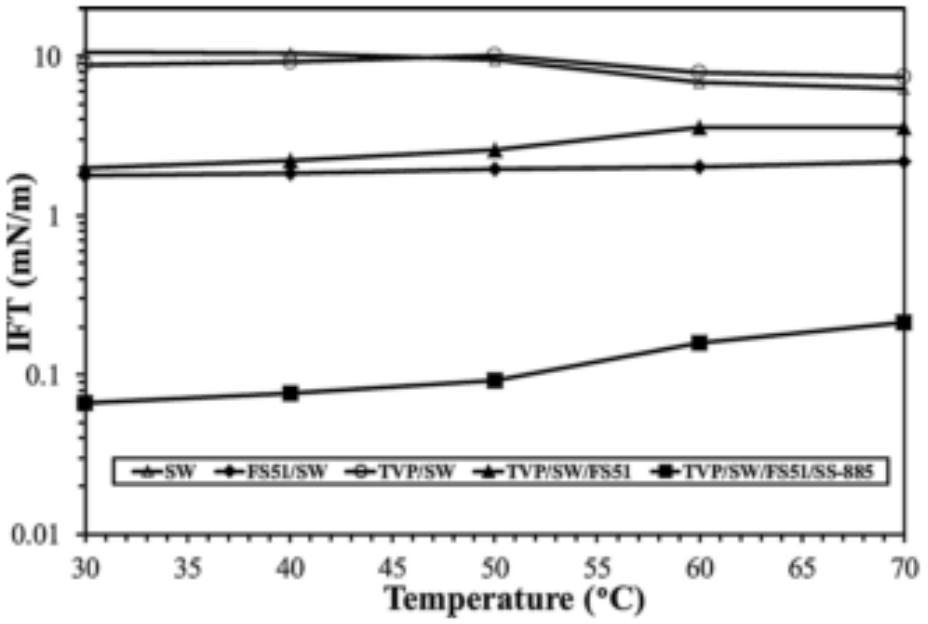

Figure 6: IFT for TVP (0.5% wt) and surfactants (0.05% wt) [20]

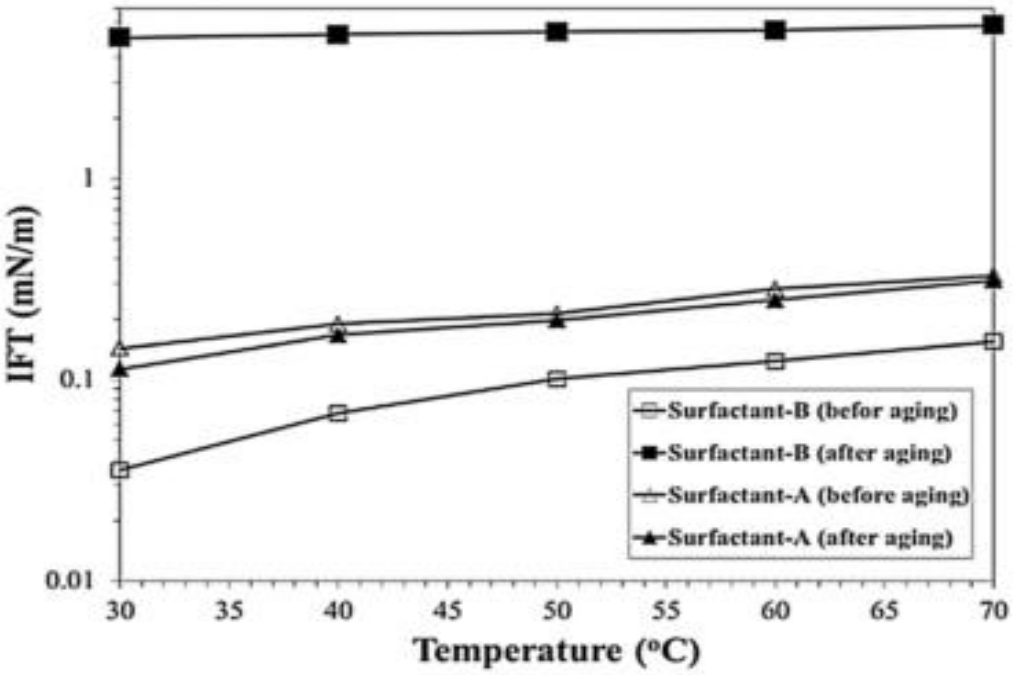

Figure 7: The effect of temperature on IFT [19]

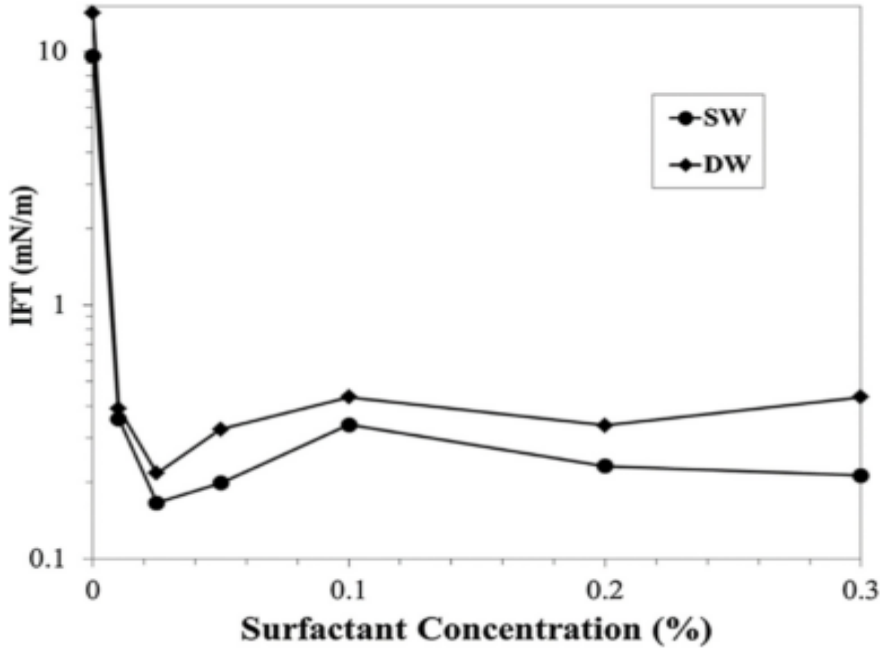

Figure 8: Effect of carboxy-betaine surfactant concentration on the IFT [19]

2.2 Slug size

Wang and Caudle studied the effect of slug size in polymer flooding and culminated that the recovery is increasing with the increase of slug starting with high increment at small sizes and become trivial at high slug sizes which indicated that there is an optimum slug after which there is no increment [35].

Maldal and Gilje evaluated the economic feasibility of using polymer assisted surfactant flood (PASF) in a specific field in Norway called Gullfaks. They used a branched sulphonate as a surfactant (5,000 ppm) and the polymer was xanthan (500 ppm), they injected a slug of xanthan after the slug of surfactant polymer in their system. At the end they concluded that PASF is effective in recovering more than 70% from the core residual oil in the laboratory, and the best temperature range for this process is about 40 to 60 °C, also they concluded that the optimum range of slug size is 0.25 to 0.5 PV with the concentration of surfactant greater than 0.4 wt%. Finally, they found that PASF process is less sensitive to the GOR in the remaining hydrocarbon and even it can mobilize dead oil [36].

Li et al. studied the effect of slug size in the breakthrough time of the ASP slug and found that its effect on the order of breakthrough is neutral [37].

2.3 Injection sequence

Ibrahim et al. discussed the laboratory aspect of using chemical EOR in Malaysian fields which located offshore and known of high temperature above 100 °C. They used actual cores from that field to do their core-flooding experiments. They found that a combination of alkali-surfactant, surfactant, and alkali-surfactant-polymer have the ability to decrease the IFT of their given field to the level desired. Also in term of recovery the incremental using ASP was 28.6% and for AS (NaOH) was 14.6% of Original OIP [38].

Dang et al. investigated the feasibility of using SP in geologically complex formations. They compared SP with water-flooding, S only and P only using a CMG simulator, and found that SP is the best solution for heterogeneous reservoir due to high displacement in both micro and macro level and in his given field the recovery amount increased sharply from $1.8x10^6$ m^3 to $6.02x10^6$ m^3 [39].

Luo et al. conducted his research to evaluate the use of P, SP, ASP and found that the incremental recovery at the end of extended water-flooding is higher in ASP then SP then P, but the instant increment in polymer flooding is higher than SP flooding because the surfactant mobilize the trap oil and it will be displaced by the extended water-flooding while the polymer displace it directly [9].

Nguyen et al. introduced a new approach to determine the optimum formulation in SP system and the injection schedule by integrating geology-driven modeling software with a robust optimizer developed by CMG Ltd. They were able to address the effect of clay content in cumulative oil as well as NPV and uncertainty analysis. They identified optimal formulations of the polymer slug and the combined SP slug beside the optimum injection schedule. They also found that SP flooding recovers the highest hydrocarbon production in comparison with only polymer flooding or surfactant flooding system [40].

Wang et al. studied the effect of adding polymer to reduce the surfactant adsorption in carbonate reservoirs. He had held a core-flooding test using natural carbonate cores from reservoir formation with length of (4.2 – 4.9 cm) and diameter of (3.76 – 3.79 cm) to observe the dynamic adsorption using betaine-type amphoteric surfactant provided by Oil Chem (USA) along with sulfonated-polyacrylamide, AN-125 provided by SNF Floerger (France) in three series; starting with only surfactant 2000 mg/L, after that polymer 2000 mg/L ahead of surfactant 2000 mg/L, then surfactant-polymer together each 2000 mg/L.

They saturated the dry core with a simulated connate water of 229,870 mg/L salinity filtered by 0.45 micron filter then loaded to the core-flooding system and the aging was overnight in 100° C and net confining pressure of 1300 with pore pressure of 3100 was used in all the tests then a simulated seawater of 57,612 mg/L was injected before the chemical injection there was no hydrocarbon saturation in this experiment, after 5 PV of chemical there was 10 PV of post seawater.

The effluent was collected at a constant time interval in test tubes and then analyzed to determine the surfactant concentration using tow-phase titration method and the TOC is used to determine the concentration of the mixture. Then a mass balance concept was used to determine the adsorption of the surfactant to the rock sample.

When slug of polymer was injected followed by surfactant, it decreased the adsorption to about 51.3%, and the SP mixture reduced it to 48.9%. This indicated that surfactant polymer flooding is better than surfactant alone not only in terms of hydrocarbon recovery but also in terms of adsorption which cost a lot of money spent on chemicals [6].

Zhu et al. concluded that the weak ASP is more favorable than strong ASP and the use of strong emulsification degree will increase the oil recovery from SP flooding by 6 – 10% [12].

Felix et al. investigated the effect of surfactant soaking for 24 hours before the polymer flooding and compared it with normal surfactant injection followed by polymer and co-injection of surfactant polymer and found that the surfactant soaking gives a higher recovery than normal injection and he attribute it to the fact that the formation of micro emulsion and capillary reduction need some time but the co-injection gives the best result [41].

2.4 Chromatographic separation & adsorption

Trogus et al. did his work at the dynamic adsorption for a mixture of surfactant to see the study the breakthrough curves, and concluded that there is a crucial difference between the high concentration slug and the low concentration slug where the fractionation increases the equivalent surfactant weight at high concentration while at low concentration the equivalent surfactant weight decreases. He attributed the increment in the effluent surfactant concentration than what has been injected to the composition of the inflowing stream and its concentration [13].

Chiou and Kellerhals studied the transportation of the surfactant polymer in micellar flooding using Berea sandstone cores, they realize that when using polymer for mobility control, it will lag behind the moving surfactant during flow in porous media. This polymer phenomenon has a strong relationship to phase separation in core tests due to cations generated as a product of the ion exchange between the surfactant and the clays. They found that core permeability is a determinant factor for the existence of polymer lag because the surfactant systems that contain polymer faced difficulties in low-permeability cores. Changing the co-surfactants found to improve the polymer transportation for certain conditions [1].

Pingping et al. studied the mechanism of ASP flooding in vertical heterogeneous reservoir and found that the flow changes direction from the high permeability formation due to the existence of some reactions either physical or chemical such as retention, adsorption and emulsion of ASP in the solution which increase the pressure because of the resistance resulted, so the flow rate decrease in high-permeability layer while increasing in the low and medium permeability layer increasing the macroscopic sweep-efficiency, considering

that the IFT is also low due to surfactant so the remaining oil at each layer will be recovered efficiently [42].

Li et al. studied the chromatographic separation of chemicals in ASP flooding. His result showed that the surfactant adsorption could be reduced to 30% by using 0.15wt% of bio-surfactant as a sacrificial-agent (Figure 9). Also the chemical breakthrough sequence in the retention test is polymer, then alkali, then surfactant. The variation in breakthrough time of the chemicals cause the chromatographic separation (Figure 10) [37].

Moreau et al. made an integrated workflow for CEOR starting from screening to formulation optimization and core-flooding evaluation in addition to simulation. They found that the adsorption in Kaolinite increases with the increasing hardness and decreases with the addition of alcohol [43].

Levitt et al. investigated the challenges facing the design of chemical EOR in carbonates formations with harsh conditions like high salinity, high temperature. They performed more than 40 core-flooding experiments with carbonate and sandstone cores of 30 cm length and 4 cm diameter using 0.38 PV slug size of SP followed by 1.53 PV polymer slug then chase water. They achieved initial water saturation (S_{wi}) of 0.48. Finally, the produced effluent was analyzed by calibrated volume test tubes for visual oil cut determination, HPLC for surfactant, conductivity for dissolved solid, rheology for viscosity and potentiometer for pH.

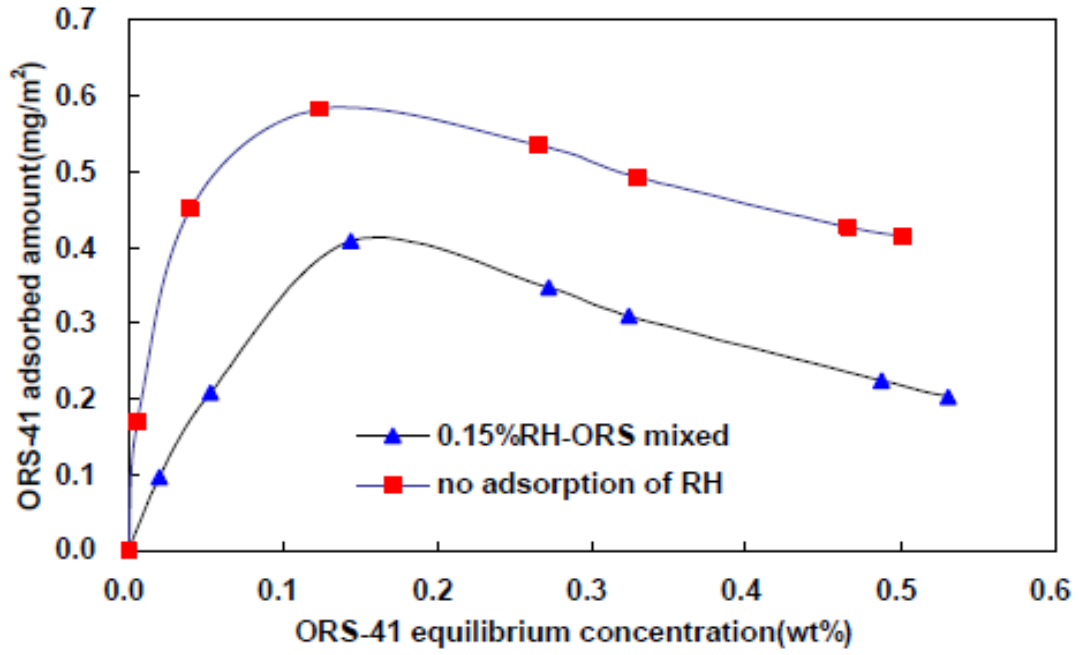

Figure 9: The adsorption amount decrease [37]

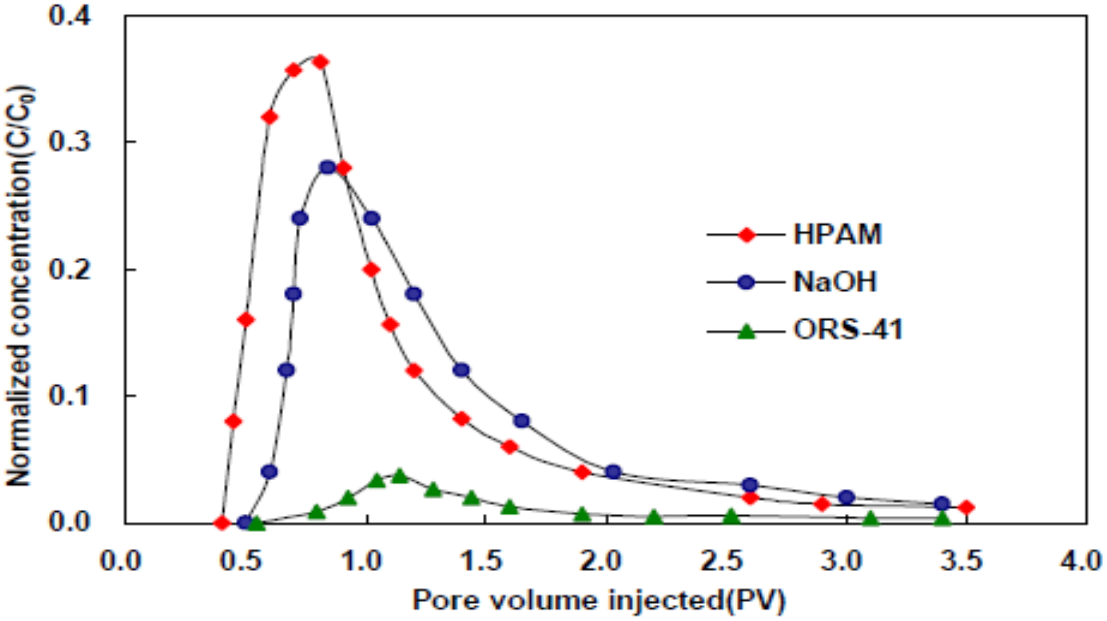

Figure 10:The relative concentration of polymer (HPAM), alkali (NaOH), and surfactant (ORS-41) [37]

They explained that the emulsion is formed only in carbonate cores not sandstone core due to the adsorption followed by desorption later of the surfactant results in emulsion formation inside the pores, or it is because of the separation between the surfactant and polymer chromatographically, which leads to polymer front free of surfactant, that lower the mobility till the surfactant arrive and mobilizes oil and rise the relative permeability of the aqueous phase. They also realized that the vuggy carbonates with large and continuum length make the traditional lab flood of SP systems even harder if it is not impossible. Finally, the molecular-weight distribution of the polymer should be optimized to improve the injectivity, at the same time maximize the viscosity [4].

Han et al. conducted a study to optimize an EOR formulation for carbonate reservoirs with high salinity and temperature especially in Arabian Gulf area. They found that the main difference between sandstone reservoirs and carbonate reservoir comes from the rock surface properties difference, such as wettability and surface charge. Their study showed that an effective slug of SP can be made without using water softening just regular seawater of Arabian Gulf. The best surfactant according to his screening criteria at the given reservoir conditions were amphoteric surfactants and the best polymers are sulfonated polyacrylamide and polysaccharide. They developed some formulations that show synergetic effects in IFT reduction and viscosity augmentation better than individual chemical performance [7].

Cao et al. thoroughly investigated the factors that affect the propagation of the flow of polymer and surfactant. He evaluated the competitive adsorption of surfactant and polymer by injecting them simultaneously; the adsorption of surfactant was reduced 50%. Both adsorption and dispersion reduce the chemical concentration during propagation. It is

mandatory to evaluate the chromatographic separation phenomenon when designing a field project because it happens in the surfactant-polymer co-injection schemes, as well as considering the in accessible pore volume when calculating the adsorption and desorption [44].

To sum up, it can be clearly seen that using surfactant and polymer together is better than using the polymer alone in terms of recovery, and many variables and effects have been studied thoroughly and some of them were slightly investigated while some were not touched.

changing the chemicals and their concentrations and combinations were very common variables that intensively been investigated, also we can see the temperature, rock type and salinity as well as the formation heterogeneity have been researched.

Table 2: Core-flooding summary

Year	Chemicals (SP)	Conditions	Slugs	Reference
1981	S: [Witco petroleum sulfonates, and Neodol 25-3S™ (ethoxysulfate) and Dowfax 2AITM (dodecyl diphenyloxide sulfonate)] P: [xanthan gum]	Berea Sandstone T: [25^{o}C] L: [10 inch] D: [2 inch] Salinity: [15,000 ppm NaCl]	Brine - oil - Brine - SP (5 PV)	[1]
1992	S: [propoxylated/ethoxylated alkyl sulfates Polyethylene glycol (PEG) as additive] P: [xanthan gum 1250 ppm]	Berea sandstone cores L: [12 inch] W: [2 inch] Salinity: [190,000 ppm] T: [47^{o}C]	Brine -S - P	[3]
1998	S: [branched sulfonate (5,000 ppm)]. P: [xanthan(500 ppm)]	Bentheimer Sandstone L = [12 inch] Salinity: [36,700 ppm], T: [50^{o}C],	Water-flooding - SP(0.5 PV) - p - sea water(2 - 5 PV)	[36]
2006	S: [ORS6-79] P: [HE-300]	Sandstone L: [5 inch] D: [1 inch] T: [119^{o}C] Salinity: [35,800 ppm]	(S&SW) - P	[38]
2009	S: [ORS-41] P: [HPAM with 21.3% degree of hydrolysis]	Sandstone L: [10 cm] D: [2.5 cm] Salinity: [3,834 ppm] T: [45^{o}C]	brine - ASP (0.3, 0.6, 1.0) PV - brine	[37]

Year	Chemicals (SP)	Conditions	Slugs	Reference
2010	S: [Diethanolamine of coconut oil, Petroleum sulfonate]. P: [HPAM with 25% degree of hydrolysis]	Sandstone L: [2 inch] D: [1 inch] T: [30^{o}C] Salinity: [20,000 ppm]	brine - 0.3 PV of (SP) - brine	[45]
2011	S: [SDS] P: [PHPAM]	Sandpack L: [14 inch] D: [1.5 inch] Salinity: [10,000 ppm]	SW-P-S-SW SW-S-P-SW	[46]
2012	S: [betaine-based amphoteric surfactants & Anionic ORS & Alpha-olefin sulfonate]. P: [HPAM & AMPS].	Berea Sandstone D: [1.5 inch] L: [20 inch] Salinity: [172,000 ppm] T: [95^{o}C]	water-flooding(2 PV) - SP(0.5 - 2 PV) - p(1 PV) - chase water	[29]
2012	S: [betaine-based amphoteric surfactants; SBET-12, SBET-16, CBET-12, CBET-16]. P: [HPAM with 24% degree of hydrolysis].	Sandpack D: [1 inch] L: [12 inch] T: [60^{o}C] Salinity: [13,659 ppm]		[30]
2013	S: [sulfate surfactant]. P: [Low MW AM-AMPS, Low MW HPAM].	Estaillades Limestone L: [12 inch] D: [1.5 inch] T: [90^{o}C] Salinity: [30,000 ppm]	Synthetic Formation Brine - SP - P - chase water	[4]

Year	Chemicals (SP)	Conditions	Slugs	Reference
2013	S: [amphoteric surfactants: carboxybetaines, sulfobetaines] P: [sulfonated polyacrylamide, polysaccharide]	Carbonate L: [4.4 cm] D: [3.8 cm] Salinity: [57,670ppm] T: [95^{o}C]	SW - SP -SW	[7]
2015	S: [amphoteric surfactant betaine-type]. P: [sulfonated polyacrylamide]	Carbonate L: [2 inch] D: [1.5 inch] Salinity: [57,612 ppm] T = [100^{o}C]	Sea water (10 PV) - S or SP or P-S (5 PV) - sea water	[6]
2015	S: [amphoteric surfactant betaine-type]. P: [sulfonated polyacrylamide]	carbonate reservoir cores L: [3.7 to 4.4 cm] D: [3.77 cm] Salinity: [57,670 ppm] T: [100^{o}C]	sea water - SP(5 PV) – seawater	[44]
2016	S: [APES (C_{14}, C_{16}, C_{18})] P: [MO4000, HPAM, KYPAM, STARPAM]	Berea sandstone L: [20 cm] D: [3.8 cm] Salinity: [25,603.89] T: [30^{o}C]	SW-SP-P-SW	[50]
2017	S: [SURF EOR ASP 4-A, SURF EOR ASP 1520, SURF EOR ASP 9100] P: [SNF AN125 VHM, SNF AN125 SH]	Sandstone Salinity: [30,000 ppm] T: [82^{o}C]	SP-P, S-P.	[49]

CHAPTER 3

METHODOLOGY

In this chapter we are going to describe the materials and the methods used in this work. The chapter will be divided to six sections: materials, rheology, contact angle measurement, core-flooding experiments, Ion analysis and Pore-scale imaging.

3.1 Materials

This section will highlight the materials used in this research and the detailed steps of preparation.

3.1.1 Brines

Synthetic formation brine with total dissolved solids (TDS) of 229,870 ppm was used to saturate the cores initially then displaced with oil to establish the initial water saturation. The composition of the formation brine is given in Table 3.

Synthetic sea water similar to Arabian Gulf water with a TDS of 57,612 ppm was used for water and chemical flooding as well as for the bulk fluid of the contact angle experiment, its composition is in Table 4.

Table 3: Formation brine composition

Salt	Concentration (mg/L)
$NaCl$	165,546
$CaCl_2.2H_2O$	69,723
$MgCl_2.6H_2O$	18,724
Na_2SO_4	2,395
$NaHCO_3$	529
TDS	229,870

Table 4: Sea water composition

Salt	Concentration (mg/L)
$NaCl$	41,041
$CaCl_2.2H_2O$	2,384
$MgCl_2.6H_2O$	17,645
Na_2SO_4	6,343
$NaHCO_3$	165
TDS	57,612

The brines were prepared carefully using deionized water. The weights of the salts were measured using an accurate weight balance up to 4 decimal digits. They have been stirred for at least three hours to insure complete dissolution, then filtered with 0.5-micron filter paper.

3.1.2 Crude oil

The crude oil used in this research was medium oil with 24.6 API and 0.89987 g/cc density measured at room temperature. Its viscosity at 90^{o}C is 3 cp and the density at that temperature is 0.77748 g/cc. It has been analyzed using Saturates Aromatic Resin Asphaltene SARA test as shown in (Table 5).

SARA analysis was done using High performance liquid chromatography (HPLC). The column used was C-18 at 40^{o}C. The oil was first dissolved in n-hexane then filtered with 0.5-micron filter to separate the Asphaltene. The Asphaltene will be held by the filter and its amount can be known by weighting the filter before and after filtration when it gets dry. The filtered solution was injected through the column to be separated to resins and aromatics. The aromatics and resins have different retention times previously determined so each one of them will be collected on its time in a separate peaker. The peaker weight will be measured dry and after evaporating the solvent from the resin or the aromatics so their amount will be determined. The amount of saturates will be determined by subtracting the measured amounts of Asphaltene, Aromatics and Resins from the original amount of the dissolved crude oil.

Table 5: SARA analysis for Crude oil

Components (g)	Composition (%)
Saturates	26.64
Asphaltene	6.90
Resin	5.54
Poly Aromatic Hydrocarbons	60.92
Total	100

3.1.3 Chemicals

We used two types of polymers and two types of surfactants in this work. They will be put together into four SP combinations.

The polymers are:

P1: Acrylamido tertiary butyl sulfonate (ATBS)/acrylamide (AM) copolymer produced by SNF FLOERGER, it has 8 million Dalton molecular weight with the structure Figure 11(a).

P2: Thermoviscosifying polymer obtained from Hengju Polymer Co. laboratories, its molecular weight is 7.08 million Dalton, it contained 8 % thermos sensitive monomer and has 3 % degree of hydrolysis with the structure Figure 11(b).

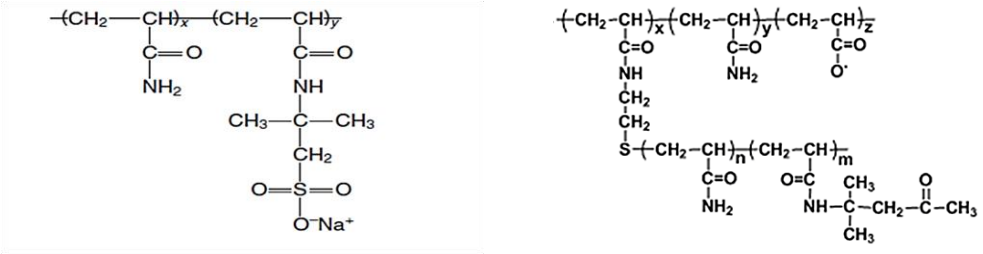

(a) (b)

Figure 11: Polymers chemical structures

While the surfactants were Amphoteric surfactant SS-880 Carboxybetaine provided by Oil Chem Teknology, USA we used (S1) to refer to it in this work. The other surfactant (S2) was Amphoteric surfactant SS-885 Carboxybetaine from the same source, both of them received in a solution with an active content of 40 %.

Those chemicals will be used with the following formulations in the contact angle, rheology and the core-flooding Table 6.

Table 6: Chemical formulations

SP combination	Surfactant	Polymer
S1P1	SS-880 (0.05% wt.)	ATBS/AM. (0.25% wt.)
S1P2	SS-880 (0.05% wt.)	TVP. (0.25% wt.)
S2P1	SS-885 (0.05% wt.)	ATBS/AM. (0.25% wt.)
S2P2	SS-885 (0.05% wt.)	TVP. (0.25% wt.)

3.2 Rheology

This part of the experiments was used to investigate the rheological properties of the polymer solutions specially shear scan. This is to understand the effect of shear on the viscosity of the ATBS/AM as well as TVP for the pure solution and in the addition of surfactant.

3.2.1 Solution preparation

The solutions are prepared with sea water described earlier. The first step is to put the solvent in a wide peaker and use magnetic stirrer and spin it to create a vortex. Then the polymer powder is added slowly on the top of the vortex to ensure easy dissolution. In the presence of surfactant, the surfactant solution is used to create the vortex.

3.2.2 Machine operation

The machine used for this set is Discovery Hybrid Rheometer (DHR3) provided by TA instrument Trios. concentric cylinder geometry is used in this case. The geometry case was first connected to the instrument followed by water lines for cooling. The cover was removed from the rotor, before the start you a zero gap calibration was done at the specific temperature we are working on. The experiment conditions and the mode should be specified from the software. Then the sample is put on the cylinder up to the mark. The cone was lowered inside the cylinder using the software navigation tool then the run was started. The results were fitted to the known models such as Carreau-Yasuda.

3.3 Contact angle

Contact angle measurements is a mean to identify the rock wettability by measuring the angle of a drop placed on a rock surface surrounded by another fluid either air or liquid. Usually the drop fluid is oil and the surrounding fluid is reservoir fluids such as sea water or EOR chemicals. In this research we are using surfactant/polymer as surrounding fluid.

3.3.1 Disc Preparation

Two types of discs were prepared: The first type was taken from carbonate outcrop rock from Riyadh and the second one from Indiana limestone core. 1-inch diameter and 3 mm thickness discs were cut and smoothed carefully with sand papers with increasing grade of fineness to reduce surface roughness effect on contact angle. The sand paper used was silicon carbide abrasive paper electro coated made in Korea.

Then they were .dried in the oven at 100^{o}C for 24 hours to evaporate all the waterThermal aging was done by immersing the discs in Crude oil at oven temperature of 90^{o}C. It was one week

for outcrop Discs and two weeks for Indiana discs to retrieve the native state reservoir wettability.

3.3.2 Drop fluid preparation

The drop fluid used here is the same Crude oil used for saturation. It is filtered with 0.7-micron filter then filled to the drop tank in the machine using a manual screw pump.

3.3.3 Bulk fluid preparation

The bulk fluid used here is a mixture of surfactant and polymer for four different combinations. It was prepared using the sea water described earlier with the polymer powder or surfactant solution at the required concentration.

3.3.4 Machine operation

We used IFT 700 Provided by VINCI Technologies for contact angle measurement Figure 12 and Figure 13. The equipment contains two tanks: one for drop fluid and one for the bulk fluid beside a high pressure high temperature cell that has two glass windows. The front window is facing a digital camera for image capturing and the back window is facing a light source to make a better vision. Also a needle is attached to the cell in the opposite direction of the disc holder to place the drop in the disc surface. Two manual screw pumps one for bulk tank and the other for the drop tank were used to establish the cell pressure and release the drop respectively. A computer software was provided by VINCI technologies used for Image analysis and angle calculation. The Cell was filled first with the bulk fluid in this case the surfactant polymer solution or sea water and connected to the bulk and drop fluid lines. Before attaching the disc holder, air bubbles were released from the bulk line to avoid trapping the bubbles inside the cell which may affect the vision.

The cell was closed by the disc holder without disc first to avoid disc contamination by oil expansion. After that, the heat was turned on to reach the required temperature, hence, the disc holder taken off and the air bubbles released from the drop line. At this stage the disc has placed on the disc holder and attached to the cell to start building the required pressure. The drop was released carefully by decreasing the drop tank pressure in a sucking like motion. As soon as the drop was released a quick increase in the bulk tank pressure was induced up to the required pressure to make sure that no other drop come out which may affect the vision. The drop angle measured for at least half an hour stabilization time. The contact angle is measured through the oil phase. The following figure is showing what is the interpretation for each contact angle value.

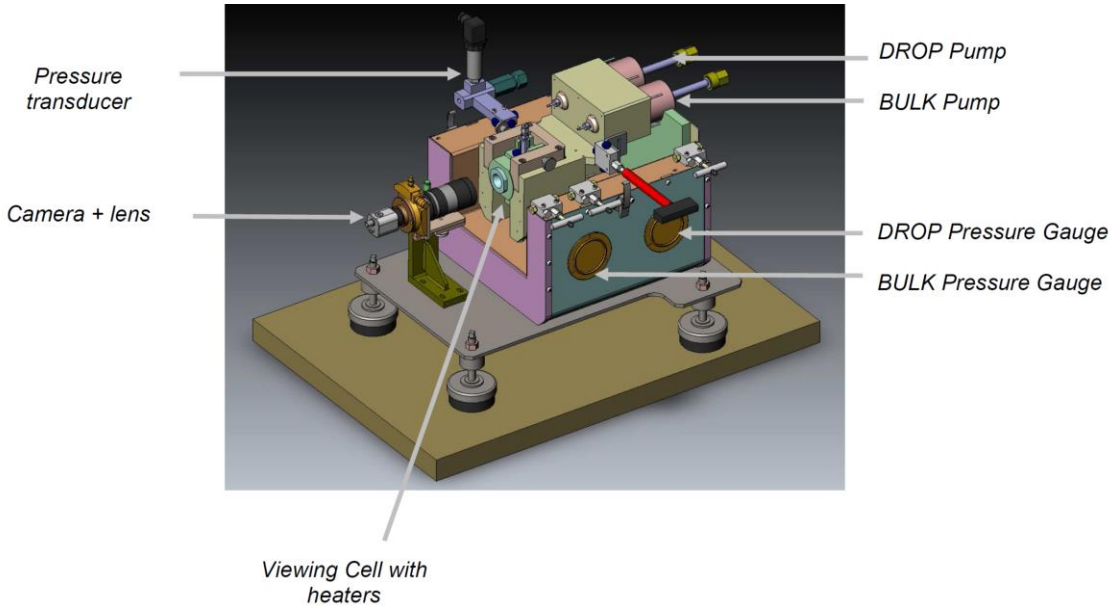

Figure 12: Schematic drawing for contact angle device (IFT700 manual)

Figure 13: VINCI HPHT contact angle device

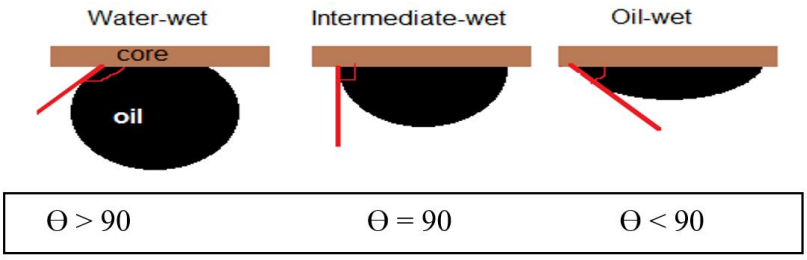

Figure 14: Contact angle interpretation

3.4 Core-flooding

Core-flooding is a way to mimic the reservoir recovery in the lab scale. It uses a cylindrical rock sample put to the same condition as the downhole formation in terms of temperature, pore pressure and overburden pressure.

3.4.1 Core Preparation

The core was first cut to small plugs 2-inch length and 1.5-inch diameter to fit the centrifuge for oil saturation. The plug surface was polished carefully using grinding surface machine to be put together as long composite core. Dean stark soxhlet assembly was used to clean the plugs by toluene solvent to make sure that there is no any trace of hydrocarbon. After that the plugs were dried overnight in 90^{o}C oven. Air permeability was measured and corrected to Klinkenberg liquid permeability.

3.4.2 Brine saturation

The saturation was done using formation water brine see (Table 3). The core was first vacuumed for three hours in in high pressure cell to remove any air from the pores. The formation brine was sucked due to the vacuuming to fill the core pore-space. 3000 psi pressure was applied for overnight using positive displacement pump. Porosity and pore volume were calculated from the weight difference between the saturated and dry core.

3.4.3 Oil saturation

Oil saturation was done by centrifuge machine provided by CoreLab company. It was done simply by displacing the formation water with Crude oil (Table 5) using different rotational speeds with gradually increasing speed starting from 1000 up to 8000 and 9000 RPM. When the required initial water saturation was reached, the cores wrapped carefully with

nylon and aluminum sheet to be transferred to aging cell without losing its saturation. The cores were immersed in Crude oil at 90^{o}C oven temperature for two weeks aging to restore the native state reservoir wettability.

3.4.4 Machine operation

The core-flooding experiment was done by VINCI core-flooding machine Figure 15. The machine consists of core holder with rubber sleeve with 1.5-inch size to fit the core inside. Four accumulators linked with displacement pumps for the injection fluids. Fluid separator or fraction collector can be used depend on the set, either effluent samples needed or not. computer software linked with the pressure transducers, pumps and separator camera to do real time monitoring for what is going on.

Firstly, the core was loaded inside the sleeve and pushed with the end faces to insure no spaces between the plugs which may cause sleeve failure. The sleeve put inside the core holder and tightened carefully to avoid any leaks, and also tight the lines very well after pushing the air bubbles inside them by the injection fluid. Secondly, the oven was turned on at 90^{o}C and the reservoir pressure was built up to 1500 psi gradually and left overnight to guarantee stabilized temperature inside the core. Finally, the injection rate was 1 cc/min for all the fluid starting with water-flooding then chemical flooding finishing with water-flooding again.

Figure 15: VINCI core-flooding system

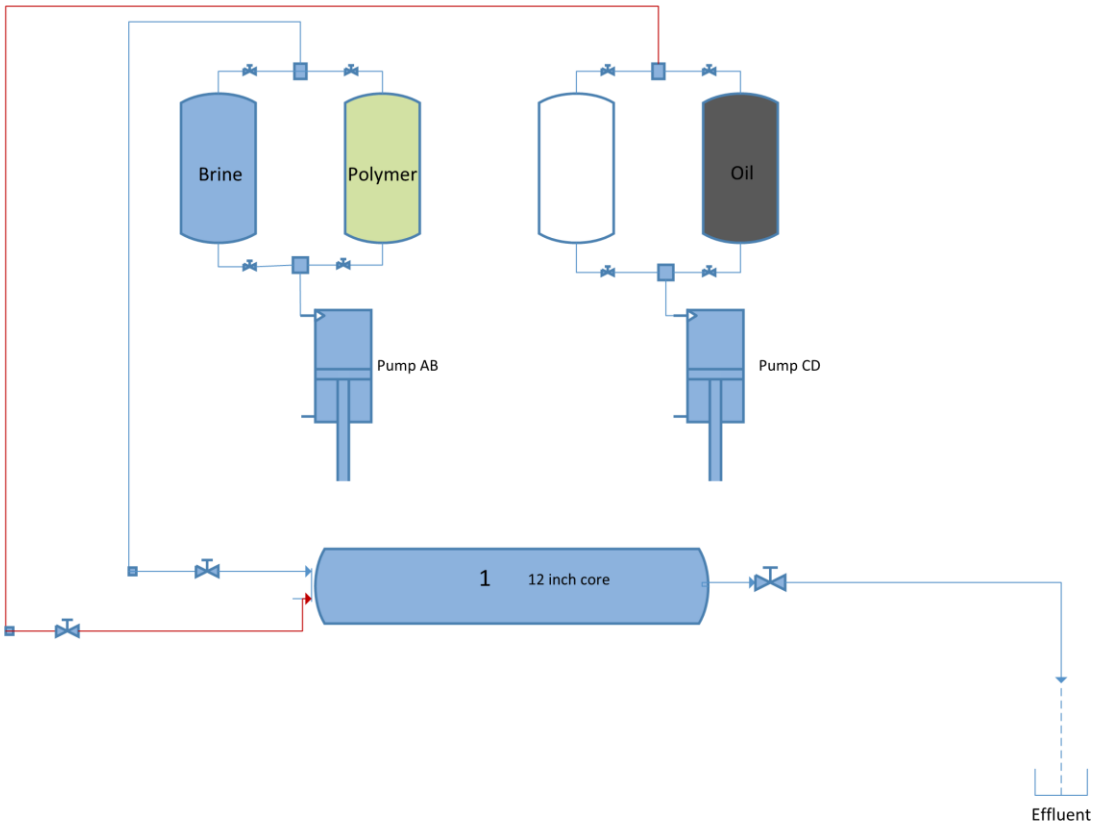

Figure 16: Schematic diagram of the core-flooding system

3.5 Effluent analysis

This part attempts to understand the ions behavior inside the rock sample and the adsorption/desorption tendencies with the carbonate rock in the presence of the injected chemical.

3.5.1 Sample preparation

The effluent sample is diluted thousand times by taking 20 microliter of the effluent and put it in 20 cc of DI water and shake it very well to ensure the solution is homogeneous and put it in closed tube to prevent evaporation.

3.5.2 Ion chromatography concept and operation

The instrument used for this set is (850 Professional IC) from Metrohm AG. The concept of this device is to separate the ions in specific columns: one for anions, and the other for cations in a way that each ion will come out at specific retention time. The detector is measuring the conductivity and then the software convert the conductivity to concentration using pre-set calibration curves.

Figure 17 shows the anions peaks at different retention times for one of the samples while Figure 18 demonstrate the cations peaks at their retention times. The calibration curves used are illustrated in Figure 19 - Figure 23.

The columns type used for anions is (Metrosep A Supp 7 - 250/4.0) with the eluent composition of Sodium carbonate. The column temperature and pressure was 45 ^{o}C and 12.95 MPa respectively. On the other hand, for cations the column type was (Metrosep C 4 – 250/4.0) with 45^{o}C temperature and 8.22 MPa pressure and the eluent composition was nitric Acid.

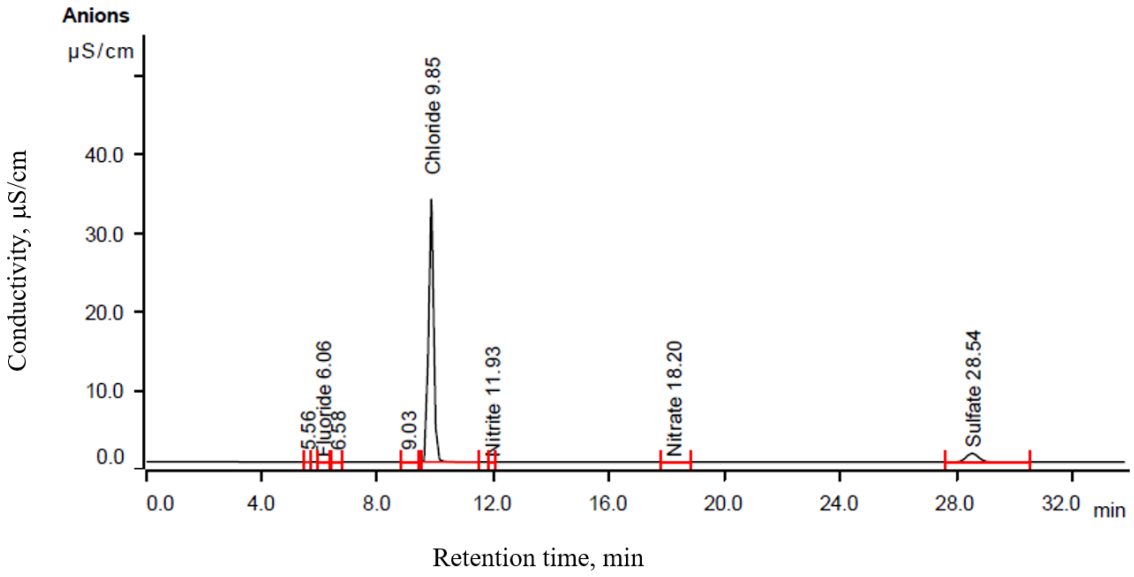

Figure 17: The anions conductivity peaks

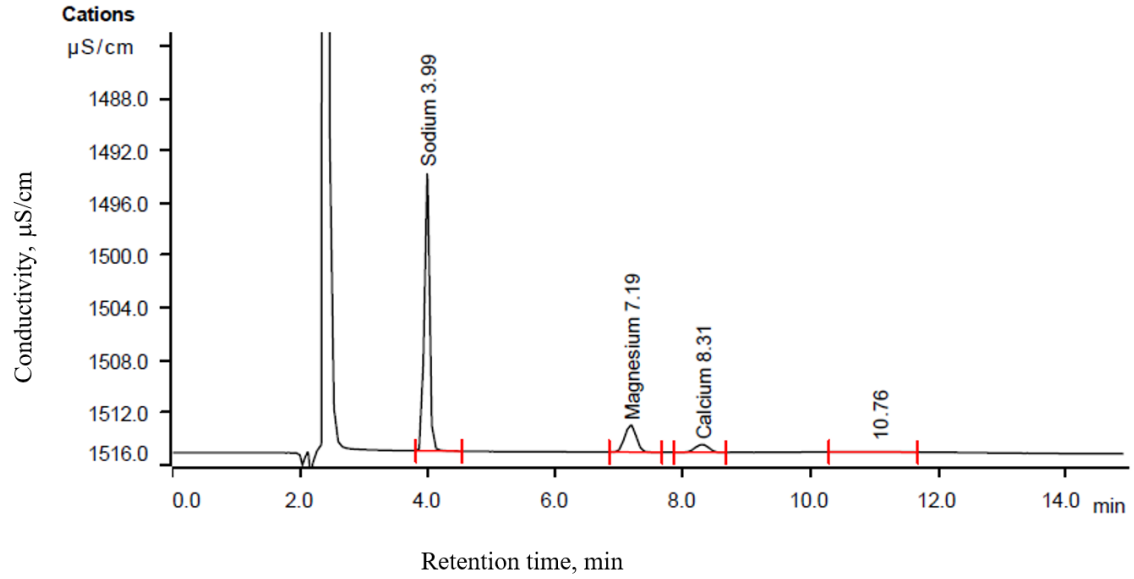

Figure 18: The cations conductivity peaks

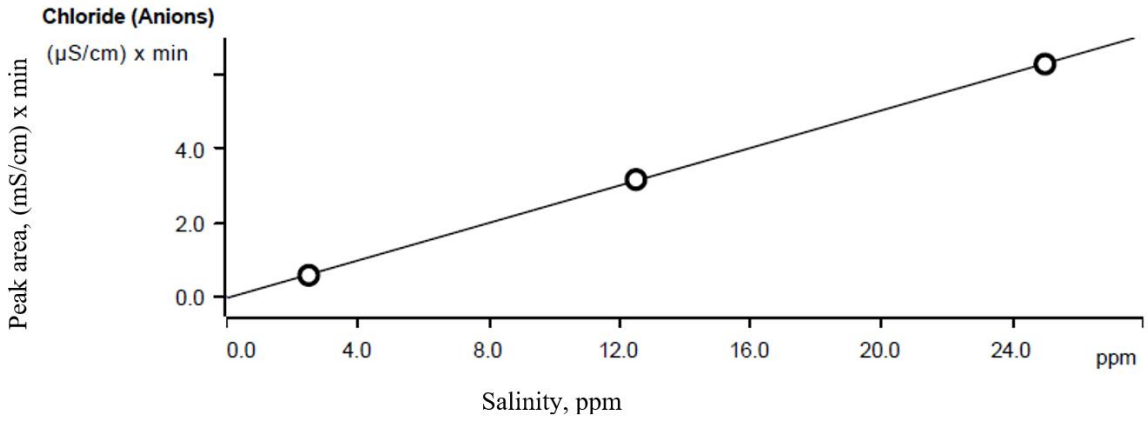

Figure 19: Chloride calibration curve

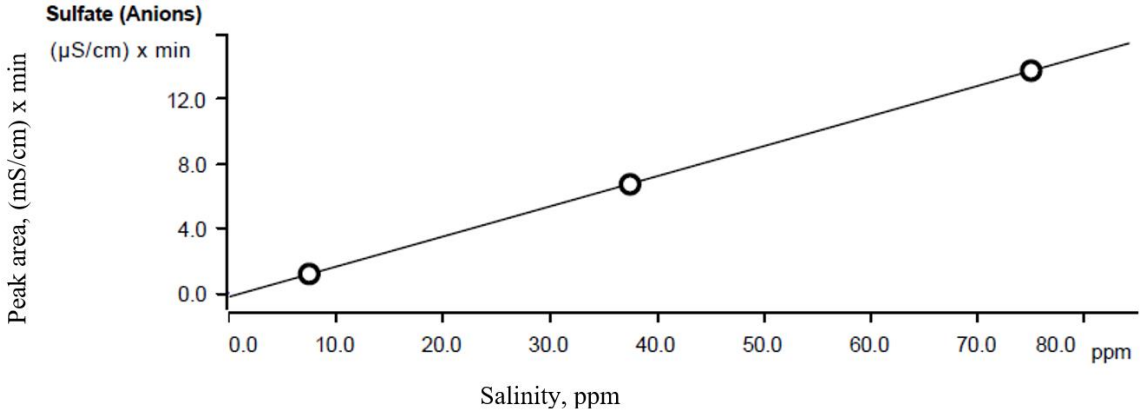

Figure 20: Sulfate calibration curve

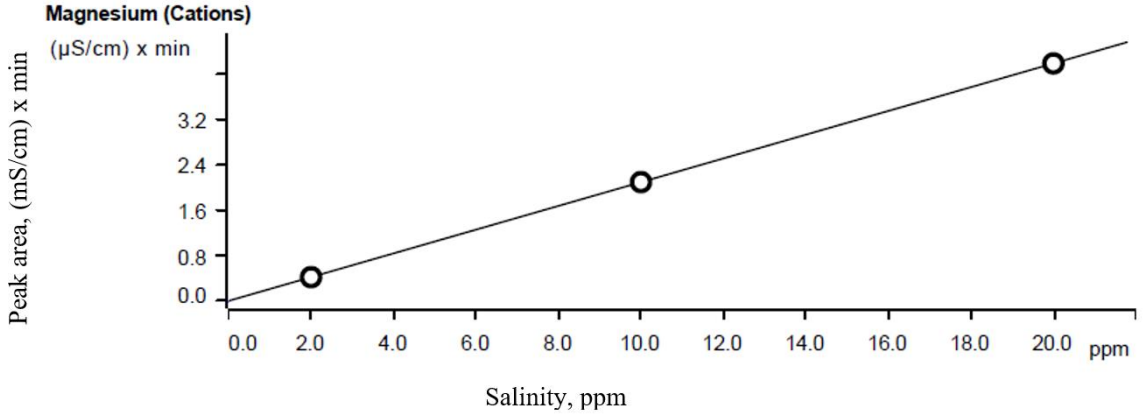

Figure 21: Magnesium calibration curve

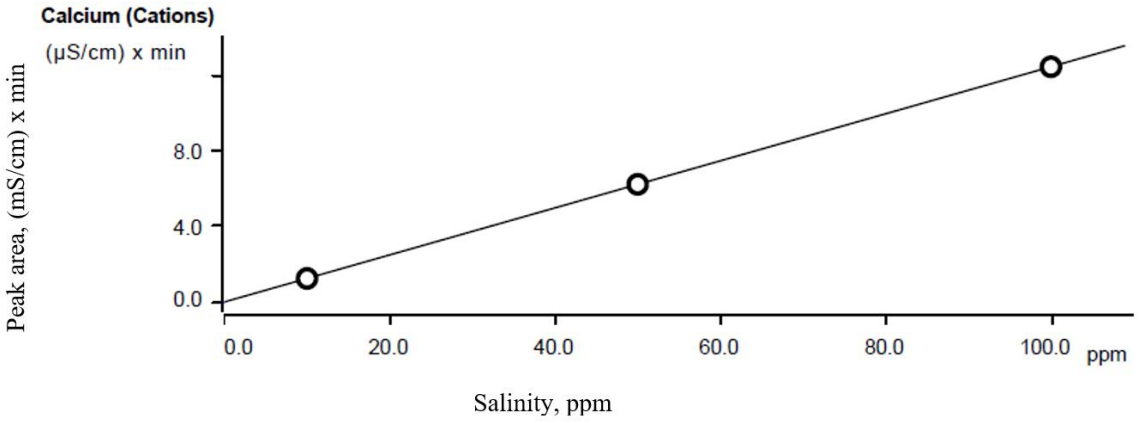

Figure 22: Calcium calibration curve

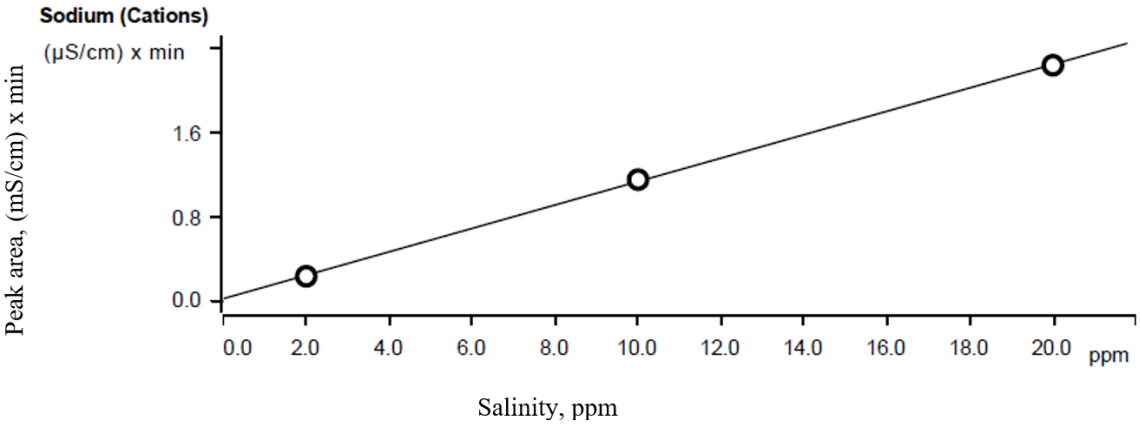

Figure 23: Sodium calibration curve

3.6 Pore-scale imaging

Pore-scale imaging is a way to understand oil recovery mechanisms by looking at the phases occupancy inside the pore by taking advantage of Micro computed tomography (Micro-CT). Coupling the slice images generated by the Micro-CT device with image processing software has invaluable advantages. It can make three dimensional maps of fluid occupancy, calculate the volume fraction of each phase using phase segmentation techniques. It can also generate pore network model, illustrate connected porosity and pore size distribution. In all the experiments the scanned portion is placed in the middle of the plug with dimension of around 3.75 mm length and 3.75 mm diameter for the first two sets and around 2.5 mm length and 2.5 mm diameter for the last two sets as explained in Figure 24.

3.6.1 Micro-CT scanner

The device used for micro-CT is Versa XRM-500 provided by Xradia a 3D X-ray microscopy optimized for non-destructive tomography Figure 25.

3.6.2 PERGEOS software

The software used for image processing is PerGeos provided by EFI company. It is comprised of advanced artifact removal techniques, filtering and analytical algorithms than can make the image obtained from the micro-CT meaningful. It has great visualization power for 2D and 3D images that makes the segmentation process easier and reliable.

3.6.3 Procedure

Four different set of core samples has put to the test, each one of the first two sets containing 6 plugs, the plug size is about 2 inches' length and 1.5-inch diameter. They were used for SP flooding; the first set for S1P2 using (CF-3 plugs) and the latter for S2P2 using (CF-4 plugs). Thermal aging at 90 ^{o}C oven temperature for 1 week for (CF-3) and (CF-4). The images were taken before flooding and after flooding using micro-CT scanner device described earlier to investigate fluid displacement and study wettability alteration in-situ. The last two sets were 2 inches in length and 1.5 diameter for each: The first one was used for individual surfactant flooding using (DF5-1 plug), and the second one was used for individual polymer injection using (DF5-2). This work is an attempt to understand the micro-scale recovery mechanism for the individual members of SP flooding and watch the wettability alteration in different phases of the flooding process. That is why the images was taken before the water-flooding, after the water-flooding and after the chemical flooding by the device mentioned above. Finally, PerGeos software was used for all the sets for image analysis to produce 3D maps for fluid occupancy and investigate the saturation changes at each phase as well as the in-situ contact angle.

Table 7: Plugs properties for micro-CT imaging

Core-flood	S1P2 (CF-3)	S2P2 (CF-4)	S1 (DF5-1)	P1 (DF5-2)
Length (inches)	11.42	11.5	1.91	1.9
Porosity	0.17	0.158	0.139	0.129
Scanned section (D,L) (mm)	(3.75, 3.75)	(3.7676, 3.767)	(2.54, 2.54)	(2.54, 2.54)
Oil permeability (md)	179	39	10.13	20.78
Pore volume (cc)	56.19	52.29	7.74	7.17
Swi	0.296	0.294	0.3	0.27
Oil volume (cc)	39.55	36.9	5.42	5.25

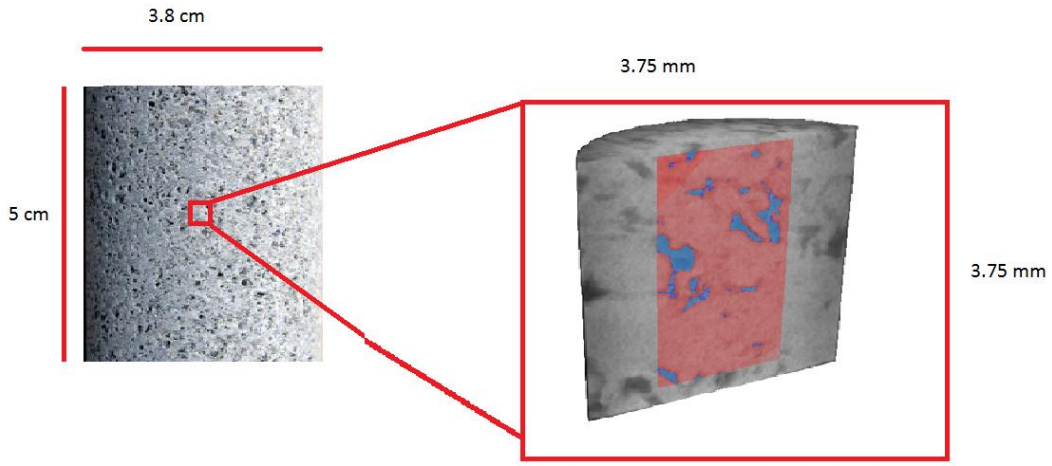

Figure 24: schematic diagram of the scanned portion

Figure 25: Micro-CT Scanner

CHAPTER 4

RESULTS AND DISCUSSIONS

4.1 Rheology

Investigating the rheological properties of the chemicals to be injected in the reservoir is really has great importance specially when dealing with heterogeneous formation. It is a mean to understand the divergence and the effect of shear in the viscosity whether it is shear thinning or shear thickening. Also, rheological properties are needed in the surface calculations for injection pressure and flowrate.

In this section we will discuss the rheological properties for the individual polymer used as well as for the chemical combinations where the surfactants are mixed with the polymers Table 6.

4.1.1 ATBS/AM Rheology

The rheological properties for ATBS has been studied using distilled water for polymer solution preparation and the temperature used was 60ºC with different polymer concentrations.

The shear scan in Figure 26 shows shear thinning behavior of the polymer which means the viscosity is reducing with the increasing shear rate. These results were fitted to the Carreau-Yasuada model and the zero-shear viscosity was calculated from the model as in Figure 27. The viscosity build up at 6.31 1/s shear rate is plotted in Figure 28.

This particular shear rate was picked based on the simplified shear rate calculation for the flow through porous media. For a flowrate of 1 cc/min, the equivalent linear injection velocity (v) used in core-flooding is 0.00735 cc/s considering the effective area as the total cross sectional area multiplied by the pore fraction. Assuming a pore diameter (d) of 93 microns. So the shear rate ($\dot{\gamma}$) will be 6.3 s^{-1} based on the following equation:

$$\dot{\gamma} = 8v/d$$

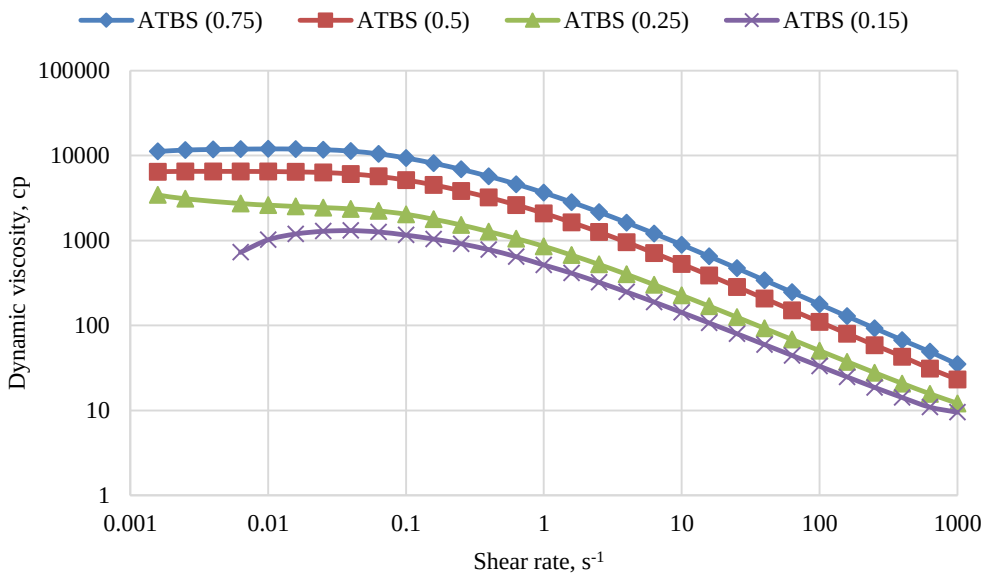

Figure 26: Shear scan for ATBS with variable concentrations in distilled water

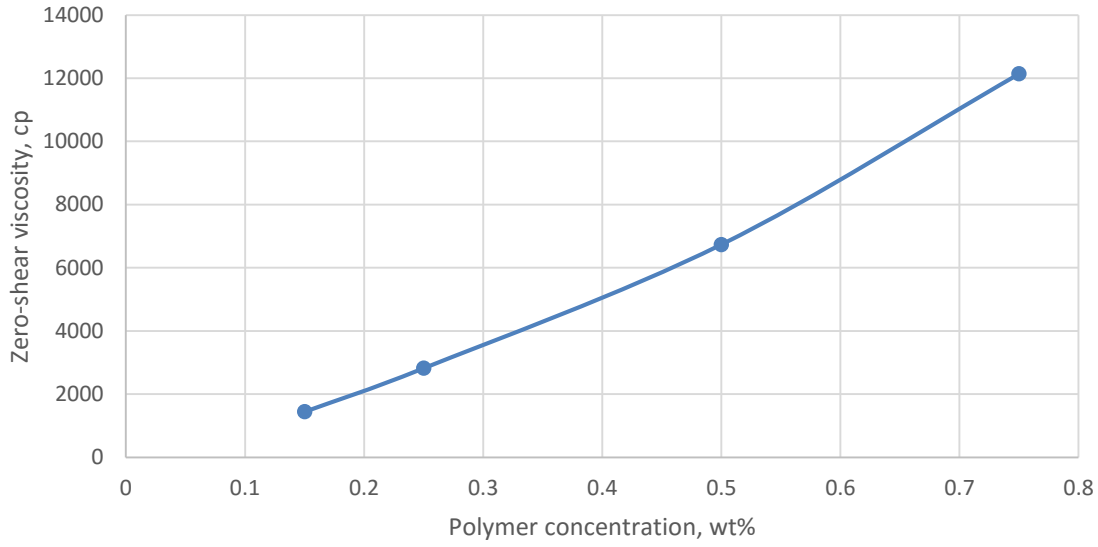

Figure 27: Zero shear viscosity build up with increasing concentration of ATBS in distilled water

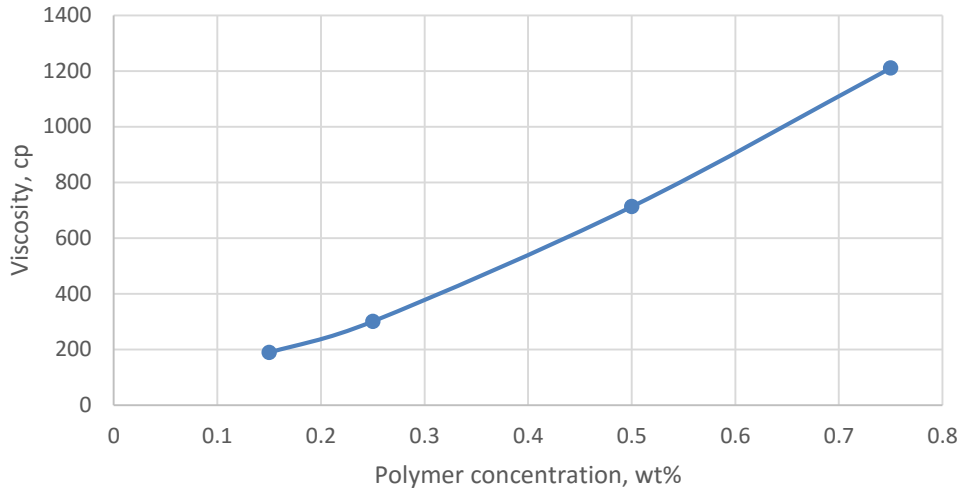

Figure 28: Viscosity build up with ATBS concentration at 6.3 1/s of shear rate

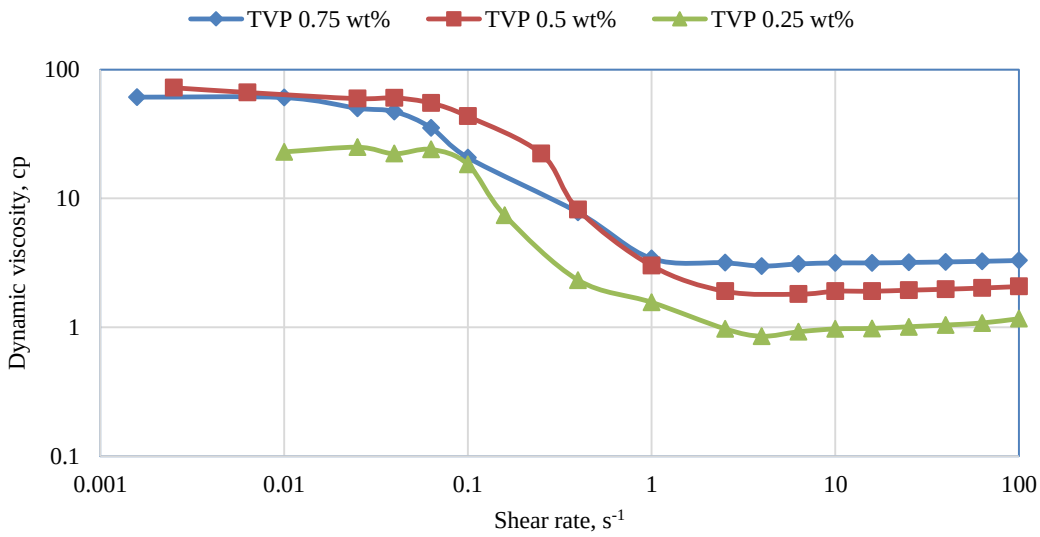

Figure 29: Shear scan for TVP with variable concentrations in sea water

4.1.2 TVP Rheology

The rheological properties of TVP has been investigated using sea water at 85^{o}C. It can be clearly seen from Figure 29 that TVP has shear thinning behavior at the shear rate range of (0.001 to 3) 1/s then there is no effect of the shear rate in the viscosity in the range (3 to 100) 1/s.

The fitted result to Carreau-Yasuada Model showed the zero-shear viscosity of TVP is building with increasing the concentration then reach plateau after 0.6 wt.% as appears in Figure 30. However, the viscosity at 6.3 1/s was directly proportional to the concentration as depicted in Figure 31.

4.1.3 SP combinations Rheology

Figure 32 shows the effect of changing chemicals on the shear scan behavior for all the SP combinations Table 6. The shear scan for S1P1 exhibits Shear thinning behavior in the range of (0.001 to 5) 1/s shear rate then no effect of shear has appeared above 5 1/s. Carreau–Yasuada model has used to fit the data and the zero-shear viscosity was found to be 35.6 cp at that temperature and salinity. While the shear scan for S2P1 showed the same shear thinning behavior at the first part then plateau at the second part. The fitted data to Carreau–Yasuada model gave a zero-shear viscosity estimation of 52.8 cp. The same trend was noticed for S1P2 and S2P2 except the zero-shear viscosity extracted by fitting the data to Carreau–Yasuada model gives 124 cp and 23.5 cp respectively.

It can be plainly noticed that the presence of surfactant has no effect of the rheology on the range of (3 to 100) 1/s shear rate because for the same polymer the two curves with two different surfactants overlapped but in the first range there is difference whether it is small

difference like in P1 or big difference like in P2. The difference in P2 confirms that there is synergism between P2 and S1 because the zero-shear viscosity has increased too much meanwhile there is antagonism between P2 and S2 because the zero-shear viscosity became very low compared to the other one.

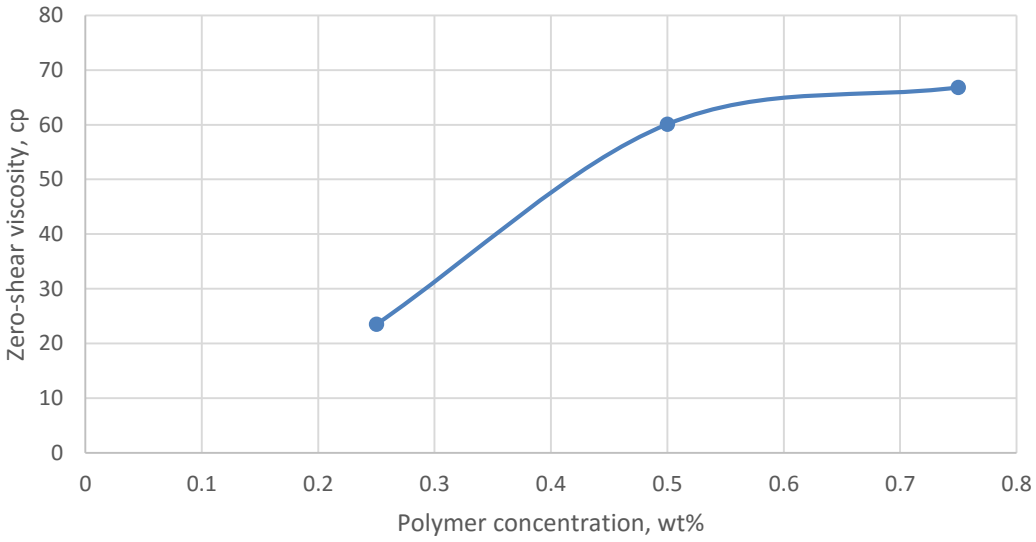

Figure 30: Zero-shear viscosity of TVP with variable concentrations in sea water

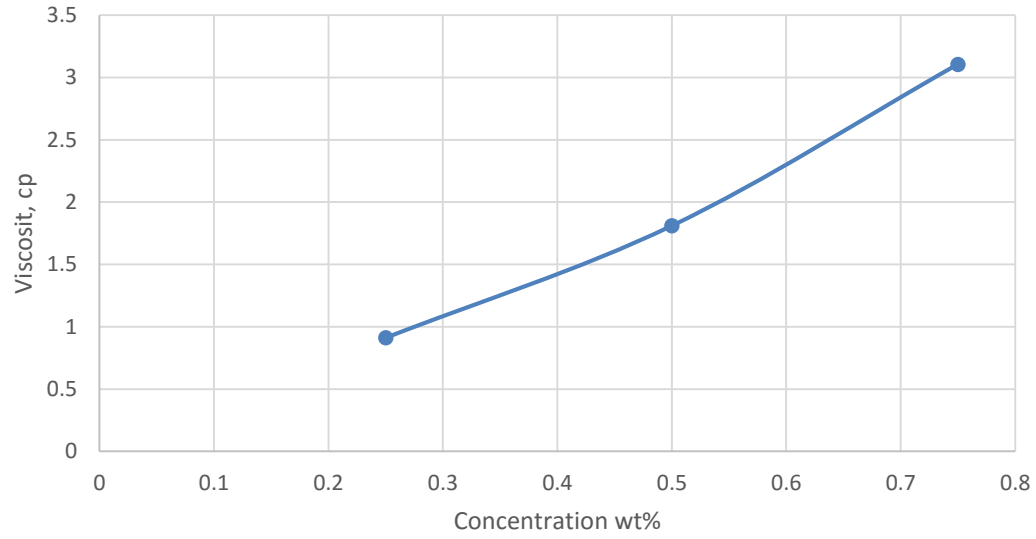

Figure 31: Viscosity buildup of TVP at 6.3 1/s shear rate

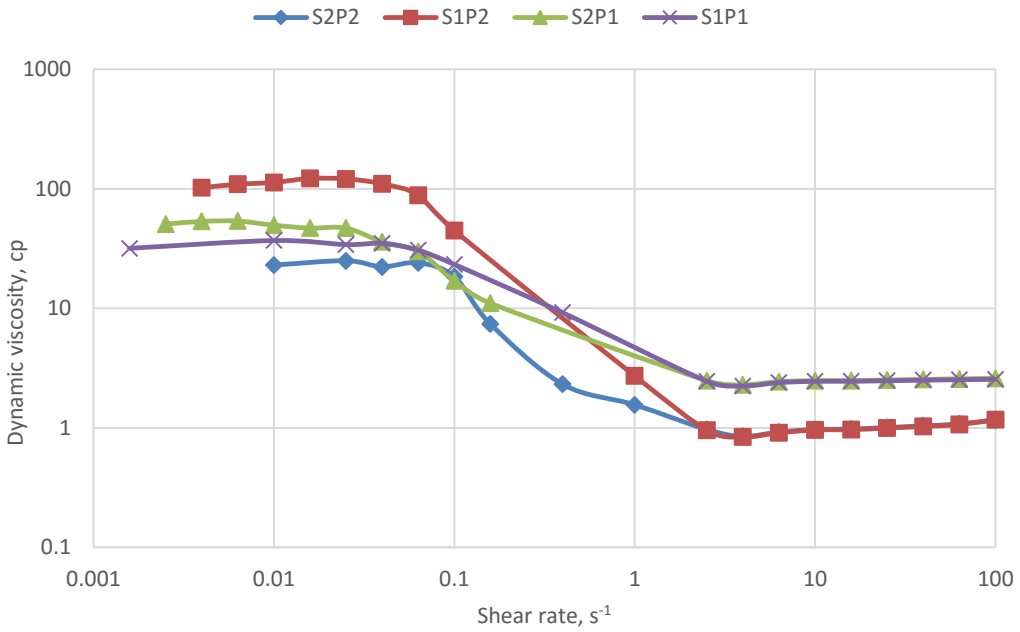

Figure 32: The effect of chemicals on rheology at 85ºC with sea water

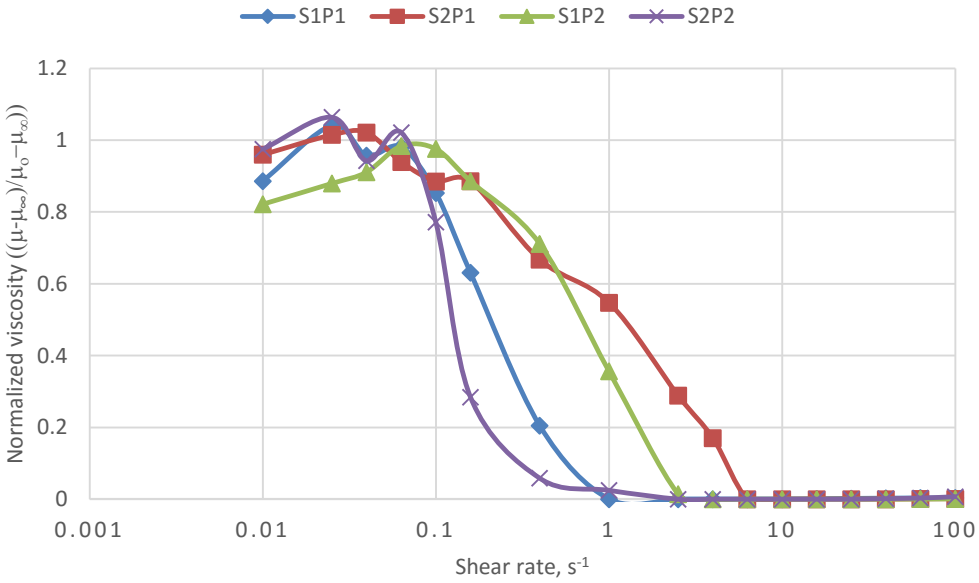

Figure 33: Normalized viscosity against the shear rate for the effect of chemicals

4.2 Contact angle

The contact angle measurements have performed in two different types of rocks for two different aging time; the first one is an outcrop rock containing pure calcite aged for one week, and the second one is an Indiana limestone rock aged for two weeks, and in which the core-flooding experiments have been performed in this research. Both of the rocks supposed to be oil-wet so the effect of aging can be investigated here as well.

4.2.1 Outcrop rock

This set of experiments was done to study the effect of the four different chemical formulation on the wettability in comparison to the sea water wettability without chemicals for one week aging time. The contact angle stabilized at 129o which means the rock is water wet as in Figure 34 (e).

The first chemical combination consists of S1; SS-880 Carboxybetaine (0.05%), and P1; ATBS/ AM copolymer (0.25%). The Solution density at 90oC is 1.00675 g/cc. Its contact angle stabilized at 52 as shown in Figure 34 (e). While S2P1 consists of SS-885 and ATBS/AM and has a density of 1.01167 g/cc at 90oC is. The measured contact angle is 34o through the oil phase indicating an oil-wet rock more than S1P1 as shown in Figure 34 (a) & (b) respectively. On the other hand, both of the forthcoming solutions consists of TVP, the former one containing the amphoteric surfactant SS-880 Carboxybetaine (0.05%) had a solution density of 1.00949 g/cc at 90oC and has a contact angle of 38o as plotted in Figure 34 (c). But the latter one containing the amphoteric surfactant SS-885 exhibited contact angle of 70o indicating a water wet rock Figure 34 (d).

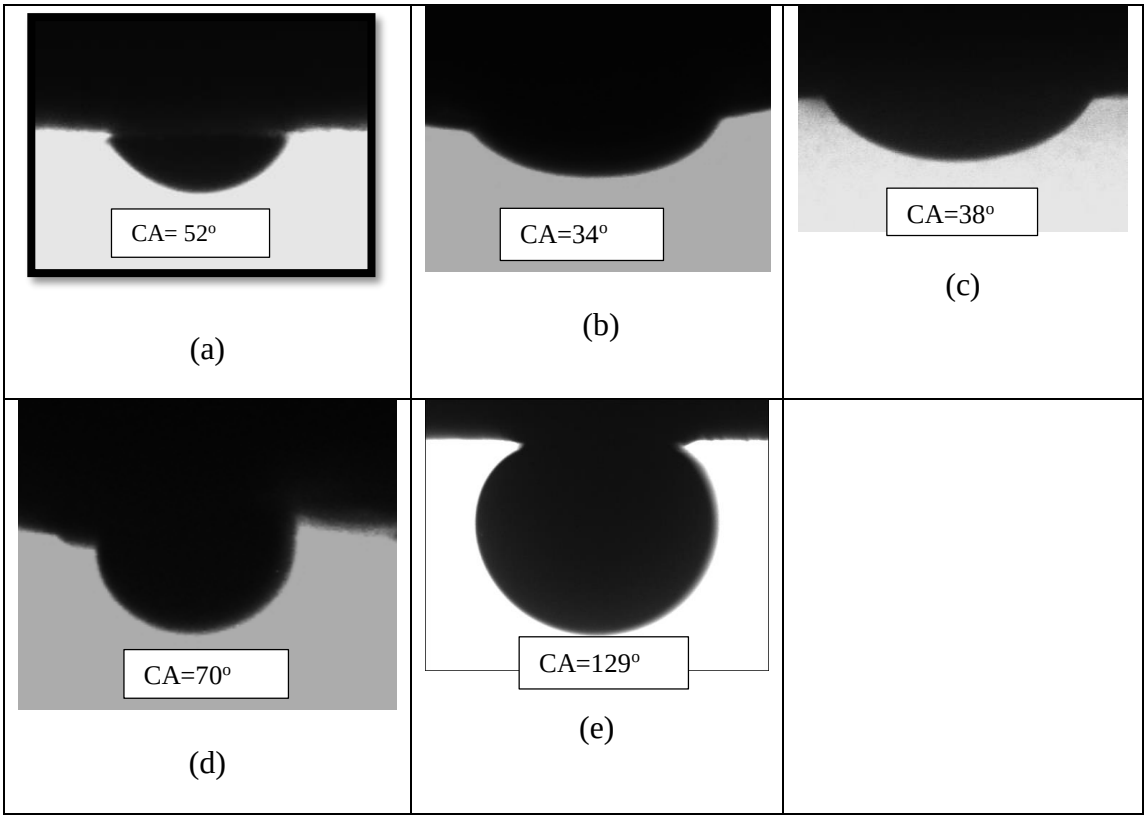

Figure 34: Contact angles for calcite outcrop (a) S1P1, (b) S2P1, (c) S1P2, (d) S2P2, (e) SW

4.2.2 Indiana limestone discs

This set of experiments is to study the effect of the four different chemicals on the wettability at Indiana limestone rock taking the sea water contact angle as a benchmark. The sea water density at 90oC was 1.00738 g/cc, the contact angle stabilized at 4o indicating original oil-wet rock as shown in Figure 35 (e). Comparing this result to the previous rock with seawater we can say that 1 week is not enough to restore the native state wettability on the disc samples. The first chemical combination consists of S1; Amphoteric surfactant SS-880 Carboxybetaine (0.05%) and P1; Acrylamido tertiary butyl sulfonate (ATBS)/acrylamide (AM) copolymer. (0.25%) The Solution density at 90oC is 1.00675 g/cc. The contact angle for S1P1 spread to the rock surface after 50 seconds showing strongly oil-wet rock as shown in Figure 35 (a). while the contact angle for second chemical combination stabilized at 12o for more than 500 seconds measured through the oil phase indicating a strongly oil-wet rock as in Figure 35 (b), this solution consists of S2; Amphoteric surfactant SS-885 Carboxybetaine. (0.05%) and P1; Acrylamido tertiary butyl sulfonate (ATBS)/acrylamide (AM) copolymer. (0.25%) and its density at 90oC was 1.01167 g/cc. Investigating the contact angle for TVP solutions with SS-880 and SS-885 Figure 35 (c)&(d) respectively resulted in extremely oil-wetness for S1; Amphoteric surfactant SS-880 Carboxybetaine (0.05%) and P2; Thermoviscosifying polymer (0.25%) with solution density at 90oC of 1.00949 g/cc. while the other solution consists of S2; Amphoteric surfactant SS-885 Carboxybetaine. (0.05%) and P2; Thermoviscosifying polymer. (0.25%) and has a density of 1.00949 g/cc, its contact angle stabilized at 22o for more than 1000 seconds measured through the wetting phase which is oil so it is strongly oil-wet.

Taking into account the benchmark contact angle of sea water as 4^{o} so the mixtures contain SS-885 in their recipe have the ability to alter the rock wettability toward water-wetness from 4^{o} to 12^{o} in combination with ATBS/AM and to 22^{o} when joining TVP. While the other surfactant recipes increased the oil-wetness to the maximum limit by forcing the oil droplet to spread to the rock surface.

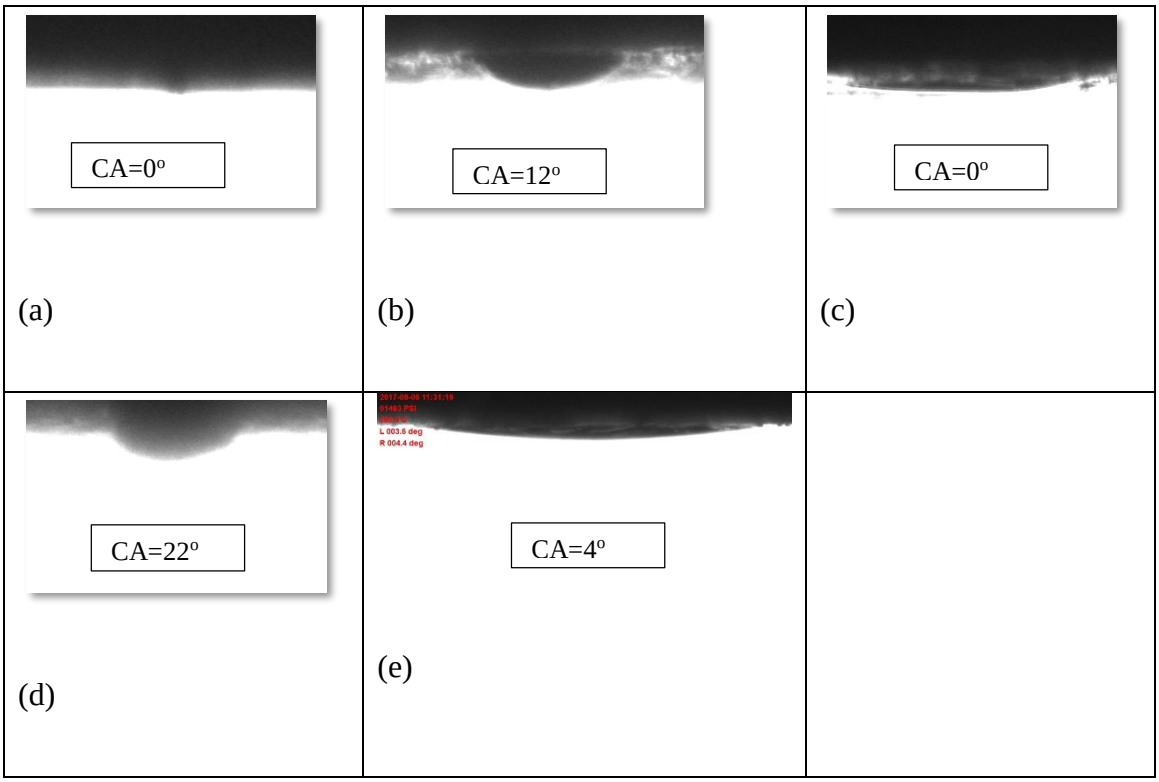

Figure 35: Contact angles for Indiana limestone (a) S1P1, (b) S2P1, (c) S1P2, (d) S2P2, (e) SW

4.3 Core-flooding results

Core-flooding experiments were done to evaluate the screened chemicals and investigate their ability to mobilize the residual oil held by capillary forces or that has been bypassed by water-flooding through fingering. Furthermore, optimize the chemical combination among the four combination as well as the slug size and sequence.

4.3.1 The effect of chemicals

Table 8 contains the detailed summary for this set of experiments.

The core-flooding experiment for S1P1 gives oil recovery of 62.8% out of the Oil Initially In Place (OIIP) by water-flooding. Chemical flooding recovered 31.29% of the Residual Oil Saturation (ROS) which represents 11.63% of the OIIP. The pressure drop stabilized after 5 PV of sea water injection because no more oil is produced and then increased dramatically when the SP injection starts due to the high polymer viscosity.

The core-flooding experiment for S2P1 showed an oil recovery of 57.7% of the (OIIP) by injecting 7 Pore Volumes (PV) of sea water. A 2.7 PV slug of S2P1 was later injected and extracted 14.87% of (ROS) which represents 6.285% of the OIIP. No more oil was produced after 4 PV of sea water injection. Water injection continued up to 7 PV to insure consistency with other core-floods.

Furthermore, the core-flooding experiment for S1P2 recovered 80.3% of the (OIIP) by injecting 7 Pore Volumes (PV) of sea water. This is an extremely high recovery for water-flooding. Nevertheless, Buckley et al. 1996 reported such a high value of water-flooding recovery although the aging in their case was two weeks [47]. A 2.7 PV slug of S1P2 was later injected and extracted 33.41% of (ROS) which represents 6.574% of the OIIP.

Finally, the core-flooding experiment for S2P2 showed an oil recovery of 58.17% of the (OIIP) by injecting 7 Pore Volumes (PV) of sea water. A 2.7 PV slug of S2P2 slug was later injected and successfully extracted 9.07% of (ROS) which represents 3.794% of the OIIP. The pressure drop stabilization indicates negligible oil production at this stage. The pressure drop increases with SP injection due to the high polymer viscosity and after the polymer breakthrough it declines again.

The combination S1P1 showed the most promising incremental recovery out of OIIP as it can be seen in Figure 36 and can be considered as the optimum combination above the other three.

Table 8: Summary of the effect of chemicals core-flooding experiments

Core-flood	S1P1	S2P1	S1P2	S2P2
Polymer concentration (% wt.)	0.25	0.25	0.25	0.25
Surfactant concentration (% wt.)	0.05	0.05	0.05	0.05
Length (inches)	11.46	11.49	11.42	11.5
Porosity	0.167	0.18	0.17	0.158
Oil permeability (md)	98.14	98	179	39
Pore volume (cc)	55.018	64.4	56.19	52.29
Swi	0.31	0.3	0.296	0.294
Initial oil volume (cc)	37.83	45.03	39.55	36.9
Residual oil after water-flooding (cc)	14.06	20.26	7.782	15.432
Recovery % of OIIP after water-flooding	62.80%	55.00%	80.30%	58.17%
Recovery % of OIIP by chemical flooding	11.63%	6.29%	6.57%	3.79%
Recovery % of ROS by chemical flooding	31.29%	13.96%	33.41%	9.07%

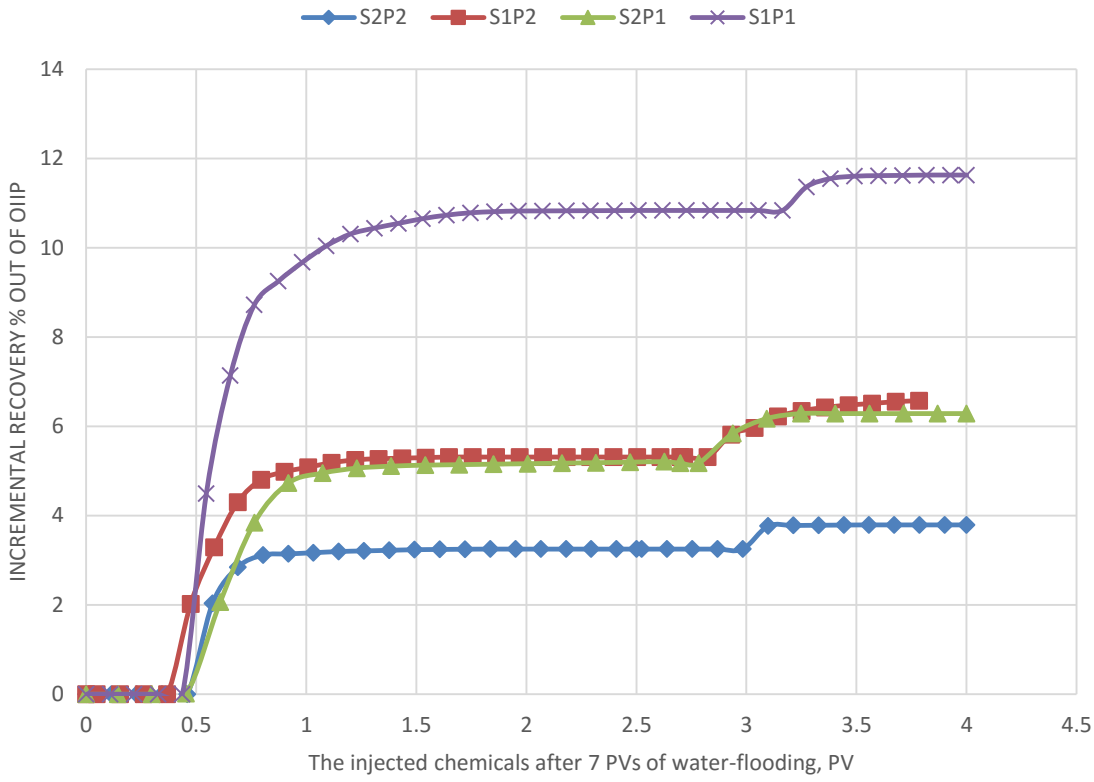

Figure 36: The effect of chemicals Incremental recovery out of OIIP

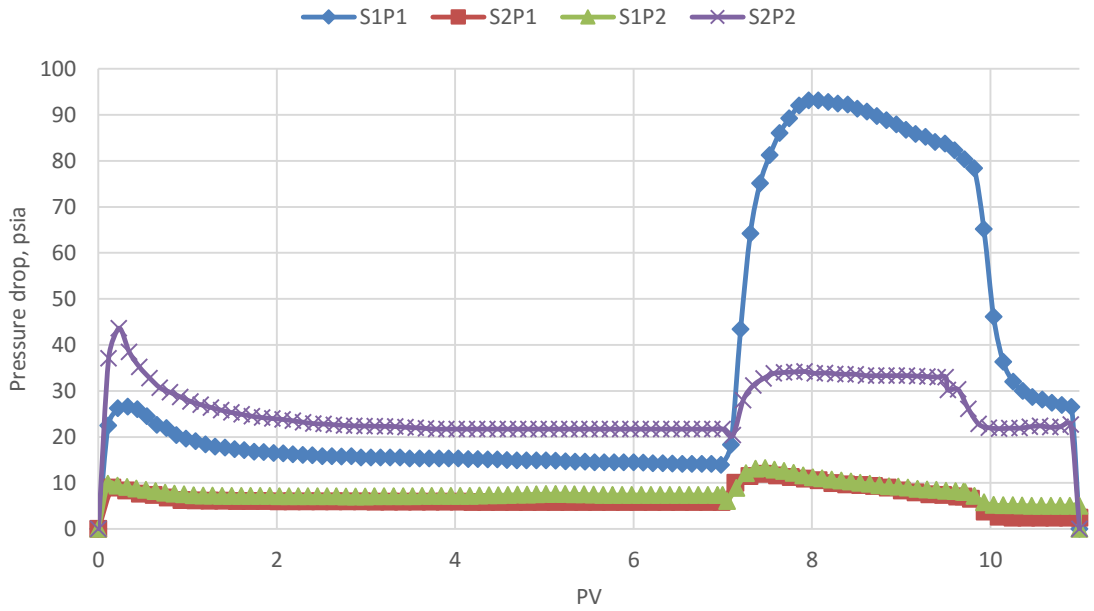

Figure 37: The effect of chemicals pressure drop

4.3.2 The effect of slug size

Three different sizes were tested to know the lowest possible sizes that gives economic recovery. The sizes start with 1.7 PV then 2.7 PV finally 3.5 PV. The SP slug to be injected was selected from the previous set. At the effect of chemical experiments the optimum one was S1P1 based on the incremental recovery obtained by the chemical injection as shown in Figure 36. The full summary of this set is elaborated in Table 9

Starting with 1.7 PV slug size core-flooding experiment, the SP slug was injected after the pre-water-flooding then followed by the post-water-flooding. The recovery profile for S1P1 flooding shows no oil has produced after 5 PV of sea water injection. The oil recovery was 56.76% of the Oil Initial In Place (OIIP) by sea water. Then 1.7 PV of S1P1 slug was injected and successfully extracted 26.24% of the Residual Oil Saturation (ROS) which represent 11.34% of the OIIP. The next size was 2.7 PV, the SP slug injected between two injections of water-flooding pre-water-flooding and post-water-flooding. Recovery profile for S1P1 flooding shows oil recovery of 62.8% of the Oil Initial In Place (OIIP) by pre water-flooding. The chemical flooding successfully extracted 31.29% of the Residual Oil Saturation (ROS) which represent 11.63% of the OIIP. The last experiment of this set was 3.5 PV slug size, the water-flooding Recovered 50.16% of the Oil Initial In Place (OIIP) by injecting 5 Pore Volumes (PV) of sea water. The chemical slug extracted 34.21% of the Residual Oil Saturation (ROS) which represent 17.05% of the OIIP.

It can be clearly seen that different plugs give different recoveries even with the same slug size. Therefore, we can make our finding from the general trend of the largest size at which the incremental recovery stabilized at 3 PV. SO the optimum slug size is 3 PV of S1P1 as explained in Figure 38.

Table 9: Summary of the effect of slug size core-flooding experiments.

Core-flood	1.7 PV S1P1	2.7 PV S1P1	3.5 PV S1P1
Polymer concentration (% wt.)	0.25	0.25	0.25
Surfactant concentration (% wt.)	0.05	0.05	0.05
Length	11.46	11.46	11.46
Porosity	0.13	0.167	0.137
Oil permeability (md)	49.5	98.14	0.7
Pore volume (cc)	43.51	55.018	44.72
Swi	0.33	0.31	0.32
Initial oil volume (cc)	29	37.83	30.5
Residual oil after water-flooding (cc)	12.54	14.06	15.2
Recovery % of OIIP after water-flooding	56.76%	62.80%	50.16%
Recovery % of OIIP by chemical flooding	11.34%	11.63%	17.05%
Recovery % of ROS by chemical flooding	26.24%	31.29%	34.21%

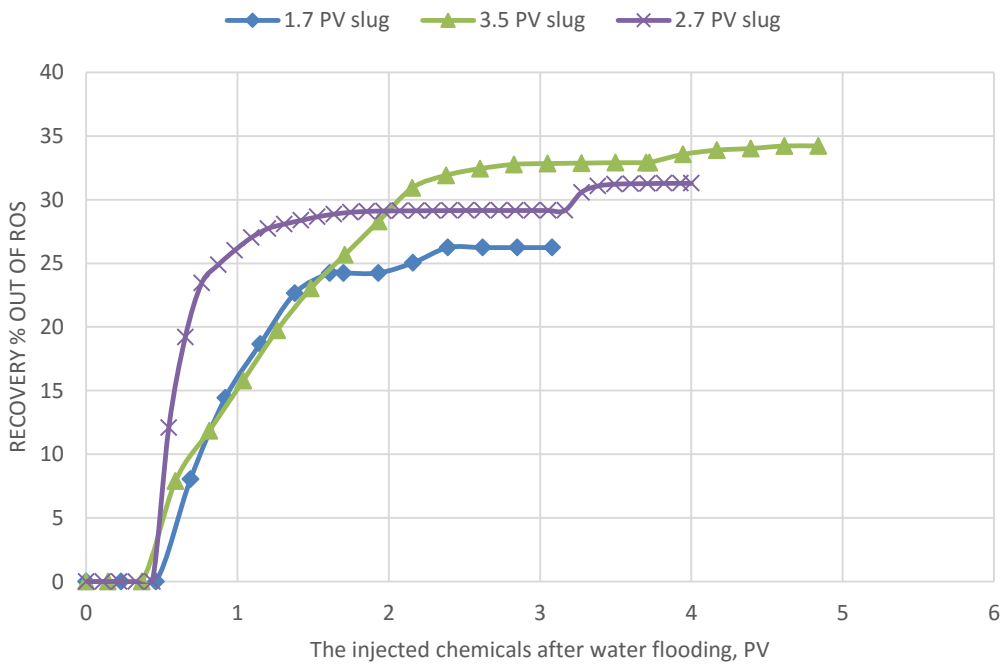

Figure 38: The effect of slug size (ROS).

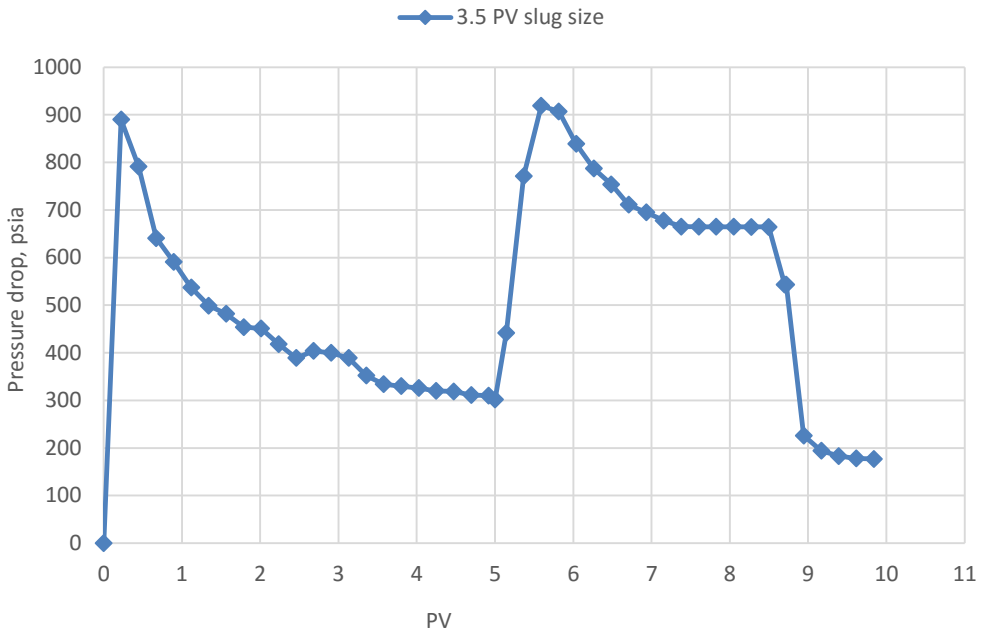

Figure 39: The effect of slug size Pressure drop

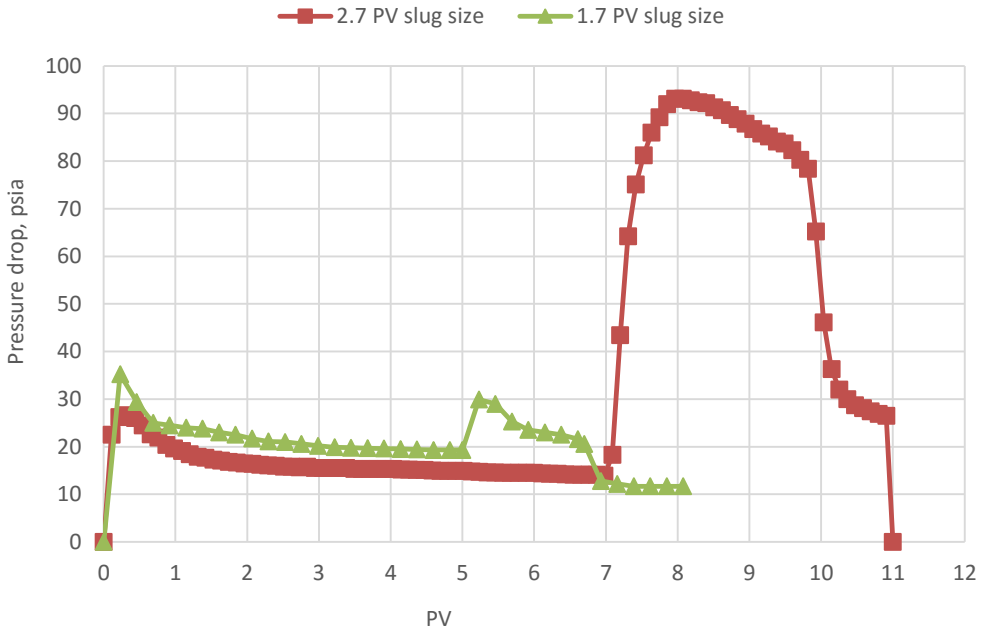

Figure 40: The effect of slug size Pressure drop

4.3.3 The effect of injection sequence

Four sequences were tested to observe which one is optimum from a recovery point of view. The recovery percent of the residual oil is considered to be the defining factor. The sequences are SW – SP – SW, SW – P – S – SW, SW – S – SW – P – SW and SW – P – SW – S – SW. The SP slug to be injected was S1P1 as previously set. The summary of the whole set will be depicted in Table 10.

The Core-flooding experiment for SW – SP – SW sequence shows oil recovery of 63.28% of the Oil Initial In Place (OIIP) by injecting 7 Pore Volumes (PV) of sea water. Then 2.7 PV of S1P1 slug was injected and successfully extracted 31.29% of the Residual Oil Saturation (ROS) which represent 11.63% of the OIIP. While SW – P – S – SW sequence depicts oil recovery of 55.7% of the Oil Initial In Place (OIIP) by injecting 5 Pore Volumes (PV) of sea water. After that 1.5 PV of P1 slug was injected followed by 1.5 PV of S1 slug then SW and extracted 17.26% of the Residual Oil Saturation (ROS) which represent 7.63% of the OIIP.

Investigating SW – S – SW – P – SW sequence shows water-flooding recovery of 52.78% of the Oil Initial In Place (OIIP) by injecting 5 Pore Volumes (PV) of sea water, a similar recovery from water-flooding was reported by[48], then 1.5 PV of S1 slug then SW then 1.5 PV of P1 slug was injected followed by SW and extracted 12.08% of the Residual Oil Saturation (ROS) which represent 5.702% of the OIIP. In the end, the analysis of the Recovery profile for SW – P – SW – S – SW sequence shows oil recovery of 52.11% of the Oil Initial In Place (OIIP) by injecting 5 Pore Volumes (PV) of sea water, then 1.5 PV of P1 slug then SW then 1.5 PV of S1 slug was injected followed by SW and extracted 25.52% of the Residual Oil Saturation (ROS) which represent 12.24% of the OIIP, it is

noted that recovery from polymer flooding is high around 9% of OIIP, [20] reported such high recovery from polymer flooding it reached 15% of OOIP.

Based on the results elaborated in Figure 41 we can obviously notice that the sequence of SW – S1P1 – SW showed the highest ROS recovery. That because it is showing synergistic effect that each one individually cannot do it and that what make SP flooding is the best. This result matched to some extent the result reported by [41] which showed the SW-SP sequence gives better recovery than SW-S-P sequence and polymer augmented surfactant soaking. Also we can notice that the recovery achieved by polymer is much more than that achieved by surfactant which match the findings of [29] that the surfactant alone doesn't increase the recovery unless there is a controlling agent for mobility.

Table 10: Summary of the effect of injection sequence core-flooding experiments

Core-flood	SW-P1-S1-SW	SW-S1P1-SW	SW-S1-SW-P1-SW	SW-P1-SW-S1-SW
Polymer conc (% wt.)	0.25	0.25	0.25	0.25
Surfactant conc (% wt.)	0.05	0.05	0.05	0.05
Length	11.44	11.46	11.38	11.45
Porosity	0.164	0.167	0.168	0.13
Oil permeability (md)	82.57	98.14	52	18.44
Pore volume (cc)	54.014	55.018	55.01	43.48
Swi	0.31	0.31	0.31	0.3
Initial oil volume (cc)	38.125	37.83	37.83	30.3
Residual oil after water-flooding (cc)	17.185	14.06	18.187	14.51
Recovery % of OIIP after water-flooding	54.92%	62.80%	51.92%	52.11%
Recovery % of OIIP by chemical flooding	7.63%	11.63%	5.70%	12.24%
Recovery % of ROS by chemical flooding	16.93%	31.29%	11.86%	25.57%

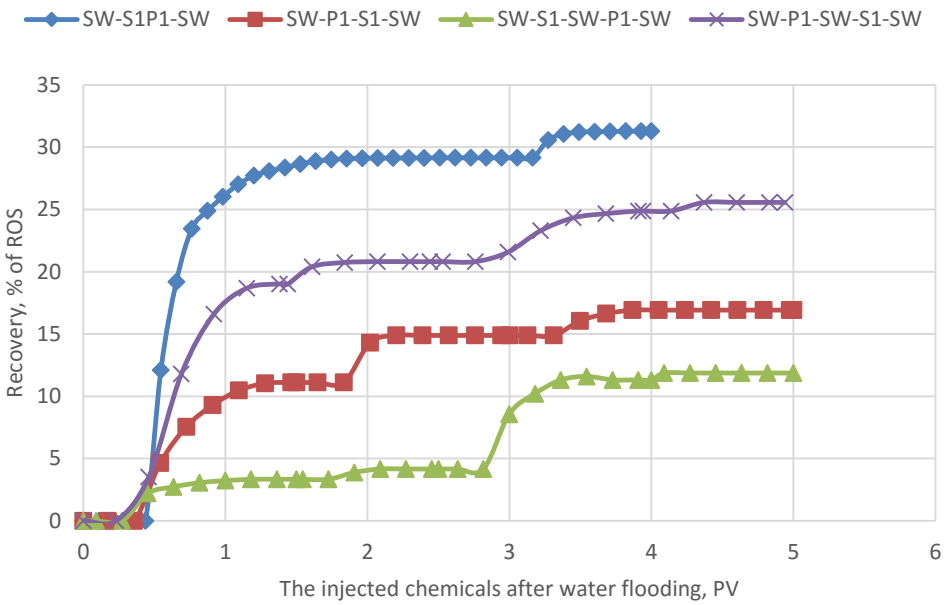

Figure 41: The effect of sequence (ROS)

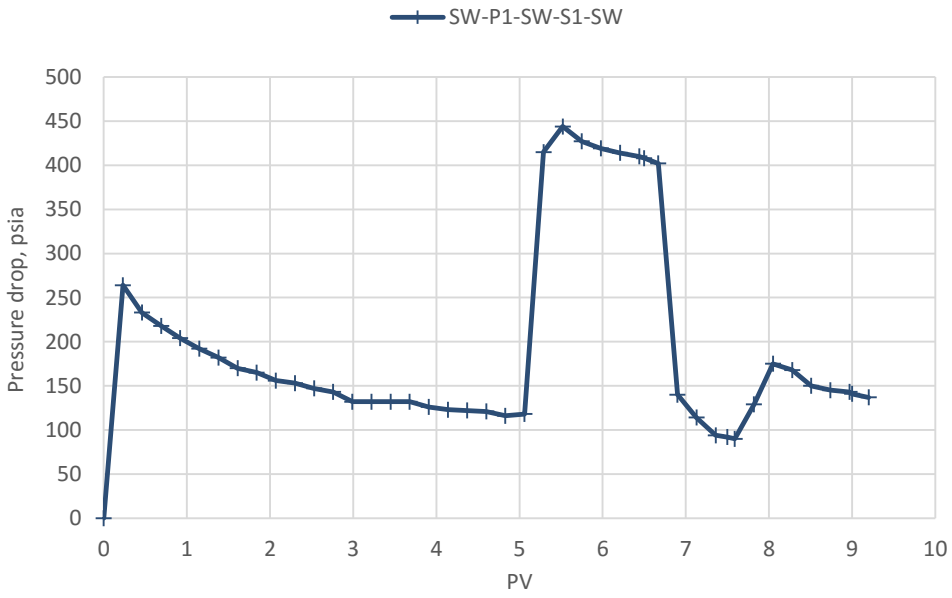

Figure 42: The effect of sequence Pressure drop

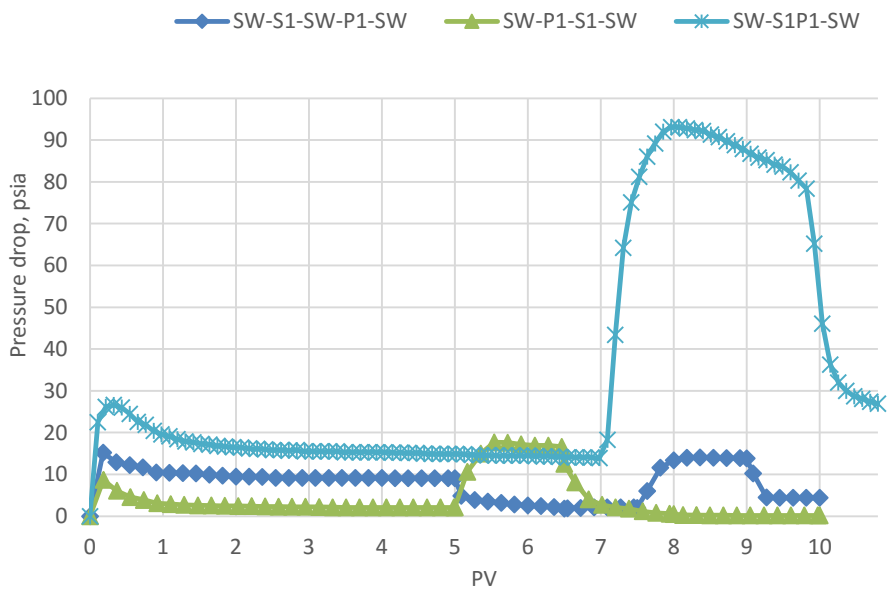

Figure 43: The effect of sequence Pressure drop

4.4 Effluent analysis

In this section we will discuss the IC results for two sets of core-flooding experiments; the effect of slug size set and the effect of chemical sequence set. This work is made in an attempt to understand the ions retention and the dissolution of the calcite as a result of mechanical erosion.

4.4.1 IC for slug size experiments (DF-1), and (DF-3)

The Calcium concentration started very high because of the formation water then decreased to a bit higher level than the original because of the dissolution from the rock surface as in Figure 44. However, in Figure 46 it diluted then stabilized at the original value at the end of SP injection.

The early injection time dilution of formation water was observed also for the rest of the ions except for the sulfate which has lower concentration in the formation water than sea water. There is an obvious retention for magnesium and sodium ions when the SP injection starts in (DF-1) as in Figure 45. While in (DF-3) the retention appeared after injecting 1 PV of SP Figure 47. The sulfate and chloride ion showed more significant retention than magnesium and sodium in both experiments.

4.4.2 IC for injection sequence experiments (CF-8), (CF-9), and (DF-4)

In (CF-8) sulfate and chloride retention is higher than that of sodium and magnesium ions as depicted in Figure 49. Meanwhile, In (CF-9) only sulfate retention was observed while the other ion were around the original injection value as plotted in Figure 51. Investigating (DF-4) we note that sulfate and chloride exhibited significant retention in comparison to the other ions as shown on Figure 53.

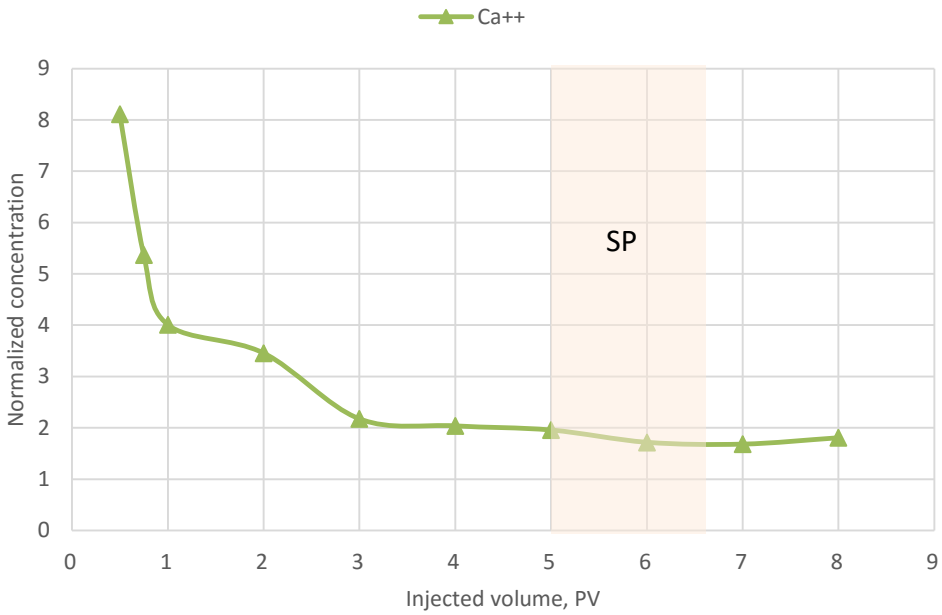

Figure 44: Concentration of calcium ions for 1.7 PV slug experiment (DF-1) normalized against the injected SW

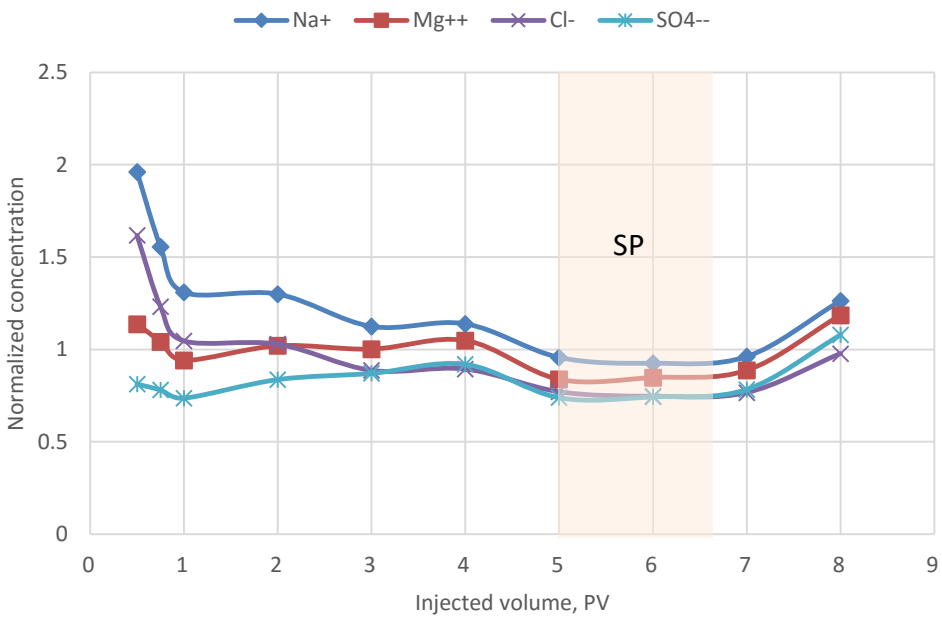

Figure 45: Concentrations of ions for 1.7 PV slug experiment (DF-1) normalized against the injected SW

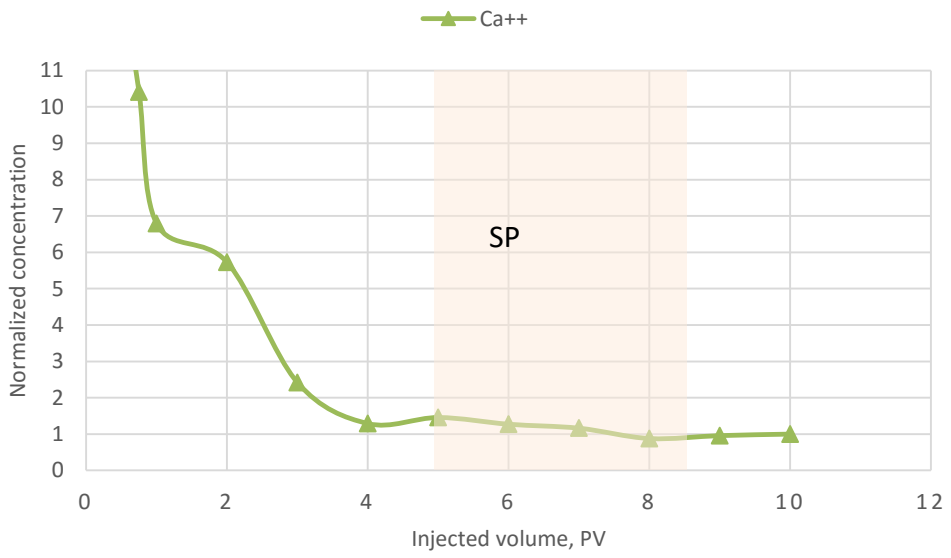

Figure 46: Concentration of calcium ion for 3.5 PV slug experiment (DF-3) normalized against the injected SW

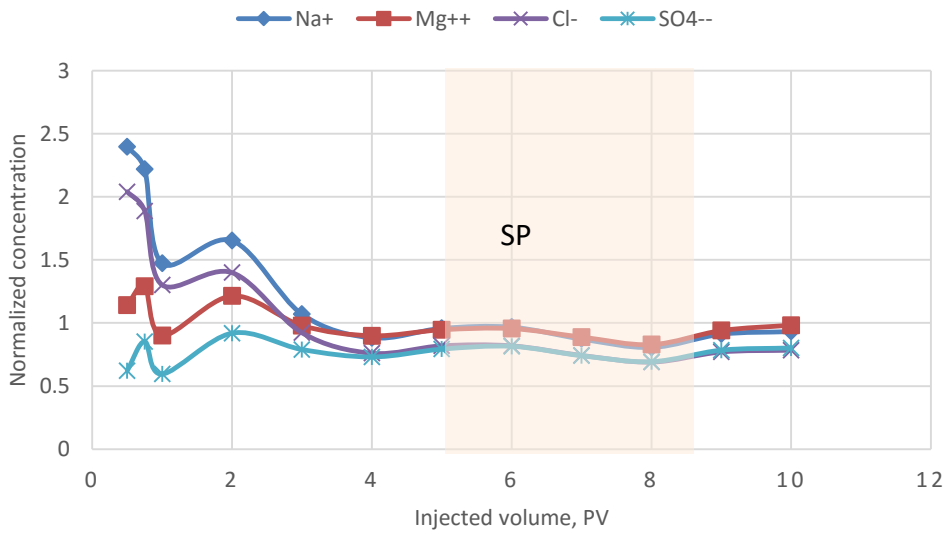

Figure 47: Concentrations of Ions for 3.5 PV slug experiment (DF-3) normalized against the injected SW

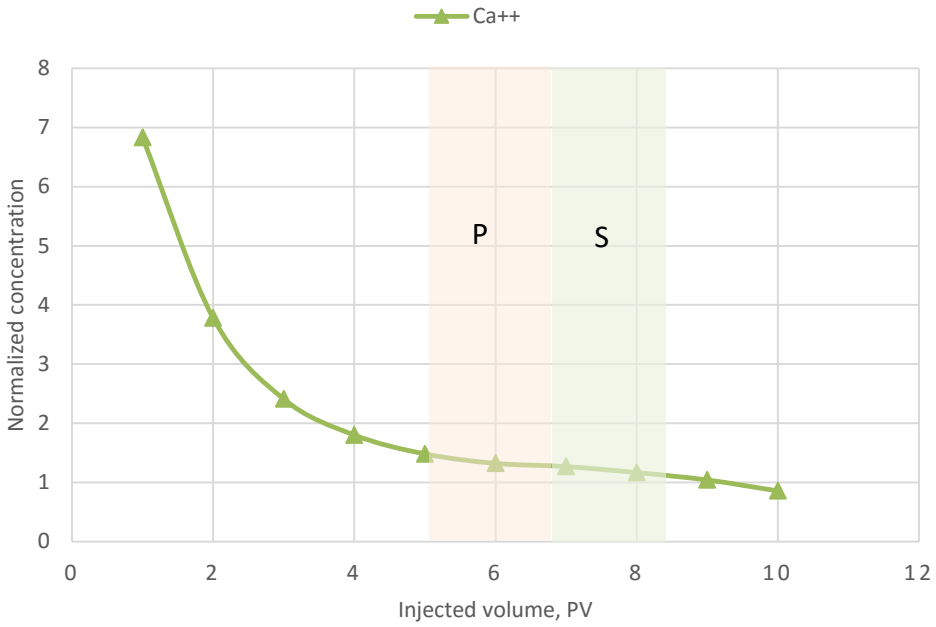

Figure 48: Concentration of calcium ion for SW-P-S-SW sequence experiment (CF-8) normalized against the injected SW

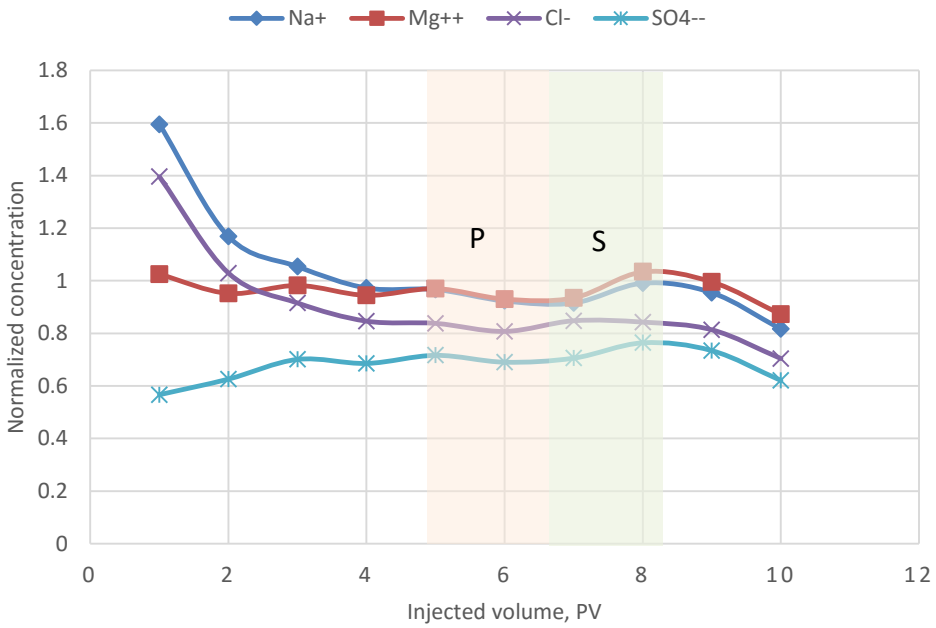

Figure 49: Concentrations of Ions for SW-P-S-SW sequence experiment (CF-8) normalized against the injected SW

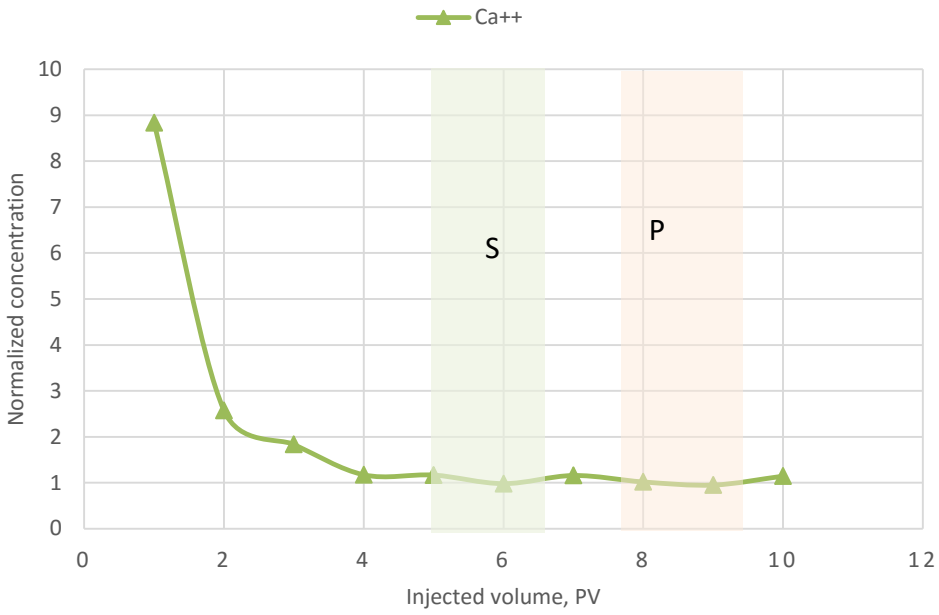

Figure 50: Concentration of calcium Ion for SW-S-SW-P-SW sequence experiment (CF-9) normalized against the injected SW

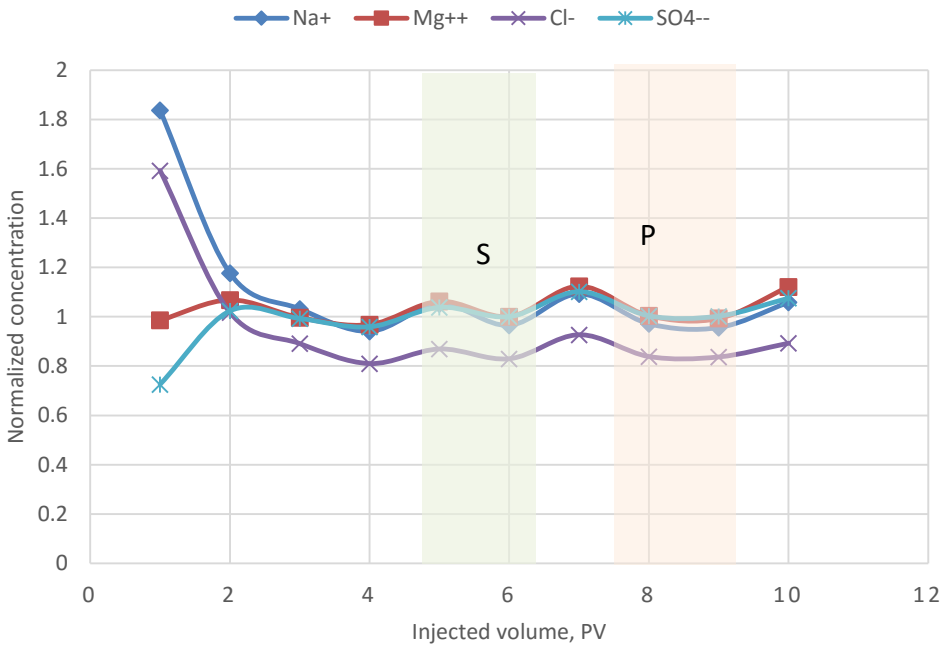

Figure 51: Concentrations of Ions for SW-S-SW-P-SW sequence experiment (CF-9) normalized against the injected SW

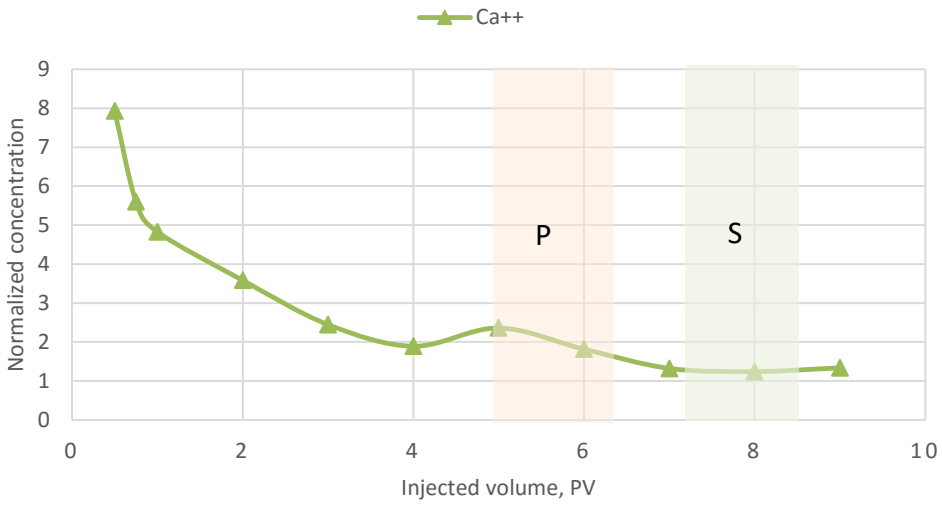

Figure 52: Concentration of calcium ion for SW-P-SW-S-SW sequence experiment (DF-4) normalized against the injected SW

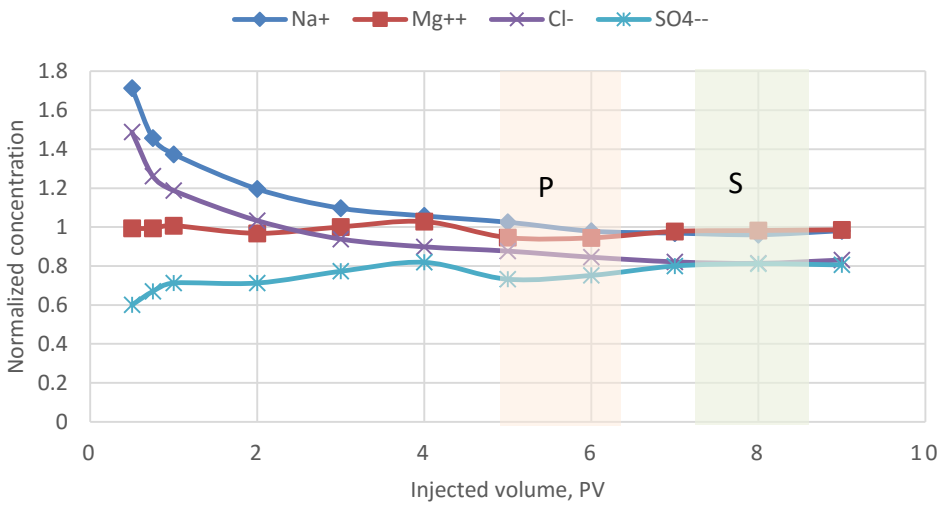

Figure 53: Concentrations of ions for SW-P-SW-S-SW sequence experiment (DF-4) normalized against the injected SW

4.5 Pore-scale imaging

At this part of the research we are going to look deep inside the rock pore space to investigate the fluid movement and the way it interacts with the surrounding rock to grasp the mechanism of recovery. Also we can know if there is any rock dissolution or pore blockage as a result of precipitation.

4.5.1 Analysis for SW-SP-SW experiment (CF3-1)

Figure 54 Illustrates a snap shot taken from the fluid map generated by PerGeos software. The two images depict a specific pore space before and after a core-flooding injection that contains pre and post water-flooding surrounding an SP flooding in the middle. The one in the left side shows the initial state of the saturated core while the final state after the chemical flooding process appears in the right side. It can be noted that, the original wettability was either extremely water wet or moderate water-wet which make the recovery mechanism mainly based on the polymer displacement. While the surfactant effect is minor in the big pores and can help in the small pores to overcome the capillary forces. The oil saturation plotted in Figure 56 showing an average initial oil saturation of 0.6065 in this segmented section in the other hand the final saturation was 0.156 in average. The remaining oil mainly has been bypassed by the injection fluids. We can note also some dissolution has happened to rock resulting in pore enlargement in some places.

4.5.2 Analysis for SW-SP-SW experiment (CF4-1)

The images shown in Figure 58 are made to investigate the recovery mechanism of SP flooding contains TVP and SS-885. Two images were taken from the fluid occupancy map at the exact place before and after the core-flooding to see the fluid movement inside the pore space.

The initial average oil saturation at the select sub volume is 0.71. By looking at the edges between the oil and water at the right image of Figure 58 it can be seen that the wettability was initially strongly to moderate water-wet. The final average oil saturation was 0.1 as shown in Figure 59.

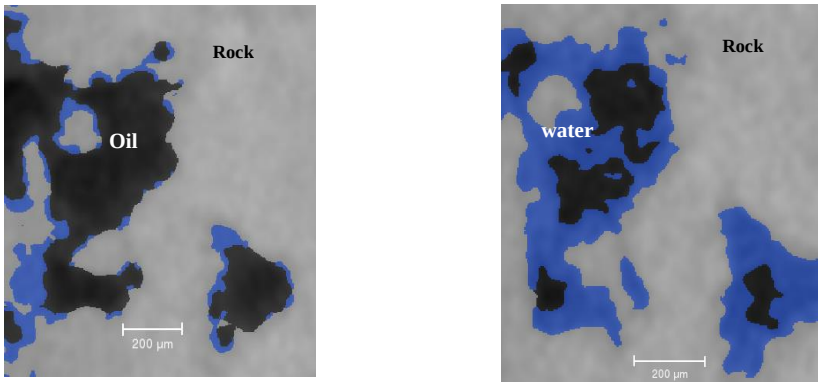

Figure 54: Fluid occupancy before and after flooding, left: before flooding, right: after flooding, gray: rock, Black: oil, Blue: water (CF3-1)

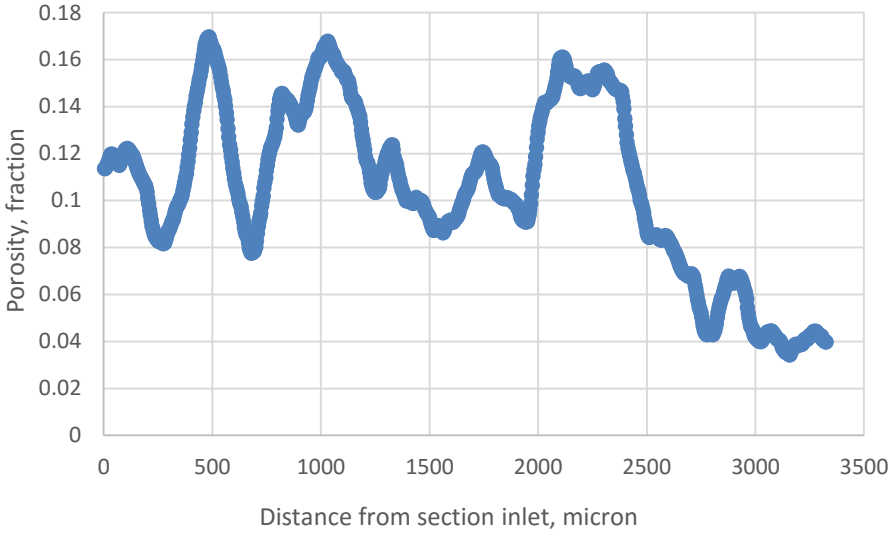

Figure 55: Connected porosity distribution for the selected sub volume (CF3-1)

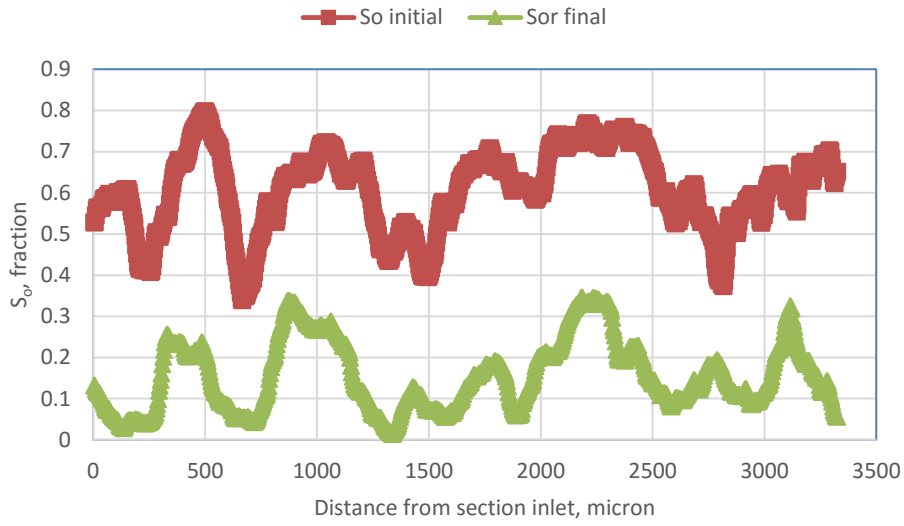

Figure 56: Initial and final oil saturation at the selected sub volume (CF3-1)

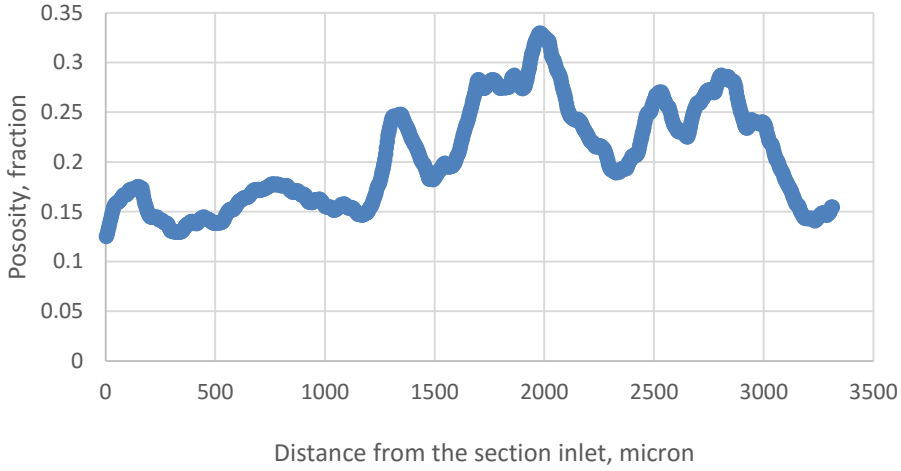

Figure 57: Connected porosity distribution for the selected sub volume (CF4-1).

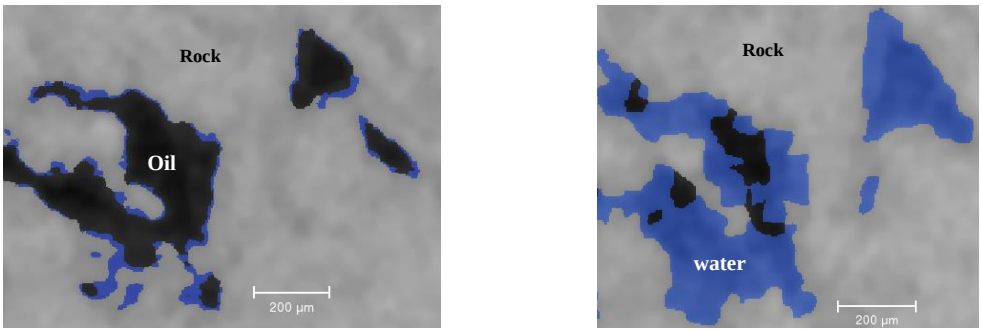

Figure 58: Fluid occupancy before and after flooding, left: before flooding, right: after flooding, gray: rock, Black: oil, Blue: water (CF4-1)

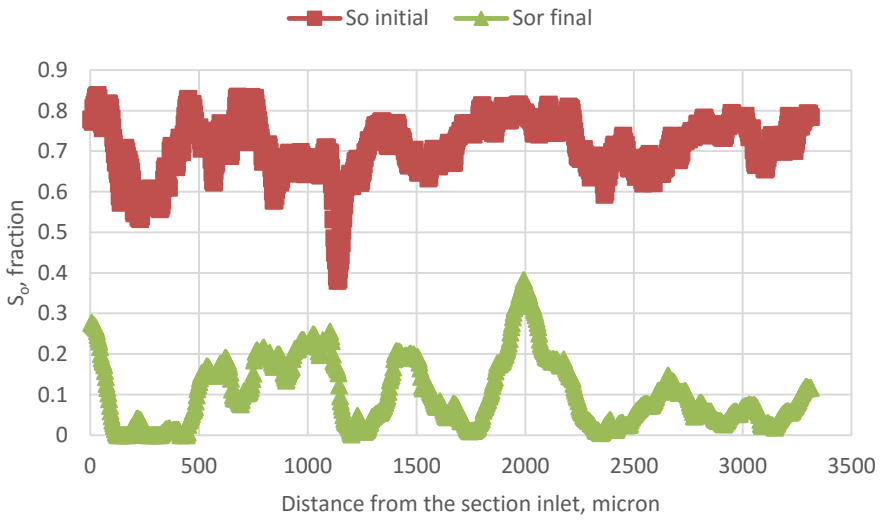

Figure 59: Initial and final oil saturation at the selected sub volume (CF4-1)

4.5.3 Analysis for SW-S1-SW experiment (DF5-1)

This time we avoided the mistakes committed at the previous experiment by scanning each step; before the water-flooding, after the water-flooding and after the chemical flooding. The chemical used in this set is only SS-880 surfactant to understand the individual effect of the surfactant flooding. Although the aging was done for this sample for 2 weeks, it seems also water-wet which means that 2 weeks are not enough to restore native state wettability. The recovery achieved by pre water-flooding translated in the image shown in Figure 60. It is obvious that the produced oil was basically by imbibition process and the oil left was due to the water breakthrough and fingering. In the other side, the images before and after chemical flooding are shown in Figure 63. All the oil left was in the middle of the pore so the recovery mechanism happened because of the micro emulsion viscosity resulted from the interaction between the surfactant and the oil at the leading fluid bank. This micro emulsion can act somehow as mobility controlling agent and give better sweep efficiency to the remaining left behind oil.

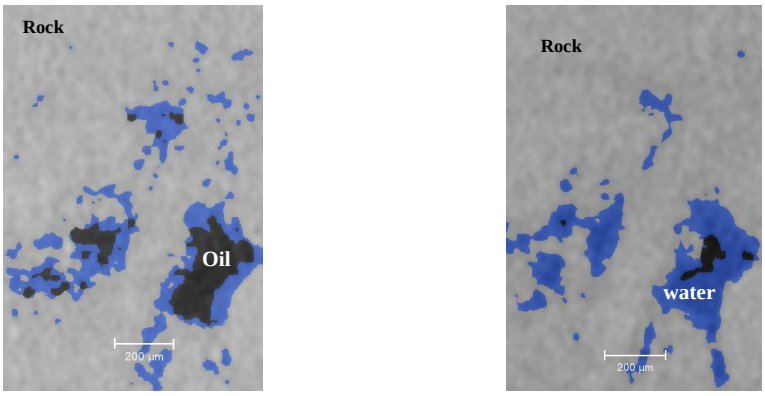

Figure 60: Fluid occupancy before and after water-flooding, left: before water-flooding, right: after water-flooding, gray: rock, Black: oil, Blue: water (DF5-1)

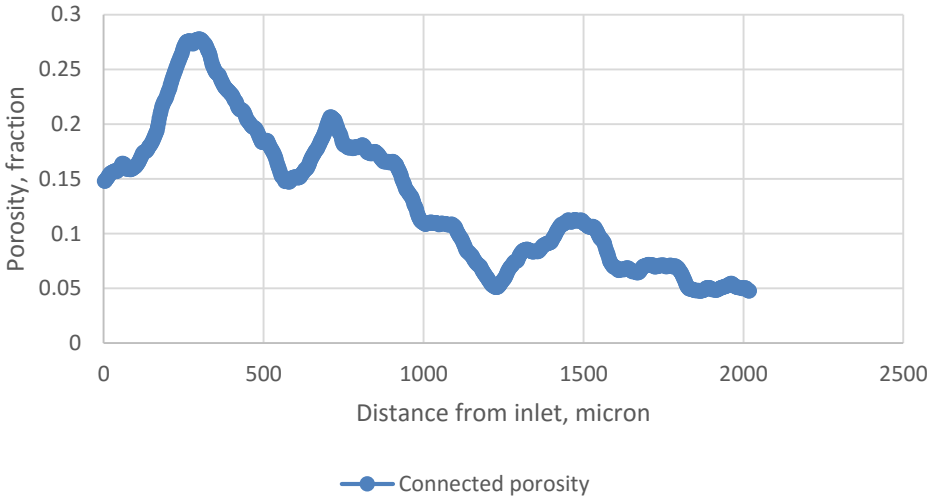

Figure 61: Connected porosity distribution for the selected sub volume for water-flooding (DF5-1)

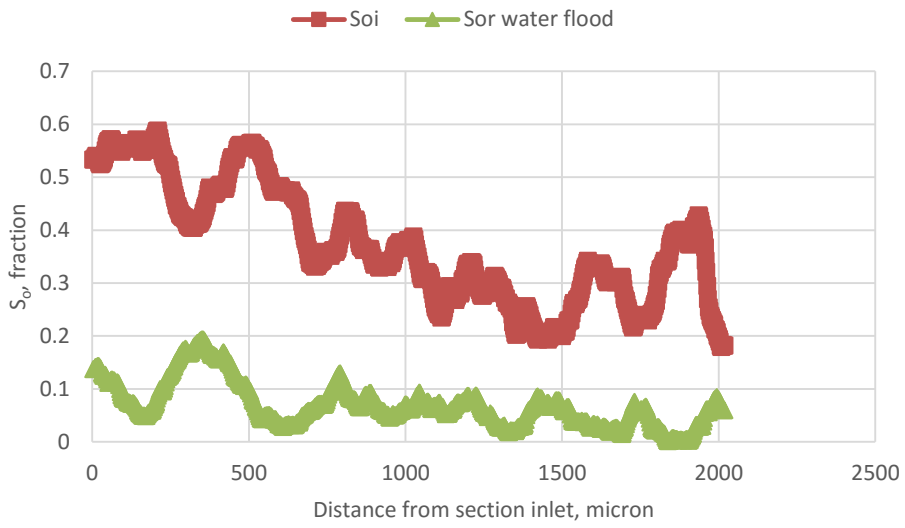

Figure 62: Oil saturation before and after water-flooding at the selected sub volume (DF5-1)

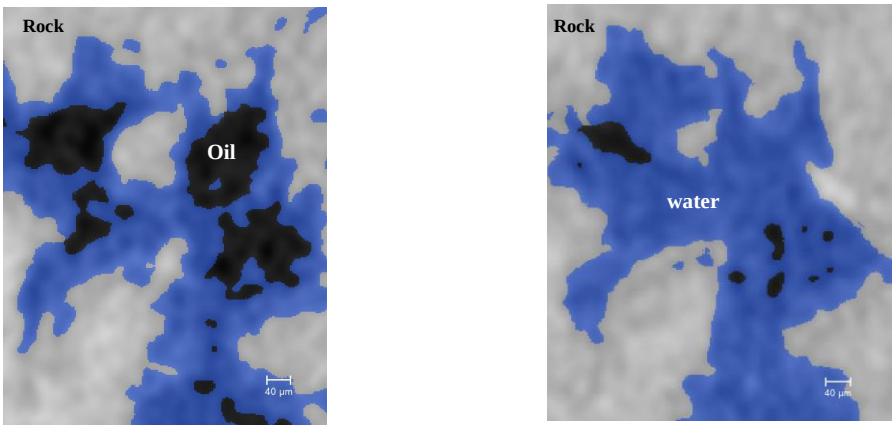

Figure 63: Fluid occupancy before and after surfactant flooding, left: before flooding, right: after flooding, gray: rock, Black: oil, Blue: water (DF5-1)

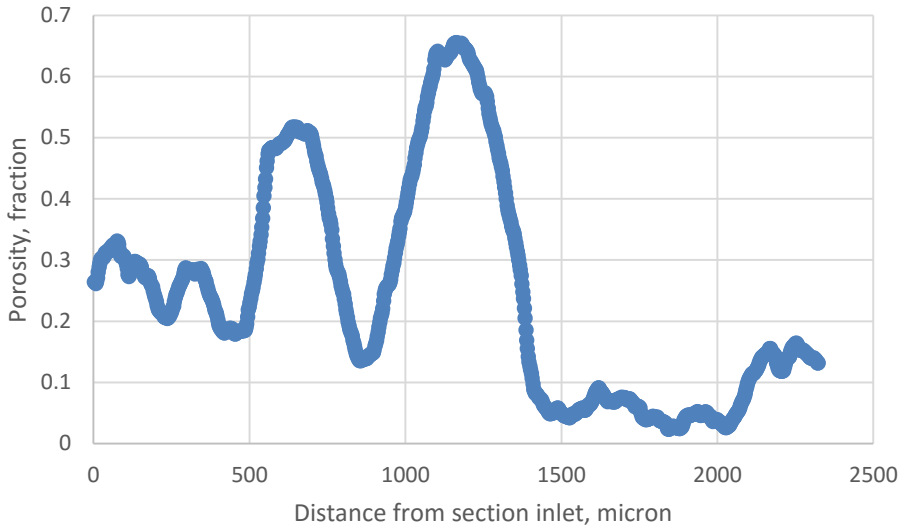

Figure 64: Connected porosity distribution for the selected sub volume for surfactant flooding (DF5-1)

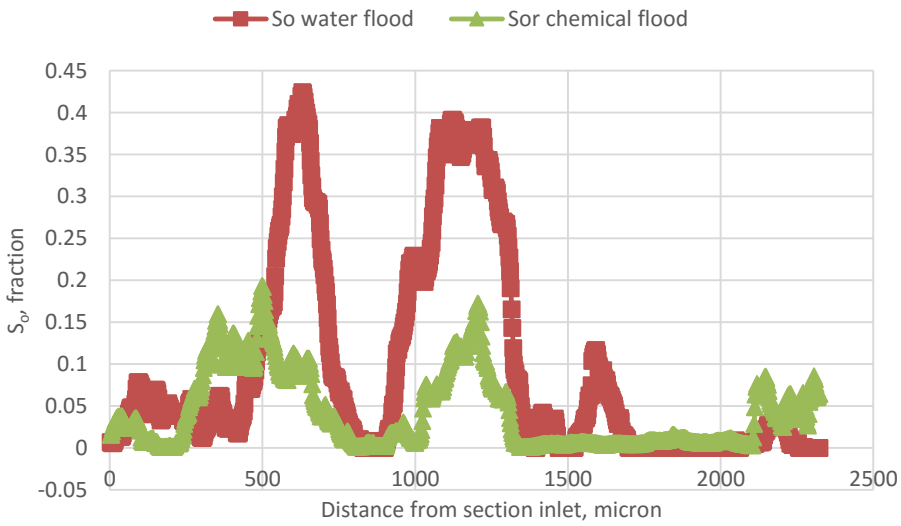

Figure 65: Oil saturation before and after Surfactant flooding at the selected sub volume (DF5-1)

4.5.4 Analysis for SW-P-SW experiment (DF5-2)

In this experiment ATBS polymer was used as the individual chemical, and the images are showing the three steps for the particular pore space from the fluid occupancy map Figure 66. The first image in the left is the initial saturated 2 weeks aged plug, its wettability is slightly oil-wet based on this image. However, the seawater has displaced the oil adhered at the rock surface efficiently and altered the rock wettability to strongly water wet. The role pf polymer became easier since its preferred mechanism is to derive the bypassed oil by piston like displacement. The average value of initial saturation was 0.33 based on the information plotted on Figure 68, while the average saturation after water-flooding was 0.095 and after the chemical flooding was 0.024.

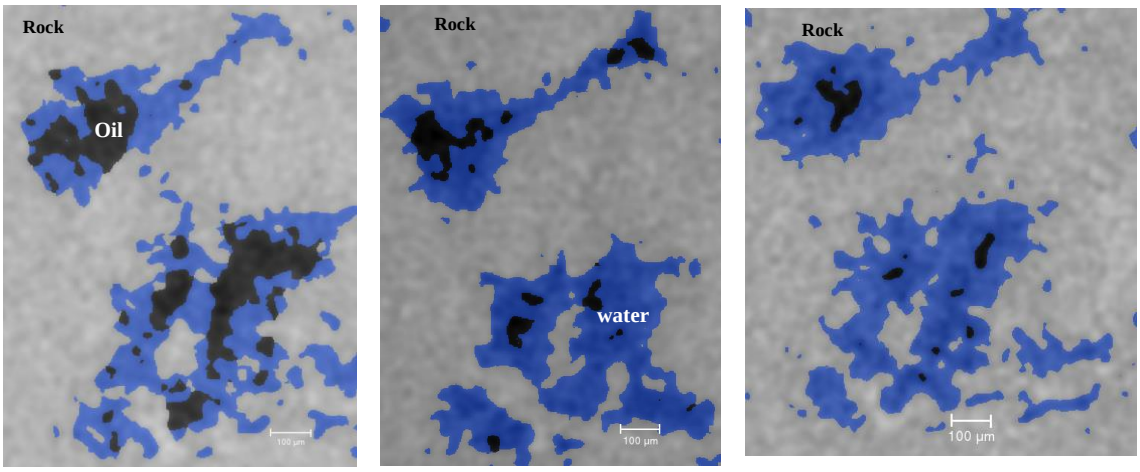

Figure 66: Fluid occupancy before and after surfactant flooding, left: before water-flooding, middle: after water-flooding right: after polymer flooding, gray: rock, Black: oil, Blue: water (DF5-2)

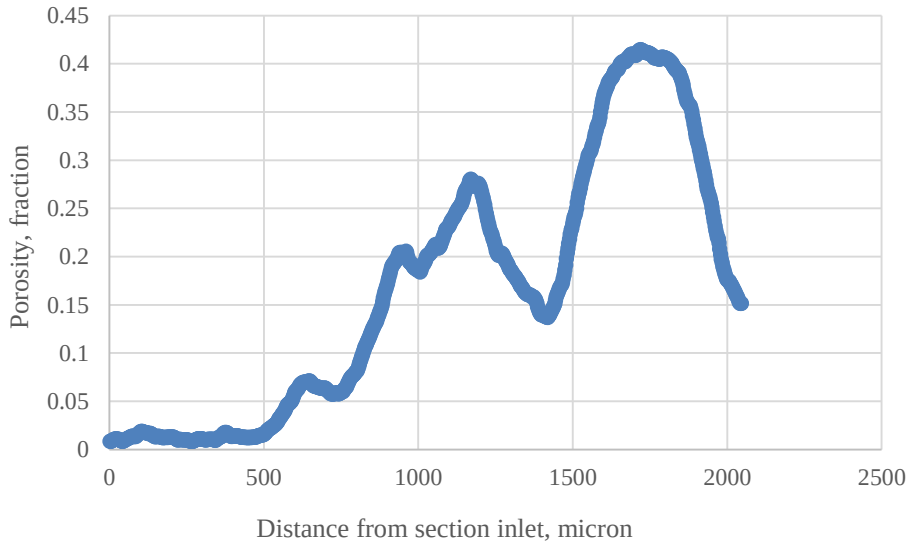

Figure 67: Connected porosity distribution for the selected sub volume for polymer flooding (DF5-2)

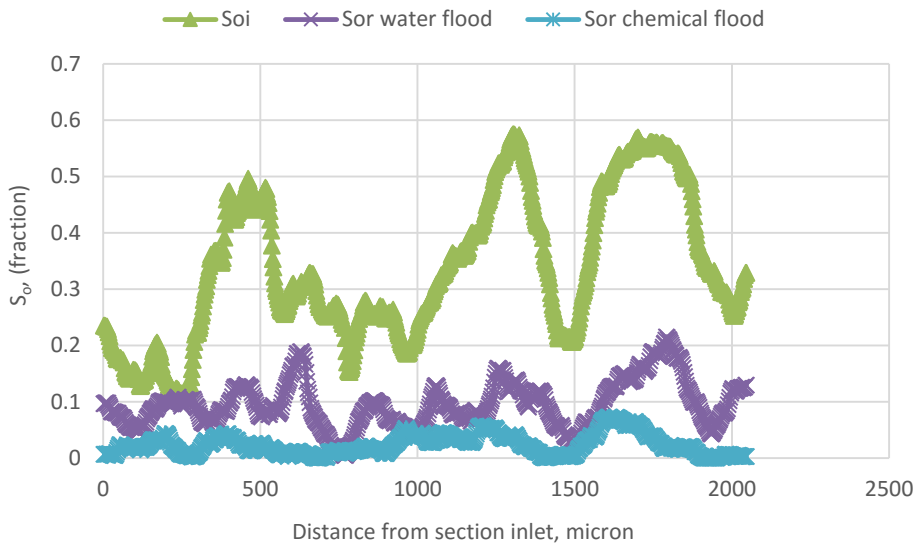

Figure 68: Oil saturation before and after polymer flooding at the selected sub volume (DF5-1)

CHAPTER 5

CONCLUSIONS AND RECOMENDATIONS

We conduct a comprehensive core-flooding study coupled with rheology and contact angle measurements. Through which, we investigated the effects of different chemical combinations for previously selected chemicals in terms of recovery, contact angle and rheology. In addition, the effects of slug size and chemical injection sequence were investigated using the optimum combination. We also coupled the work by ion concentration analysis for effluents as well as pore3-scale imaging. The following remarks can be extracted from this:

5.1 Conclusions

- The presence of surfactant has no effect on the rheology of the mixture at rates between (3 and 100) 1/s. For the same polymer, the rheologies obtained with two different surfactants overlapped.
- At shear rates ranging between (0.001 and 3) the mixture containing ATBs/AM exhibit small difference. However, TVP works better with SS-880 than SS-885.
- Two weeks thermal aging is enough to restore the original wettability for calcite rock discs while one week is too short.
- The combination S1P1 showed the most promising incremental recovery out of OIIP and can be considered as the optimum combination above the other three.

- The slug size showed almost directly proportional relationship with the recovery out of the residual oil saturation (SOR) which emphasizes that continuous injection of chemical is advantage then the defining factor will be the tolerable cost.
- We can obviously notice that the sequence of SW – S1P1 – SW showed the highest ROS recovery.
- Ion concentration analyses for Calcium ion showed dissolution in most of the cases.
- The adsorption of Sodium and magnesium ion in the presence of polymer have noticed while no effect of the surfactant in their adsorption.

5.2 Recommendations

- To avoid the uncertainties induced by doing the core-flooding optimization on different core plugs, it is better to clean the same sample by solvents and dry it and use it to insure the same pore size distribution and ganglia. However, the capability to restore original conditions especially after the introduction of chemicals must be investigated. Simulators history match and upscale results might provide a more reliable option.
- Studying the dynamic adsorption for the surfactant and polymer is important but the suitable procedure for measuring the concentration should have the ability to remove the effect of hydrocarbon presence in the solution.
- For the micro-CT imaging, it is better to do the experiment in a core-flooding system coupled with the micro-CT scanner to be able to take images at more steps. In addition, it would avoid issues associated with the sample placement which may result in losing the pore space under investigation.
- Using light oil for the micro-CT imaging is good because workflow is based on density, the higher the density contrast the better differentiation and visualization of the different phases.

References

[1] C. S. S. P. E. M. Chiou and G. E. S. P. E. M. Kellerhals, "Polymer/Surfactant Transport in Micellar Flooding," *Soc. Pet. Eng.*, no. October, pp. 603–612, 1981.

[2] N. Arihara, T. Yoneyama, Y. Akita, and L. XiangGuo, "Oil Recovery Mechanisms of Alkali-Surfactant-Polymer Flooding," in *Proceedings of SPE Asia Pacific Oil and Gas Conference and Exhibition*, 1999.

[3] W. T. Osterloh and J. M. . Jante, "Surfactant-polymer flooding with anionic PO/EO surfactant microemulsions containing polyethylene glycol additives," in *SPE/DOE Enhanced Oil Recovery …*, 1992.

[4] D. Levitt, A. Klimenko, S. Jouenne, M. Chamerois, and M. Bourrel, "Overcoming Design Challenges of Chemical EOR in High-Temperature, High Salinity Carbonates," in *SPE Middle East Oil and Gas Show and Conference*, 2013, pp. 1–15.

[5] M. S. Azad and A. S. Sultan, "Extending the Applicability of Chemical EOR in High Salinity , High Temperature & Fractured Carbonate Reservoir Through Viscoelastic Surfactants," in *SPE Annual Technical Symposium and Exhibition held in Al-Khobar, Saudi Arabia*, 2014.

[6] J. Wang, M. Han, A. B. Fuseni, and D. Cao, "Surfactant Adsorption in Surfactant-Polymer Flooding for Carbonate Reservoirs (2).pdf," in *SPE Middle East Oil and Gas Show and Conference*, 2015.

[7] M. Han, A. Alsofi, A. Fuseni, X. Zhou, S. Hassan, and S. Aramco, "IPTC 17084 Development of Chemical EOR Formulations for a High Temperature and High Salinity Carbonate Reservoir," *Iptc*, vol. March, no. 1–13, pp. 1–13, 2013.

[8] H. S. Al-Hashim, V. Obiora, H. Y. Al-Yousef, F. Fernandez, and W. Nofal, "Alkaline surfactant polymer formulation for carbonate reservoirs," *Pet. Sci. Technol.*, vol. 23, no. 5–6, pp. 723–746, 2005.

[9] P. Luo, Y. Wu, and S. Huang, "Optimized Surfactant – Polymer Flooding for Western Canadian Heavy Oils," in *SPE Heavy Oil Conference Canada, 2013*, 2013.

[10] C. Glover, M. Puerto, J. Maerker, and E. Sandvik, "Surfactant Phase Behavior and Retention in Porous Media," *SPE J.*, vol. 19, no. 3, pp. 183–193, 1979.

[11] S. Adkins, P. Liyanage, G. W. P. Pinnawala Arachchilage, T. Mudiyanselage, U. Weerasooriya, and G. Pope, "A New Process for Manufacturing and Stabilizing High-Performance EOR Surfactants at Low Cost for High-Temperature, High-Salinity Oil Reservoirs," *Proc. SPE Improv. Oil Recover. Symp.*, 2010.

[12] Y. Zhu, M. Lei, and Y. Zhang, “Effects of Emulsification on Oil Recovery and Produced Liquid Handing in,” 2015.

[13] F. J. Trogus, R. S. Schechter, G. a. Pope, and W. H. Wade, “Adsorption of Mixed Surfactant Systems,” *J. Pet. Technol.*, vol. 31, no. 6, pp. 769–778, 1979.

[14] Y. Zhu, Y. Zhang, Q. Hou, H. Yuan, and G. Jian, “IPTC 16433 Effect of Main Factors on Oil Recovery of Surfactant-Polymer Flooding,” in *IPTC*, 2013.

[15] H. Mohammadi, M. Delshad, and G. a Pope, “Mechanistic Modeling of Alkaline / Surfactant / Polymer Floods,” *Spe 110212*, no. 2006, pp. 1–13, 2008.

[16] R. Tabary, B. Bazin, F. Douarche, and P. Moreau, “Surfactant Flooding in Challenging Conditions : Towards Hard Brines and High Temperatures,” *Spe 164359*, pp. 1–16, 2013.

[17] C. T. Q. Dang, Z. J. Chen, N. T. B. Nguyen, W. Bae, and T. H. Phung, “Development of Isotherm Polymer/Surfactant Adsorption Models in Chemical Flooding,” *SPE Asia Pacific Oil Gas Conf. Exhib.*, 2013.

[18] M. S. Kamal, A. S. Sultan, U. A. Al-Mubaiyedh, I. A. Hussien, and M. Pabon, “Evaluation of Rheological and Thermal Properties of a New Fluorocarbon Surfactant–Polymer System for EOR Applications in High-Temperature and High-Salinity Oil Reservoirs,” *J. Surfactants Deterg.*, vol. 17, no. 5, pp. 985–993, 2014.

[19] M. S. Kamal, A. S. Sultan, and I. A. Hussein, “Screening of amphoteric and anionic surfactants for cEOR applications using a novel approach,” *Colloids Surfaces A Physicochem. Eng. Asp.*, vol. 476, pp. 17–23, 2015.

[20] M. S. Kamal, A. S. Sultan, U. A. Al-Mubaiyedh, I. A. Hussein, and Y. Feng, “Rheological Properties of Thermoviscosifying Polymers in High-temperature and High-salinity Environments,” *Can. J. Chem. Eng.*, vol. 93, no. 7, pp. 1194–1200, 2015.

[21] M. S. Kamal, A. S. Sultan, U. A. Al-Mubaiyedh, and I. A. Hussein, “Review on Polymer Flooding: Rheology, Adsorption, Stability, and Field Applications of Various Polymer Systems,” *Polym. Rev.*, vol. 55, no. August 2016, pp. 491–530, 2015.

[22] P. Somasundaran and H. S. Hanna, “Adsorption of Sulfonates on Reservoir Rocks,” *Soc. Pet. Eng. J.*, vol. 19, no. 4, 1979.

[23] J. Lu and G. A. Pope, “Optimization of Gravity-Stable Surfactant Flooding,” no. April, pp. 27–30, 2015.

[24] S. P. E. Journal, C. A. Miller, G. J. Hirasaki, C. A. Miller, and M. Puerto, “Recent Advances in Surfactant EOR Recent Advances in Surfactant EOR,” no. NOVEMBER, pp. 3–5, 2008.

[25] L. Zhenquan, A. Zhang, X. Cui, L. Zhang, L. Guo, and L. Shan, “A Successful

Pilot of dilute Surfactant-Polymer Flooding in Shengli Oilfield," *SPE Improv. Oil Recover. Symp.*, pp. 1–6, 2013.

[26] V. A. Tabrizy, "Investigation of CO 2 Enhanced Oil Recovery Using Dimensionless Groups in Wettability Modified Chalk and Sandstone Rocks," *J. Pet. Eng.*, vol. 2014, no. March, pp. 1–16, 2014.

[27] Y. Wang, F. Zhao, B. Bai, J. Zhang, W. Xiang, X. Li, and W. Zhou, "Optimized Surfactant IFT and Polymer Viscosity for Surfactant- Polymer Flooding in Heterogeneous Formations," in *SPE Improved Oil Recovery Symposium*, 2010, pp. 1–11.

[28] S. Solairaj, "New Method of Predicting Optimum Surfactant Structure for EOR," University of Texas at Austin, 2011.

[29] M. A. Bataweel, A. . Y. Shivaprasad, and H. A. T. A. U. Nasr-El-din, "Low-Tension Polymer Flooding Using Amphoteric Surfactant in High Salinity/High Hardness and High Temperature Conditions in Sandstone Cores," in *SPE Enhanced Oil Recovery …*, 2012, pp. 1–23.

[30] A. Feng, G. Zhang, J. Ge, P. Jiang, H. Pei, J. Zhang, and R. Li, "Study of Surfactant-Polymer Flooding in Heavy Oil Reservoirs," *SPE Heavy Oil Conf. Canada, 2012*, no. June, pp. 1–10, 2012.

[31] Y. Zhu, X. Liu, and J. Fan, "Developments of ASP / SP Flooding Formulations for Huabei Fault Block Reservoir," pp. 0–9, 2015.

[32] P. A. L. Alanis, A. M. Alsofi, J. Wang, and M. Han, "Toward an Alternative Bio-Based SP Flooding Technology : I. Biosurfactant Eevaluation," in *SPE Enhanced Oil Recovery Conference*, 2015.

[33] X. Wu, M. Han, B. H. Zahrani, and L. Guo, "Effect of Surfactant-Polymer Interaction on the Interfacial Properties for," no. Sheng 2011, 2015.

[34] D. Magzymov, C. Qiao, R. T. Johns, and T. Pennsylvania, "SPE-181651-MS Impact of Surfactant Mixtures on Microemulsion Phase Behavior," no. September, pp. 26–28, 2016.

[35] G. C. Wang and B. H. Caudle, "Effects of Polymer Concentrations, Slug Size And Permeability Stratification in Viscous Waterfloods," *Spe*, 1970.

[36] T. Maldal and E. Gilje, "Evaluation and economical feasibility of polymer-assisted surfactant flooding for the Gullfaks field, Norway," *... Eval. …*, no. April, pp. 161–168, 1998.

[37] D. Li, M. Shi, D. Wang, Z. Li, H. Fei, and D. O. Co, "Chromatographic Separation of Chemicals in Alkaline Surfactant Polymer Flooding in Reservoir Rocks in the Daqing Oilfield," *Spe Oilf. Chem. Symp. Woodlands Tx 420222009 Proc.*, no. 200937, 2009.

[38] Z. Ibrahim, a a a Manap, P. a Hamid, H. V Yee, L. P. Hong, K. Wyatt, Petronas, P. R. E. S. & S. C. I. Serv, and S. Inc, "Laboratory Aspect of Chemical Eor Processes Evaluation for Malaysian Oilfields," *Spe Asia Pacific Oil Gas Conf. (Adelaide, Aust. 9/11-13/2006) Proc.*, no. 200711, 2006.

[39] C. T. Q. Dang, Z. Chen, N. T. B. Nguyen, W. Bae, T. H. Phung, C. Univ, S. Univ, and Vietsovpetro, "Successful Story of Development and Optimization for Surfactant-Polymer Flooding in a Geologically Complex Reservoir," *Spe Enhanc. Oil Recover. Conf. [Eorc] (Kuala Lumpur, Malaysia, 7/19-21/2011) Proc.*, no. 201149, 2011.

[40] N. T. B. Nguyen, Z. Chen, L. X. Nghiem, and C. Modelling, "A New Approach for Optimization and Uncertainty Assessment of Surfactant-Polymer Flooding," no. 1, pp. 1–17, 2014.

[41] U. Felix, T. O. Ayodele, and O. Olalekan, "Surfactant-Polymer Flooding Schemes (A Comparative Analysis)," in *Nigeria Annual International Conference and Exhibition held in Lagos, Nigiria*, 2015.

[42] S. Pingping, W. Jialu, Y. Shiyi, Z. Taixian, and J. Xu, "Study of Enhanced-Oil-Recovery Mechanism of Alkali / Surfactant / Polymer Flooding in Porous Media From Experiments," *SPE J.*, vol. 14(2), no. June, pp. 237–244, 2009.

[43] P. Moreau, M. Morvan, P. Rivoal, B. Bazin, F. Douarche, J.-F. Argillier, and R. Tabary, "An Integrated Workflow for Chemical EOR Pilot Design," *Spe 129865*, no. April, pp. 1–11, 2010.

[44] D. Cao, J. Wang, M. Han, and A. J. Alshehri, "Comprehensive Effects on the Propagation of Surfactant and Polymer Flow," in *Spe Enhanced Oil Recovery Conference [Eorc] (Kuala Lumpur, Malaysia, 8/11-13/2015) Proceedings*, 2015.

[45] Y. Wang, F. Zhao, B. Bai, J. Zhang, W. Xiang, X. Li, and W. Zhou, "Optimized Surfactant IFT and Polymer Viscosity for Surfactant- Polymer Flooding in Heterogeneous Formations," *SPE Improv. Oil Recover. Symp.*, pp. 1–11, 2010.

[46] A. Samanta, K. Ojha, A. Sarkar, and A. Mandal, "Surfactant and Surfactant-Polymer Flooding for Enhanced Oil Recovery," *Adv. Pet. Explor. Dev.*, vol. 2, no. 1, pp. 13–18, 2011.

[47] J. S. Buckley, C. Bousseau, and Y. Liu, "Wetting Alteration by Brine and Crude Oil: From Contact Angles to Cores," *SPE J.*, vol. 1, no. 3, pp. 341–350, 1996.

[48] P. A. L. Alanis, A. M. Alsofi, J. Wang, and M. Han, "Toward an Alternative Bio-Based SP Flooding Technology : I. Biosurfactant Eevaluation," *SPE Enhanc. Oil Recover. Conf.*, 2015.

[49] Hassan, A. A., Abdullah, M. B., Abdulrahim, A. M., Marliere, C., & Hocine, S. (2017). SPE-183933-MS Surfactant-Polymer Flooding: Chemical Formulation Design and Evaluation for the Raudhatain Lower Burgan RALB Reservoir in Kuwait.

[50] Zhu, Y., & Lei, M. (2016). Studies on Surfactant-Polymer Combination Flooding Formulations for a High Salinity Reservoir, 1–9. https://doi.org/10.2118/179759-MS

APPENDIX A

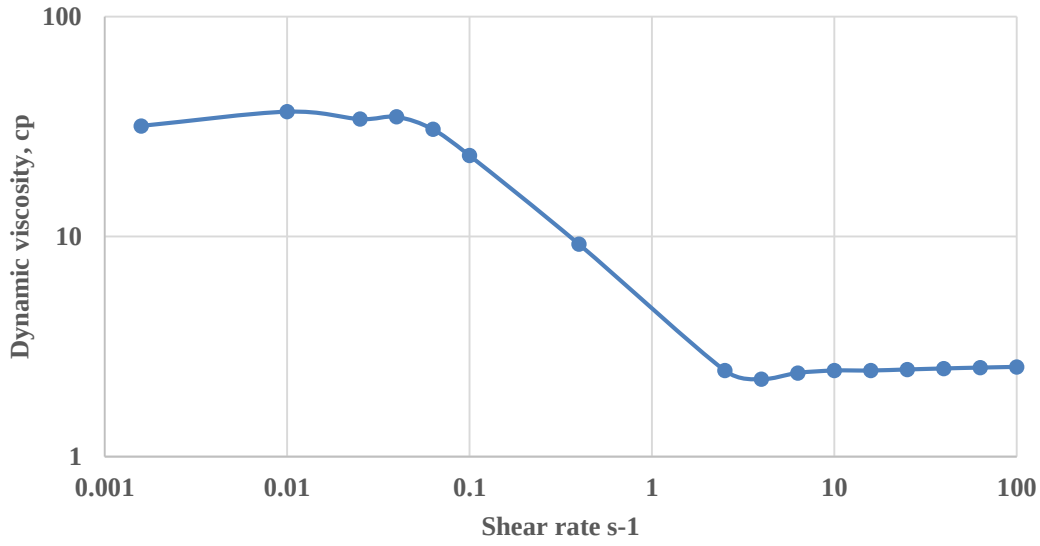

Figure 69: Shear scan for S1 0.05 wt.% and P1 0.25 wt.% prepared in sea water at 85ºC

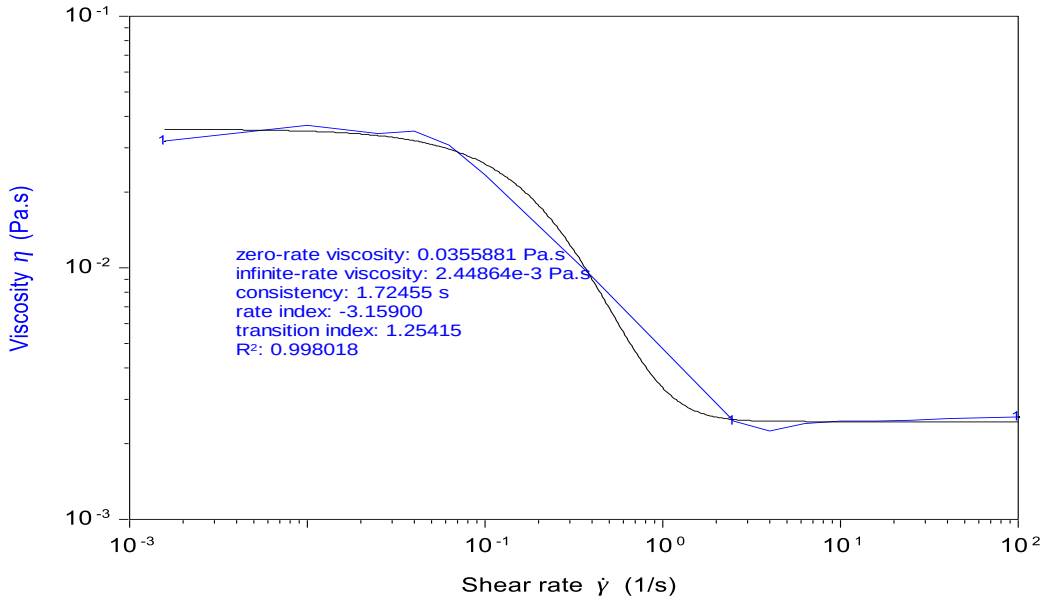

Figure 70: Carreau - Yasuada fitting for S1P1

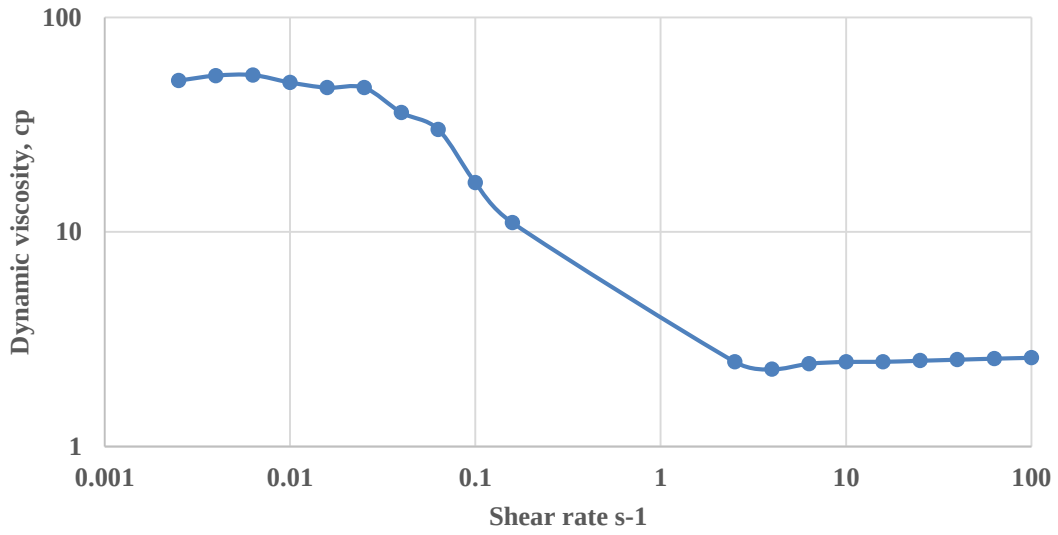

Figure 71: Shear scan for S2 0.05 wt.% and P1 0.25 wt.% prepared in sea water at 85°C

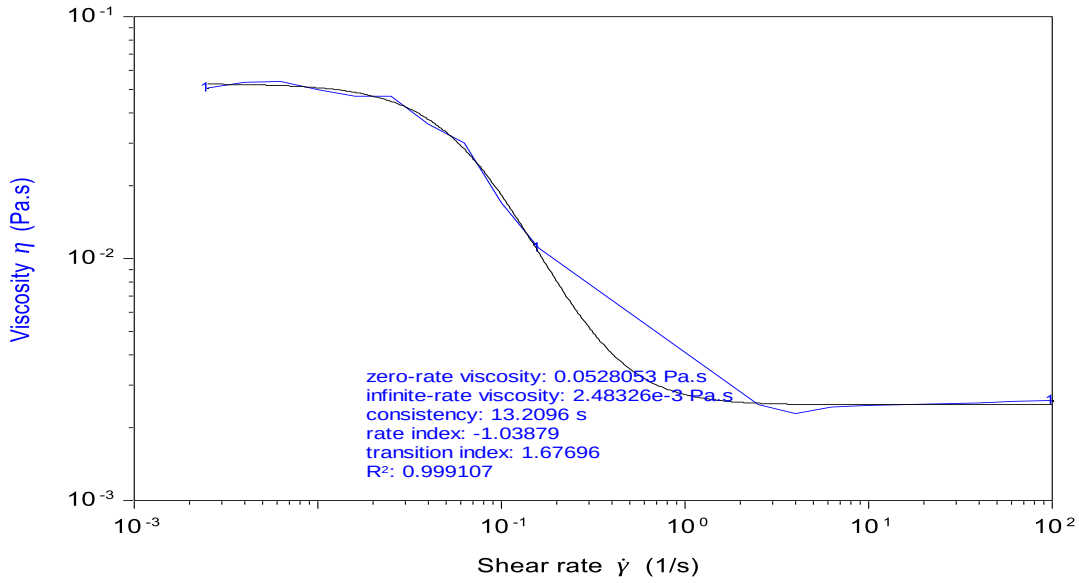

Figure 72: Carreau - Yasuada fitting for S2P1

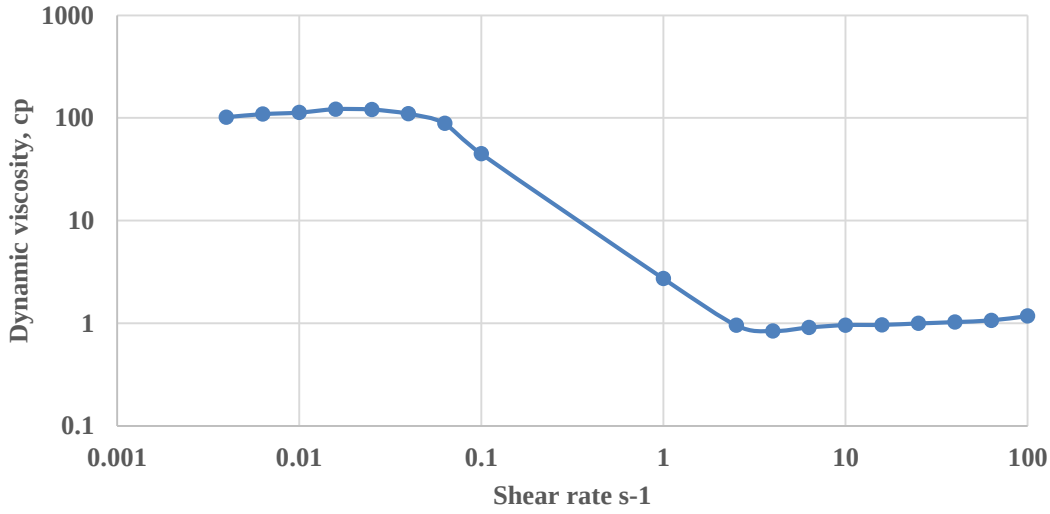

Figure 73: Shear scan for S1 0.05 wt.% and P2 0.25 wt.% prepared in sea water at 85ºC

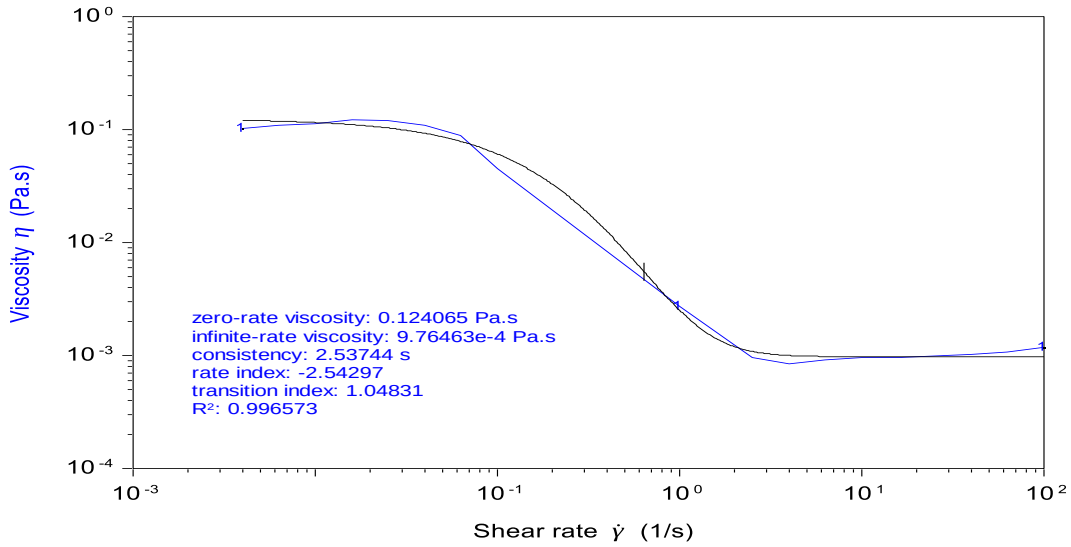

Figure 74: Carreau - Yasuada fitting for S1P2

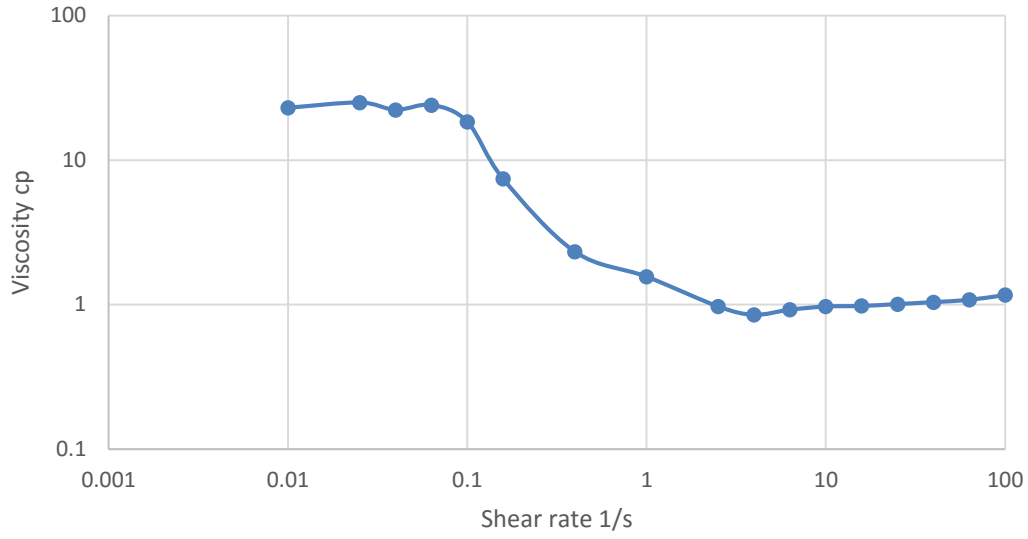

Figure 75: Shear scan for S1 0.05 wt.% and P2 0.25 wt.% prepared in sea water at 85ºC

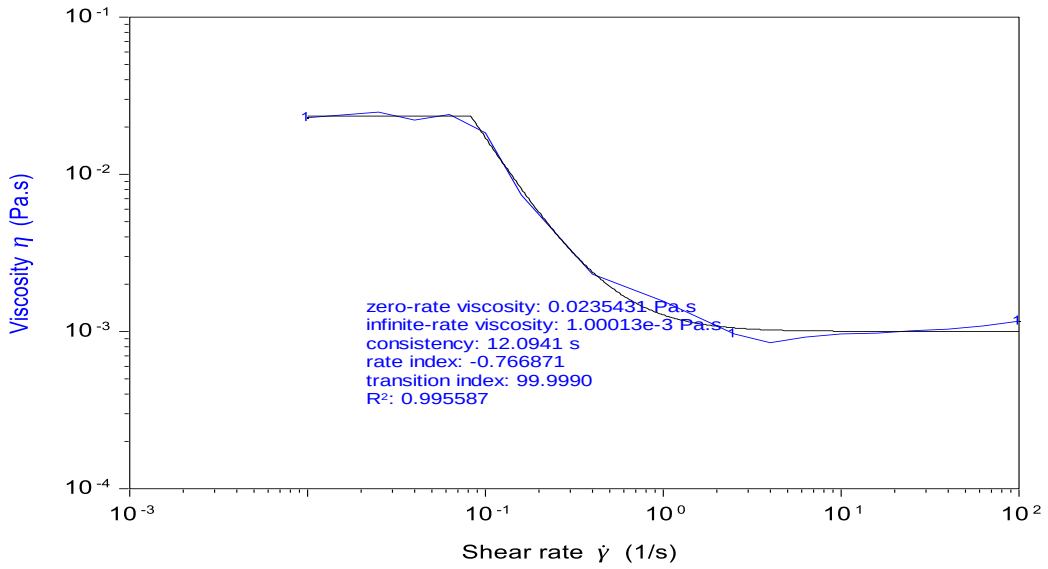

Figure 76: Carreau - Yasuada fitting for S1P2

APPENDIX B

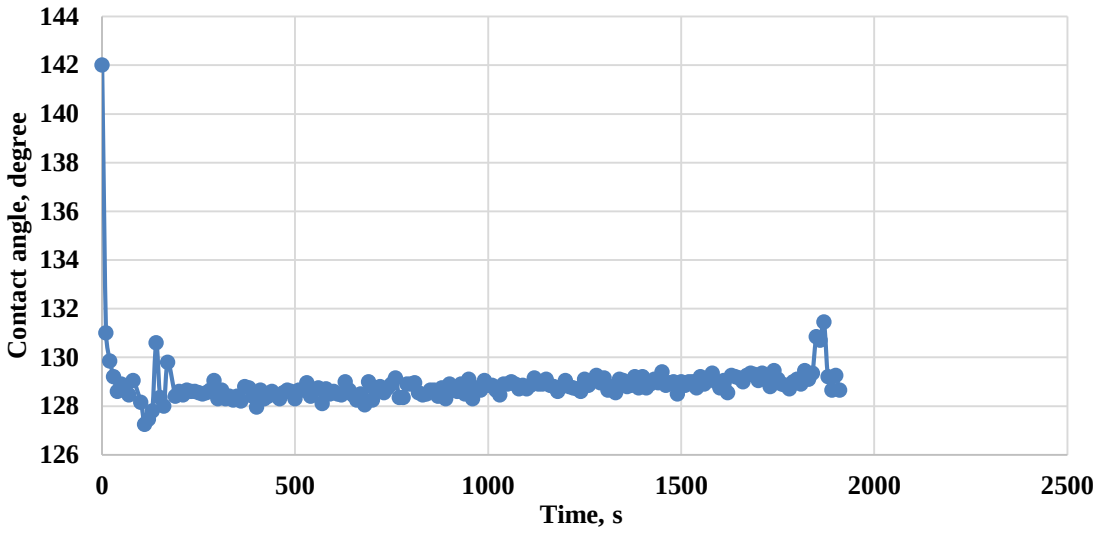

Figure 77: Contact angle for Sea water at outcrop

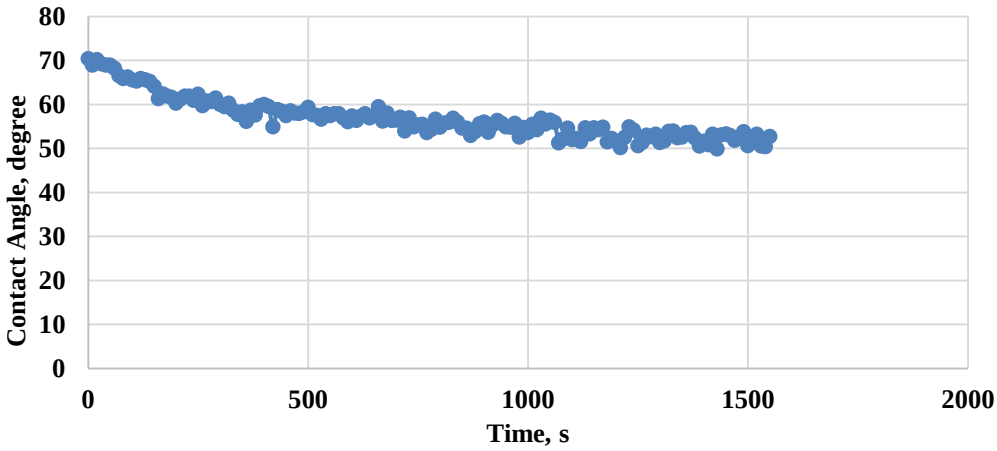

Figure 78:Shows the contact angle for S1P1 at outcrop

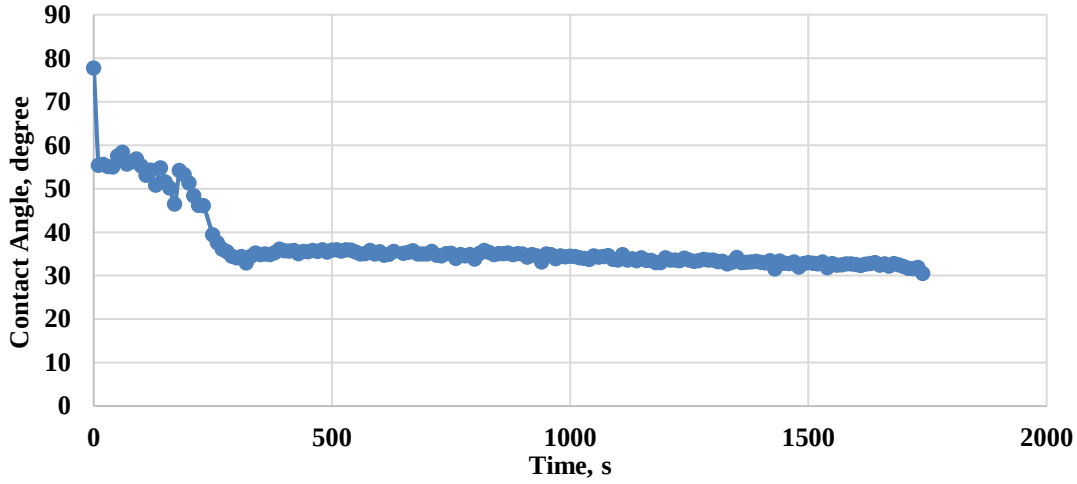

Figure 79:Shows the contact angle for S2P1 at outcrop

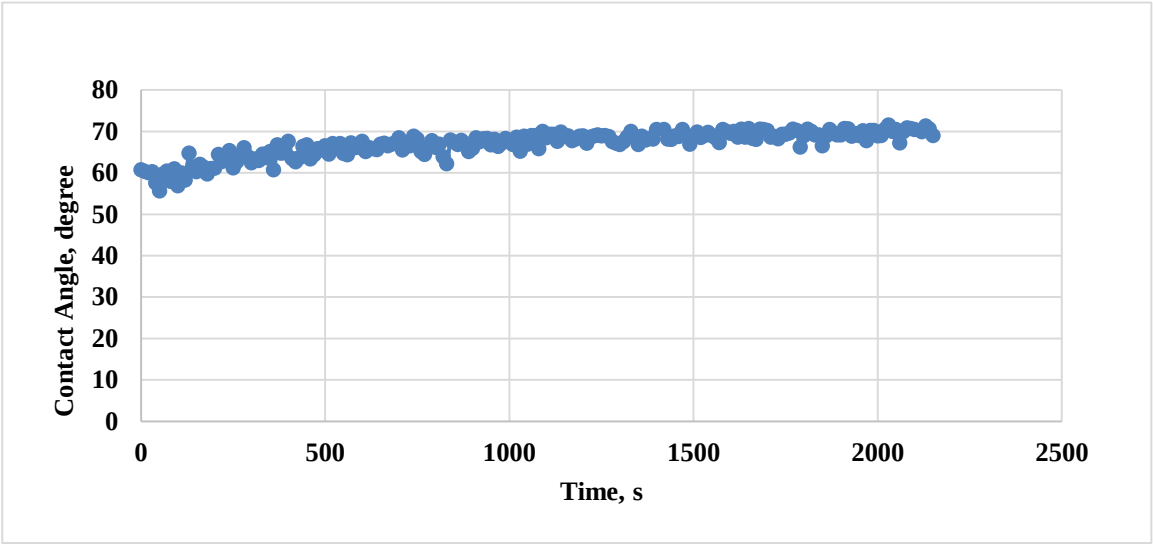

Figure 80: Shows the contact angle for S1P2 at outcrop

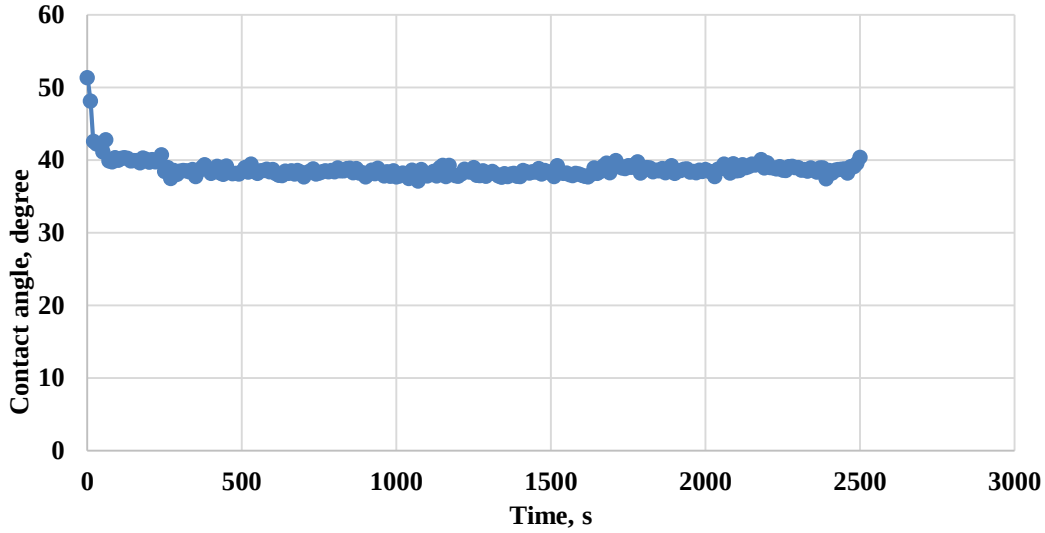

Figure 81: Shows the contact angle for S2P2 at outcrop

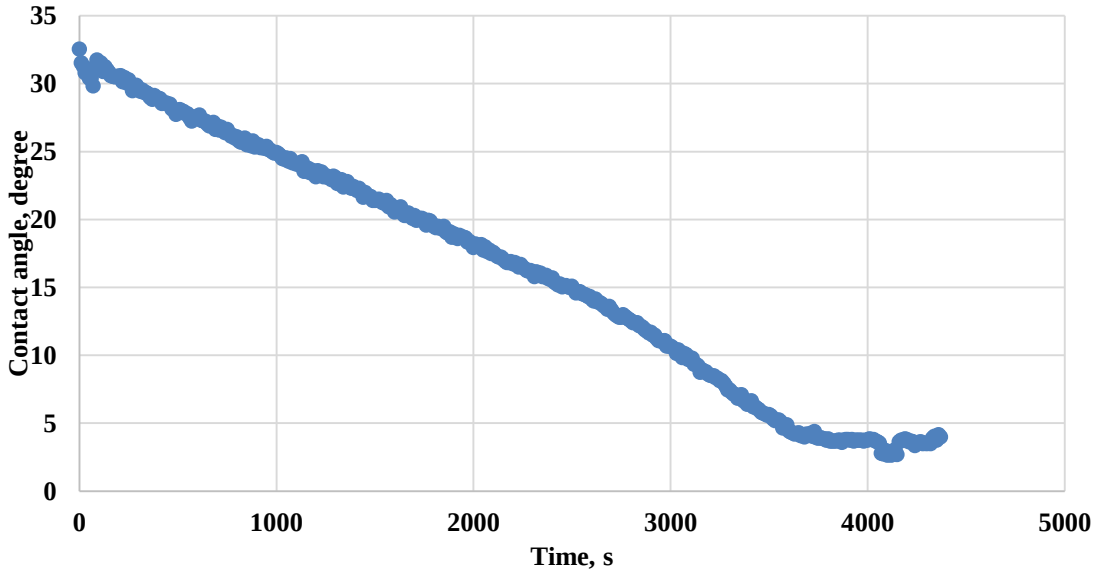

Figure 82: Contact angle for sea water at Indiana limestone

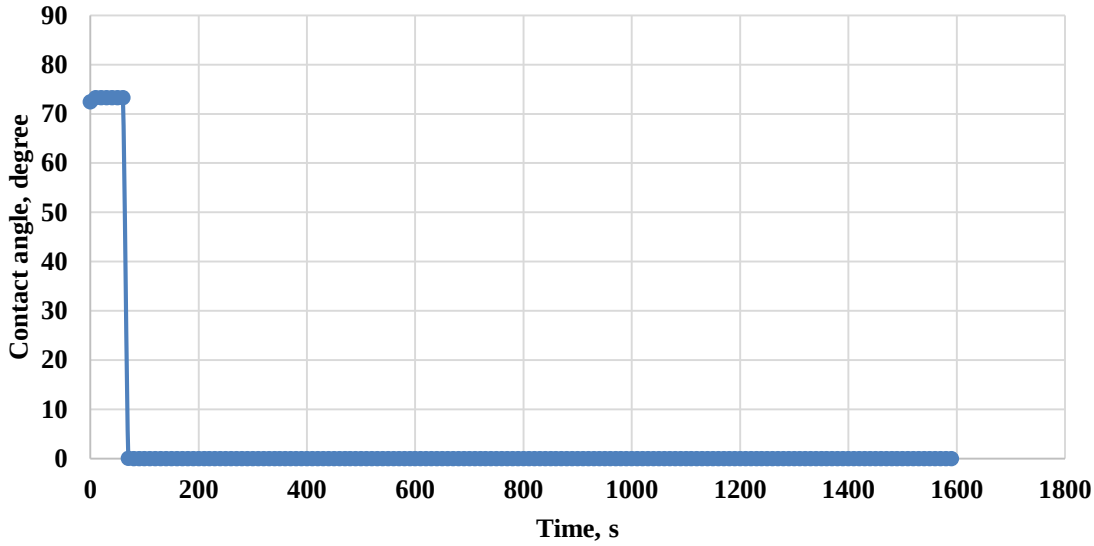

Figure 83: Contact angle for S1P1 Indiana limestone

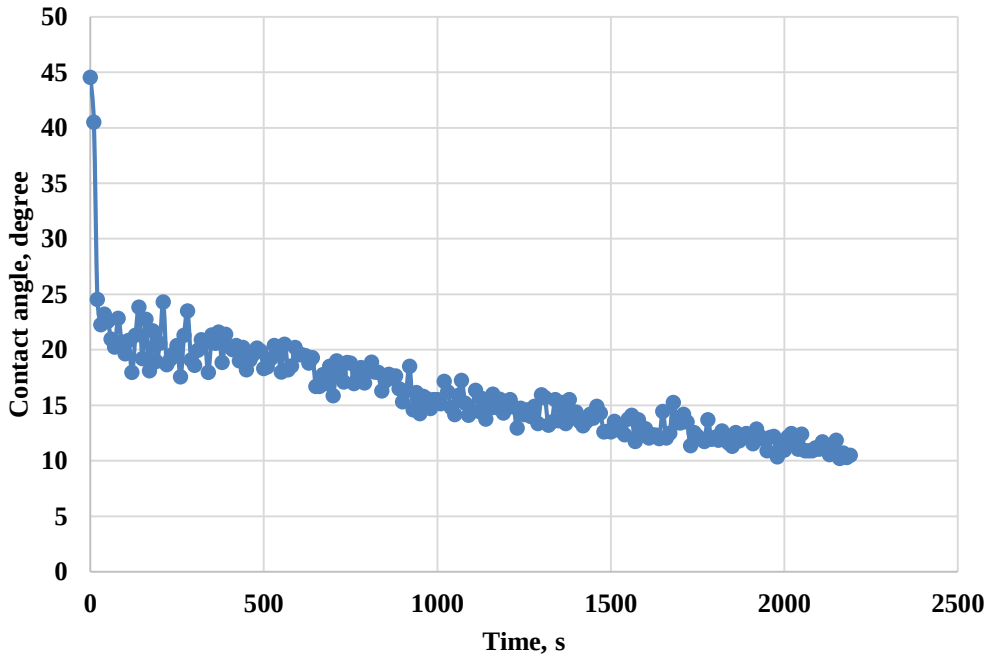

Figure 84: Contact angle for S2P1 Indiana limestone

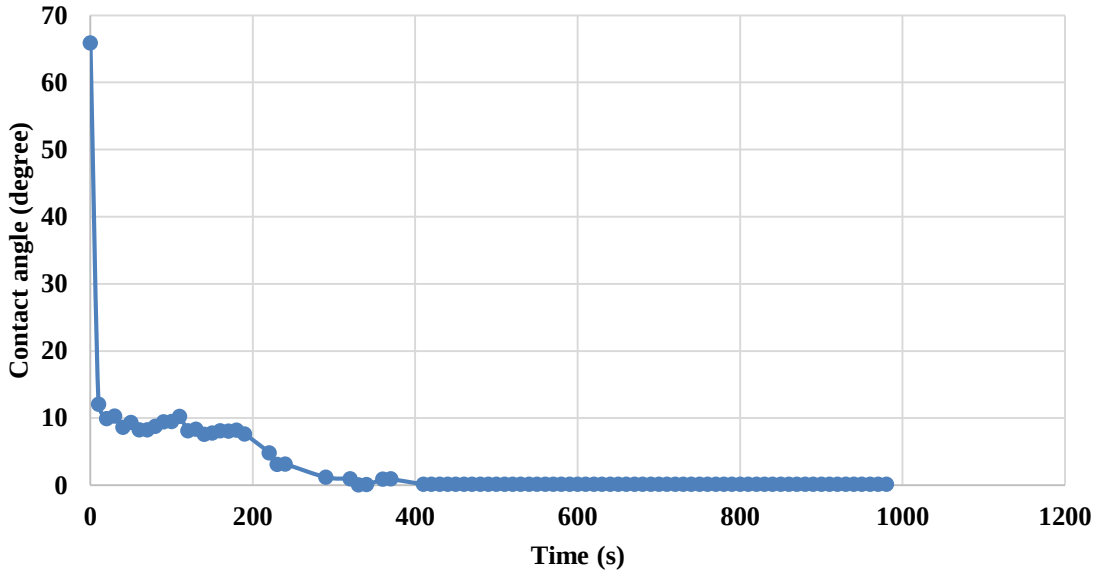

Figure 85: Contact angle for S1P2 Indiana limestone

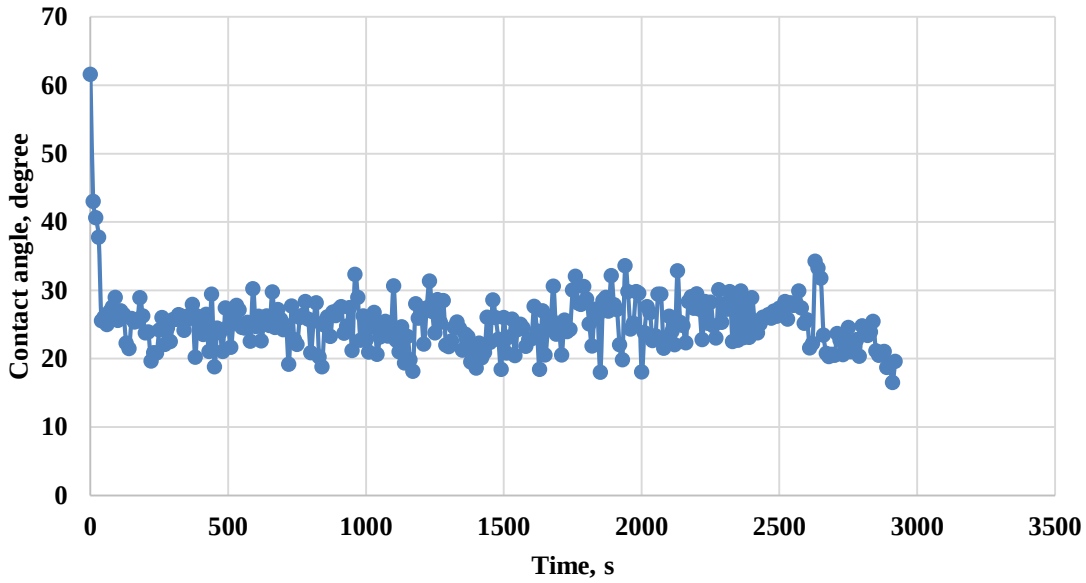

Figure 86: Contact angle for S2P2 Indiana limestone

APPENDIX C

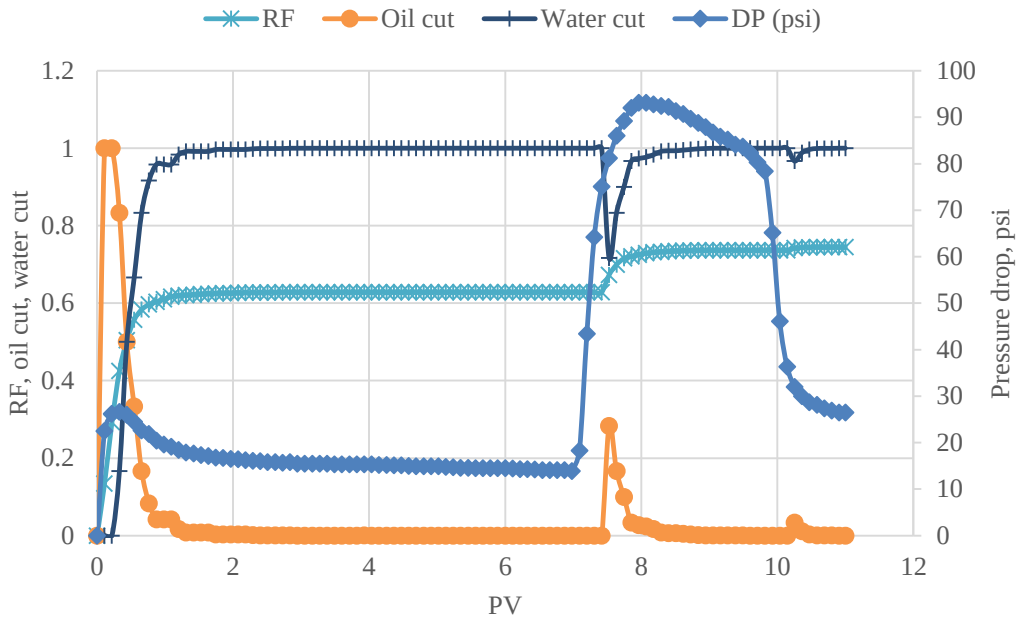

Figure 87: The recovery and Pressure drop S1P1 flooding

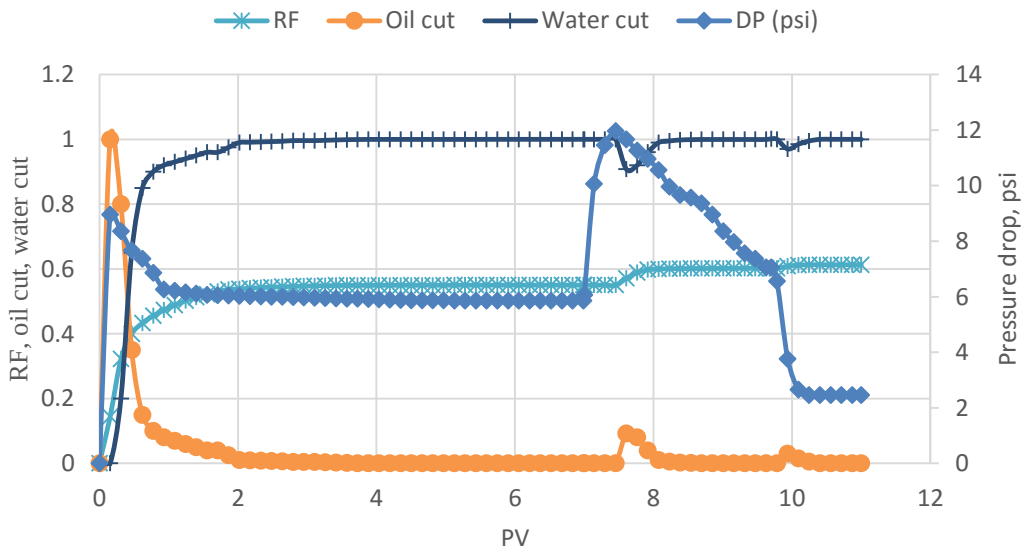

Figure 88: The recovery and Pressure drop S2P1 flooding

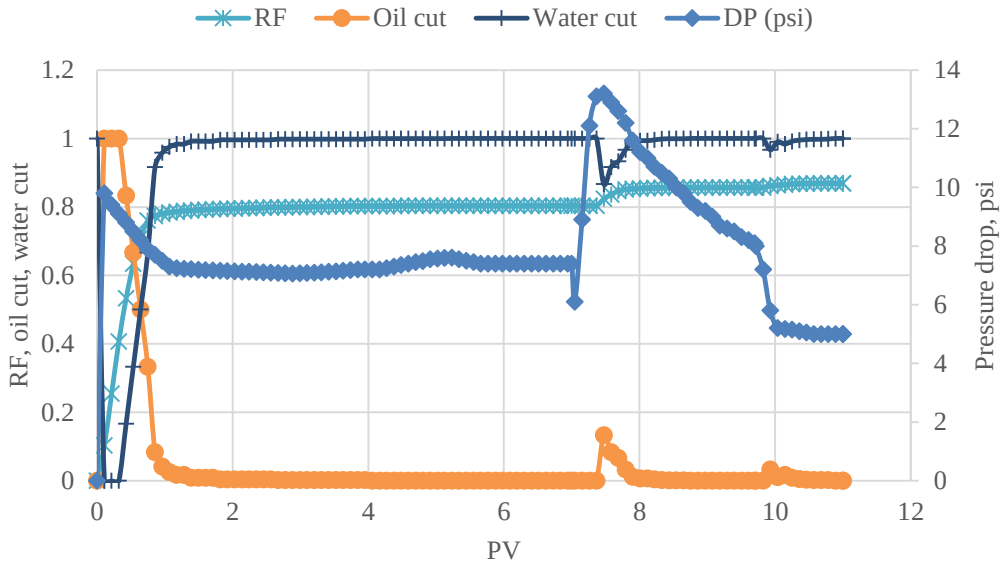

Figure 89: The recovery and Pressure drop for S1P2 flooding

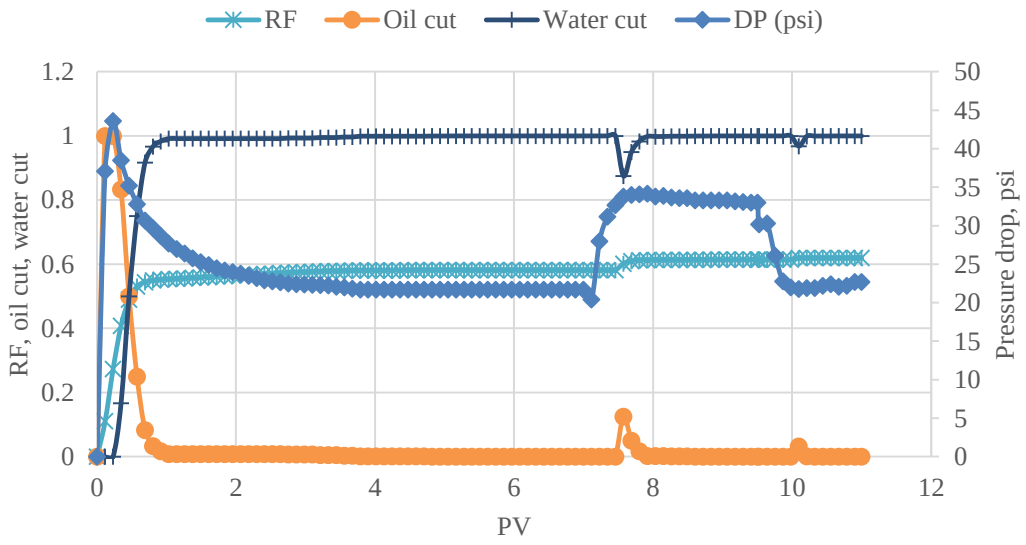

Figure 90: The recovery and Pressure drop for S2P2 flooding

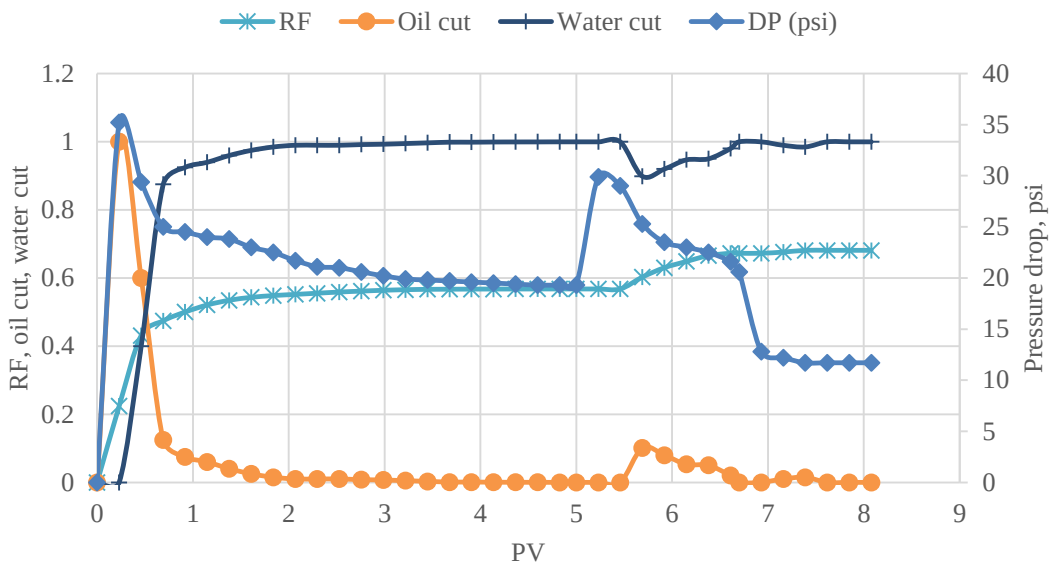

Figure 91: The recovery and Pressure drop for 1.7 PV slug size

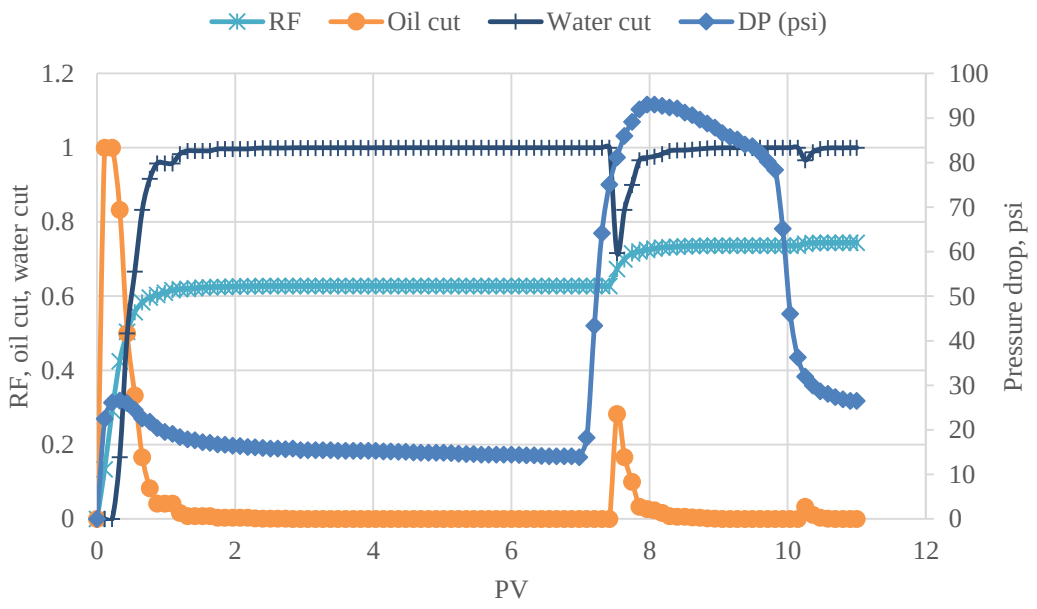

Figure 92: The recovery and Pressure drop for 2.7 PV slug size

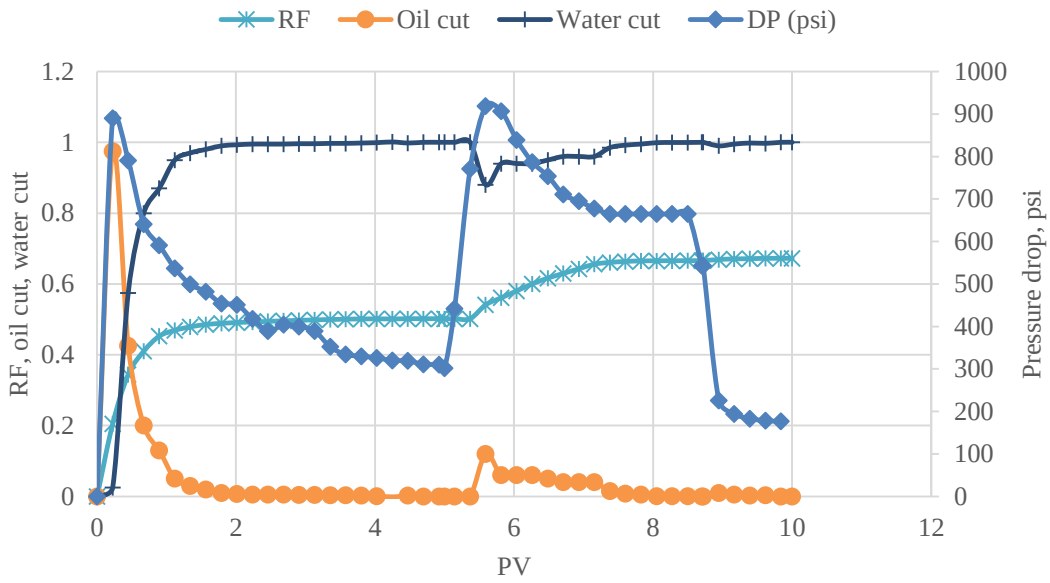

Figure 93: The recovery and Pressure drop for 3.5 PV slug size

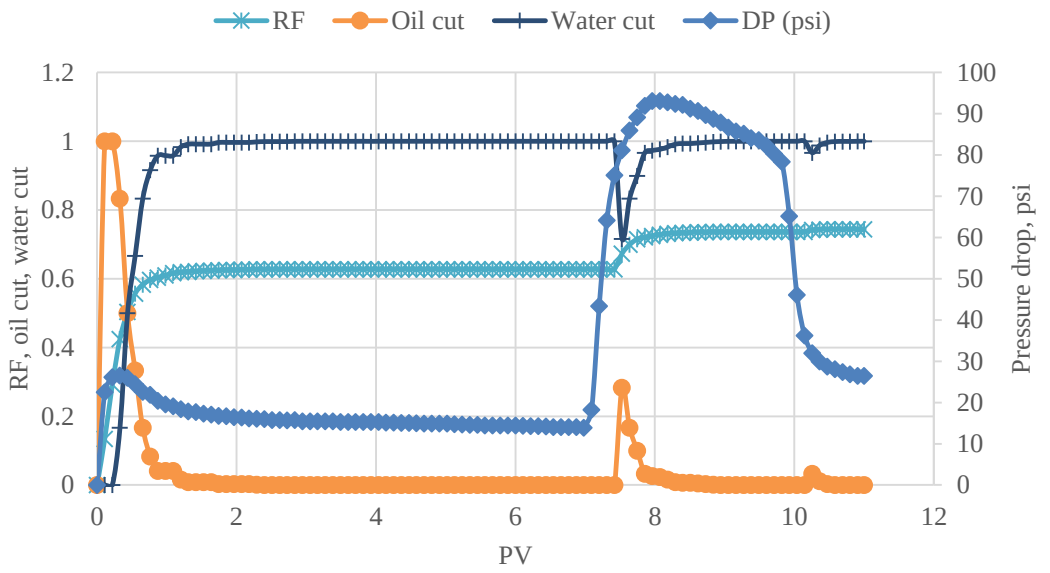

Figure 94: The recovery and Pressure drop SW-SP-SW sequence

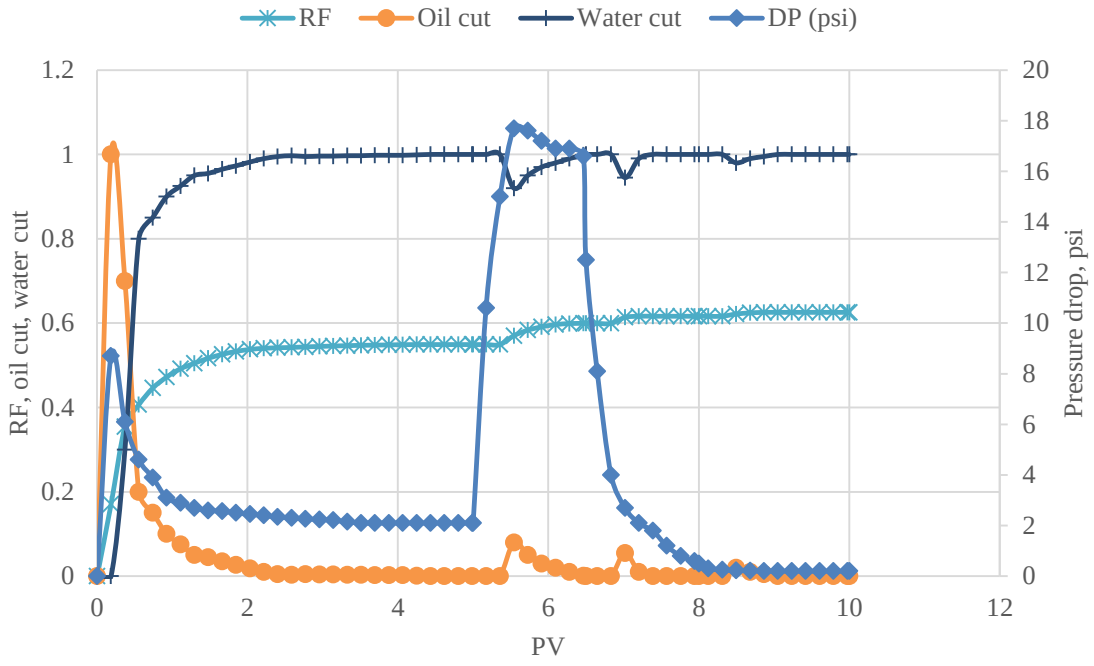

Figure 95: The recovery and Pressure drop for SW-P-S-SW sequence

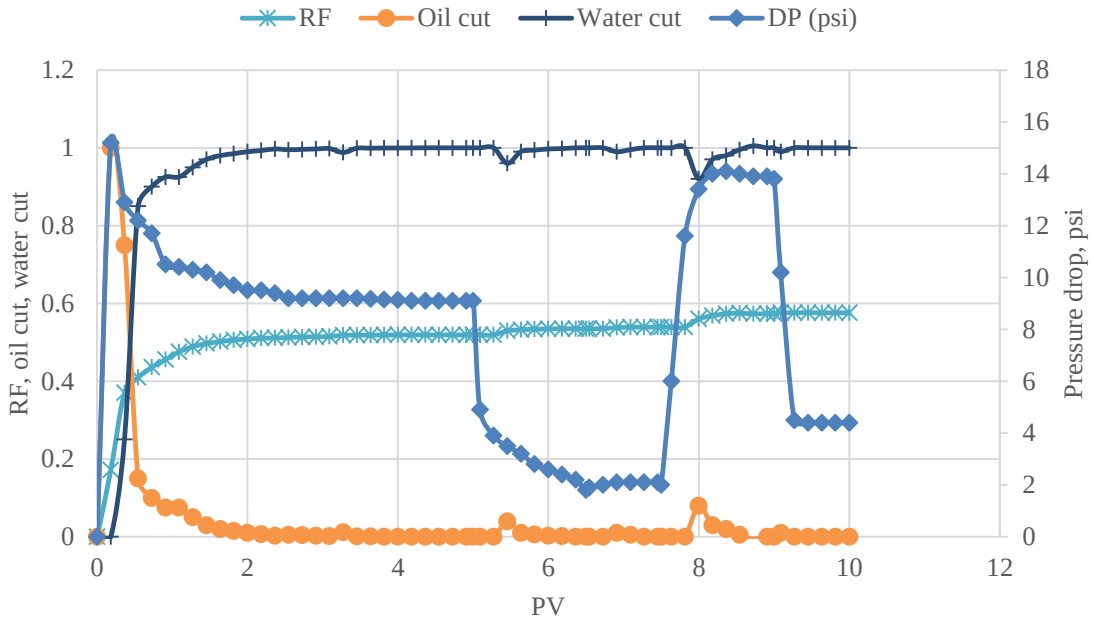

Figure 96: The recovery and Pressure drop for SW-S-SW-P-SW sequence

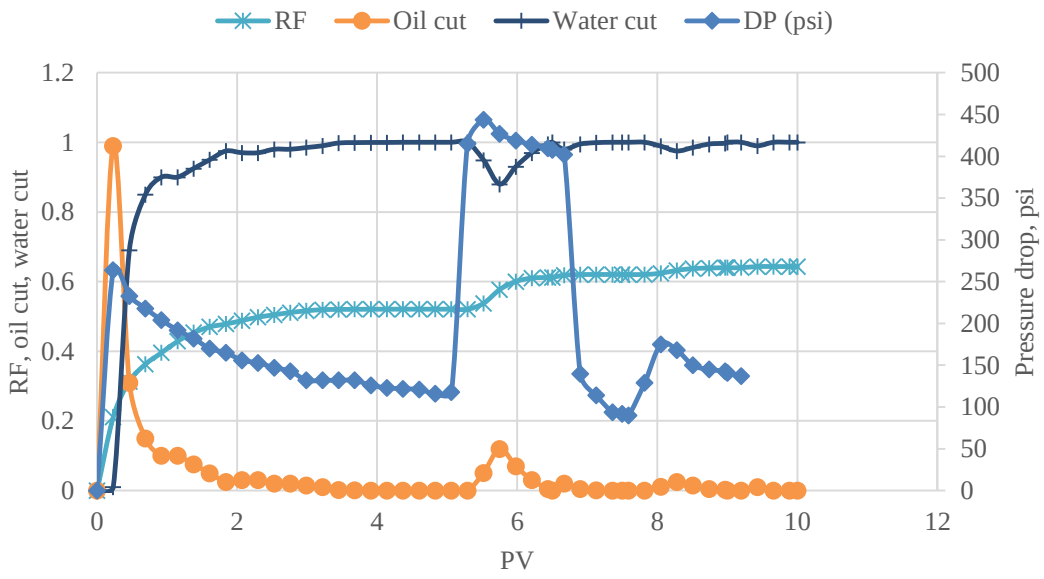

Figure 97:The recovery and Pressure drop for SW- P -SW- S -SW sequence

APPENDIX D

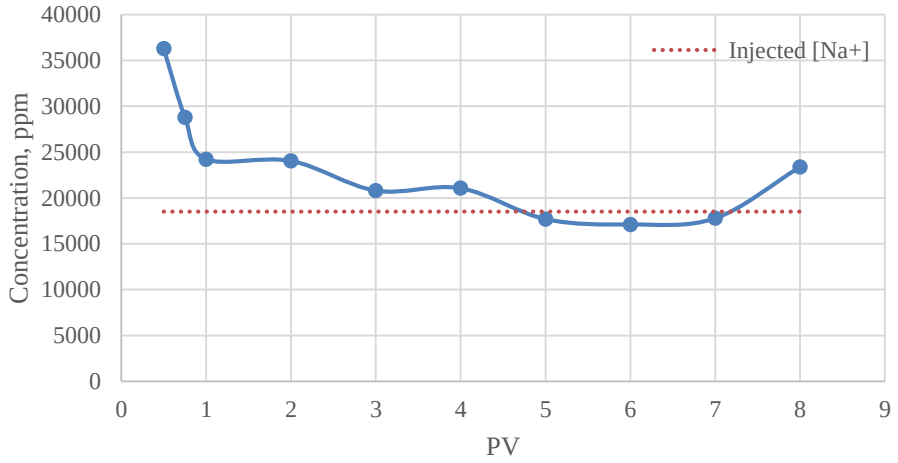

Figure 98: Sodium concentration for 1.7 PV slug size experiment (DF-1)

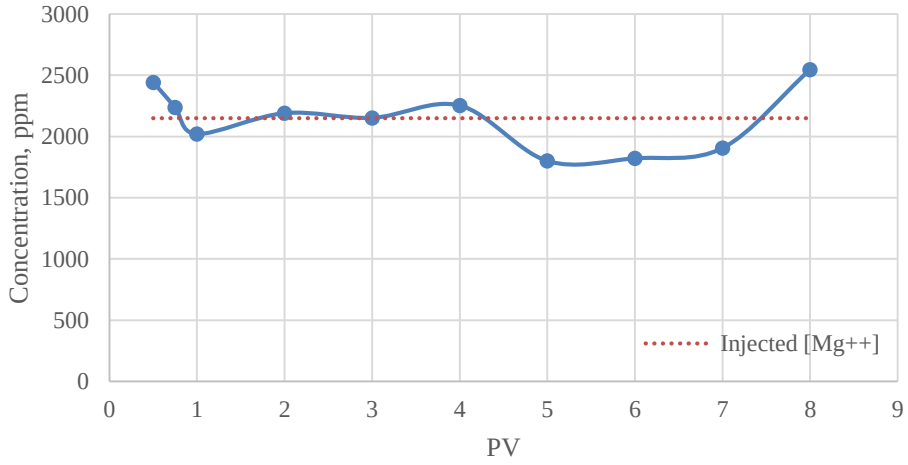

Figure 99: Magnesium concentration for 1.7 PV slug size experiment (DF-1)

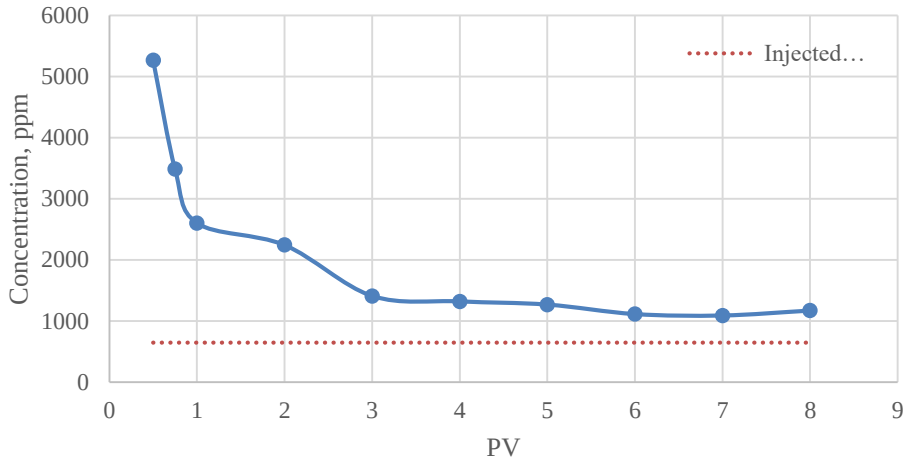

Figure 100: Calcium concentration for 1.7 PV slug size experiment (DF-1)

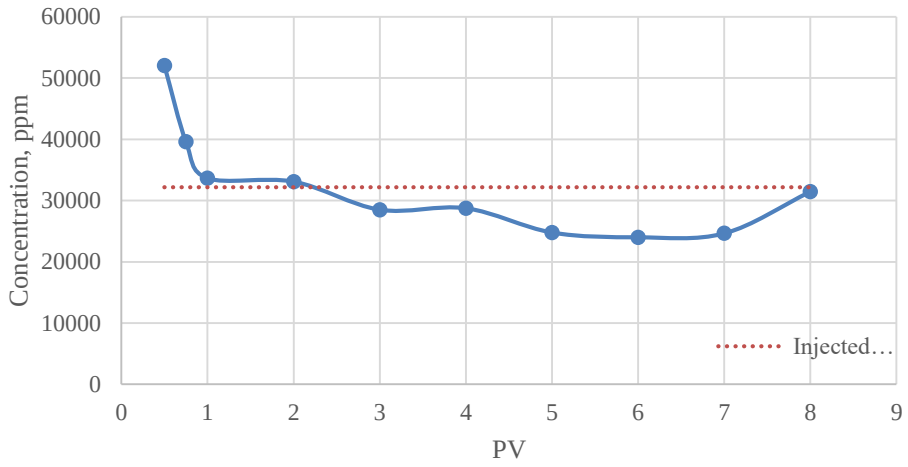

Figure 101: Chloride concentration for 1.7 PV slug size experiment (DF-1)

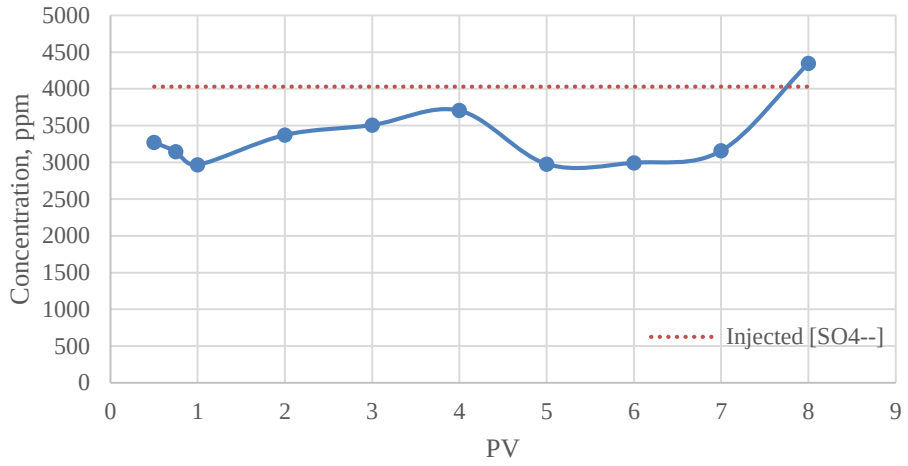

Figure 102: Sulfate concentration for 1.7 PV slug size experiment (DF-1)

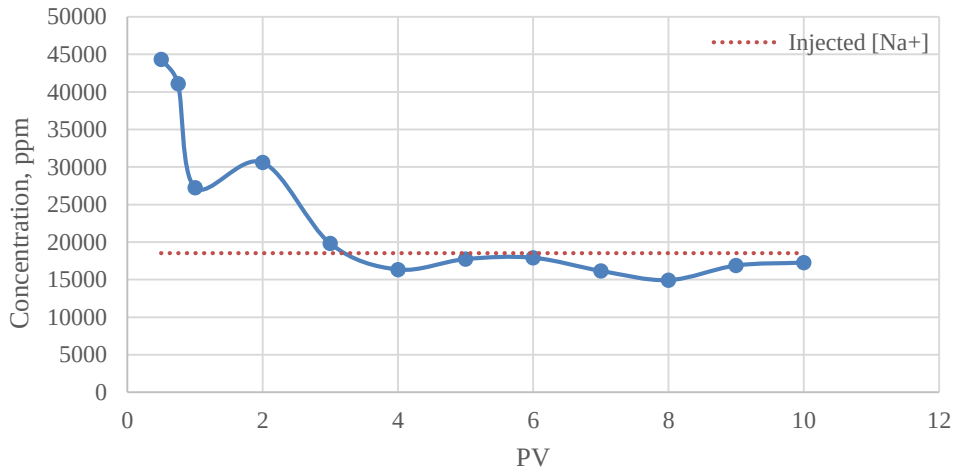

Figure 103: Sodium concentration for 3.5 PV slug size experiment (DF-3)

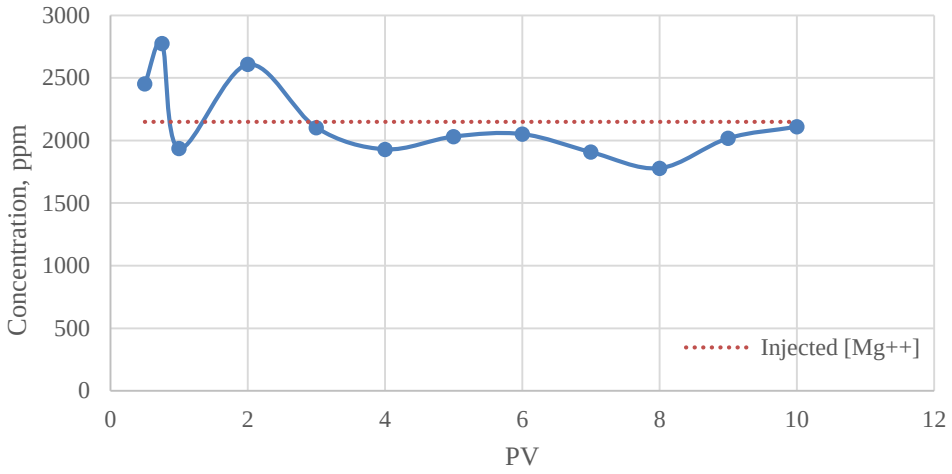

Figure 104: Magnesium concentration for 3.5 PV slug size experiment (DF-3)

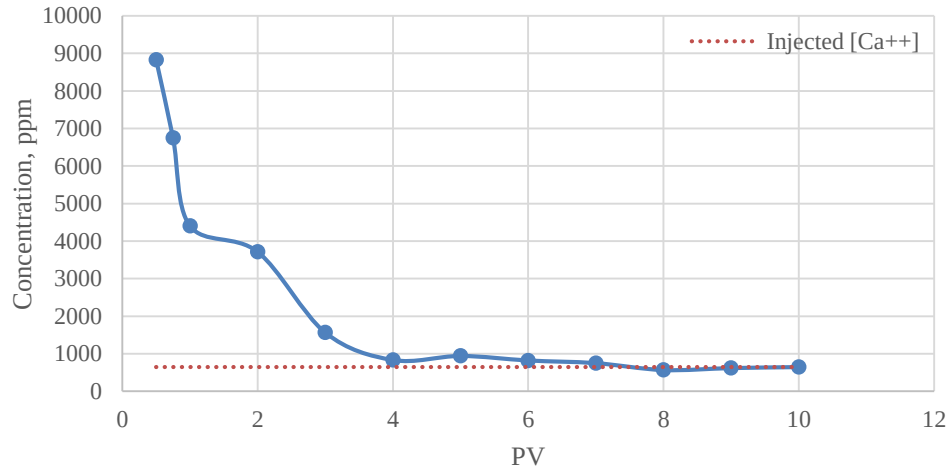

Figure 105: Calcium concentration for 3.5 PV slug size experiment (DF-3)

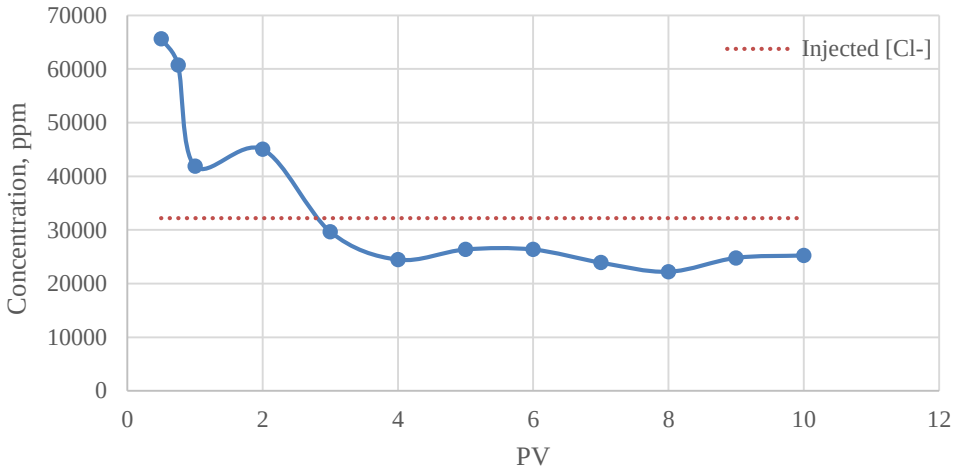

Figure 106: Chloride concentration for 3.5 PV slug size experiment (DF-3)

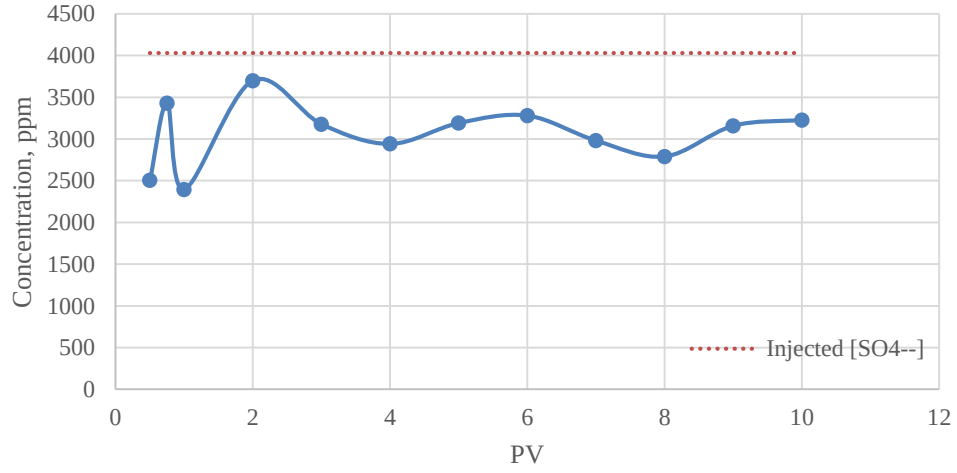

Figure 107: Sulfate concentration for 3.5 PV slug size experiment (DF-3)

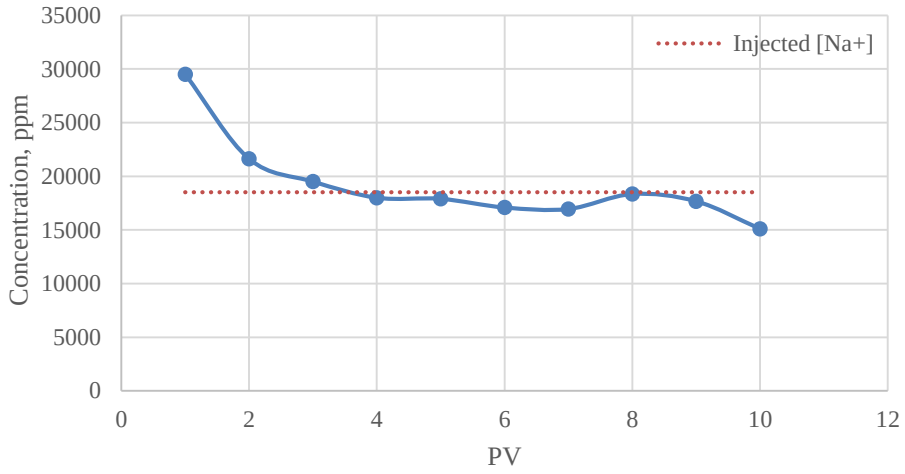

Figure 108: Sodium concentration for SW-P-S-SW sequence experiment (CF-8)

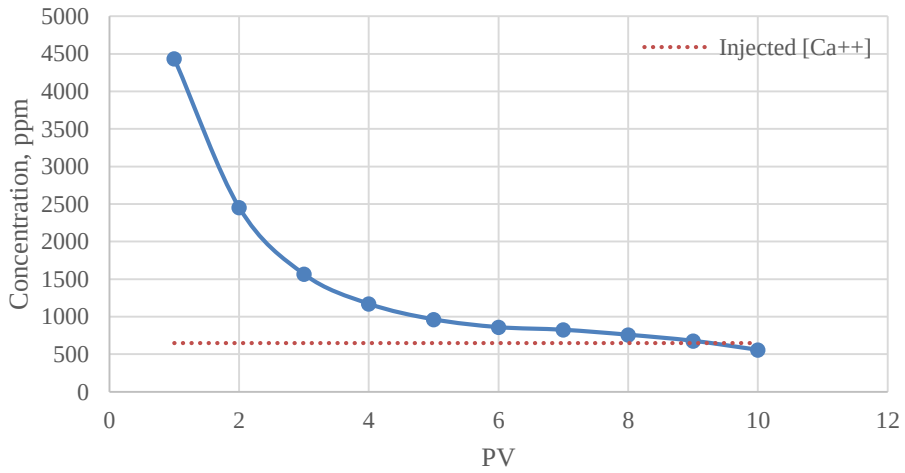

Figure 109: Calcium concentration for SW-P-S-SW sequence experiment (CF-8)

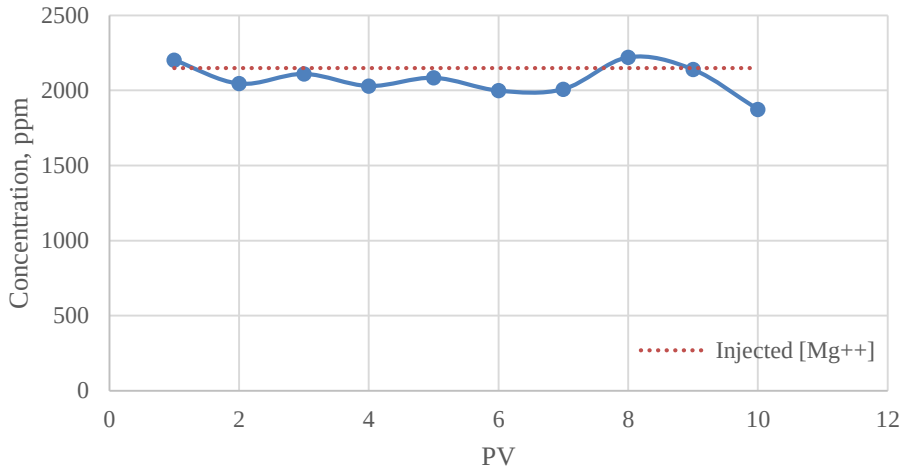

Figure 110: Magnesium concentration for SW-P-S-SW sequence experiment (CF-8)

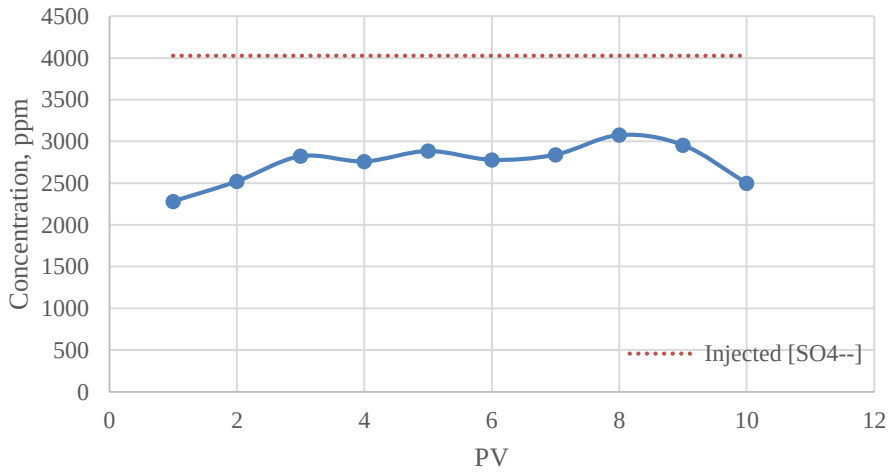

Figure 111: Sulfate concentration for SW-P-S-SW sequence experiment (CF-8)

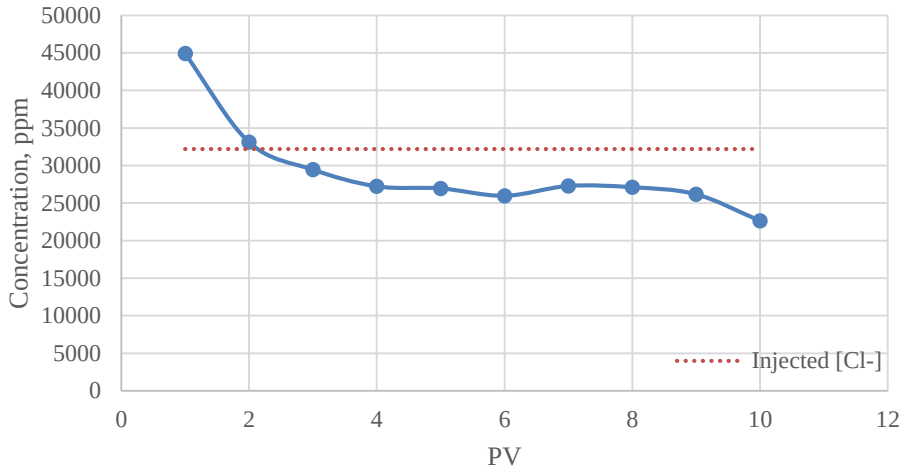

Figure 112: Chloride concentration for SW-P-S-SW sequence experiment (CF-8)

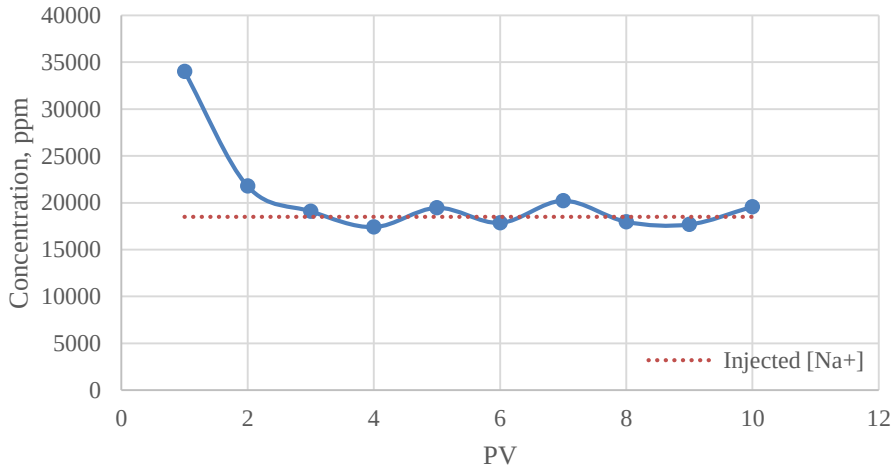

Figure 113: Sodium concentration for SW-S-SW-P SW sequence experiment (CF-9)

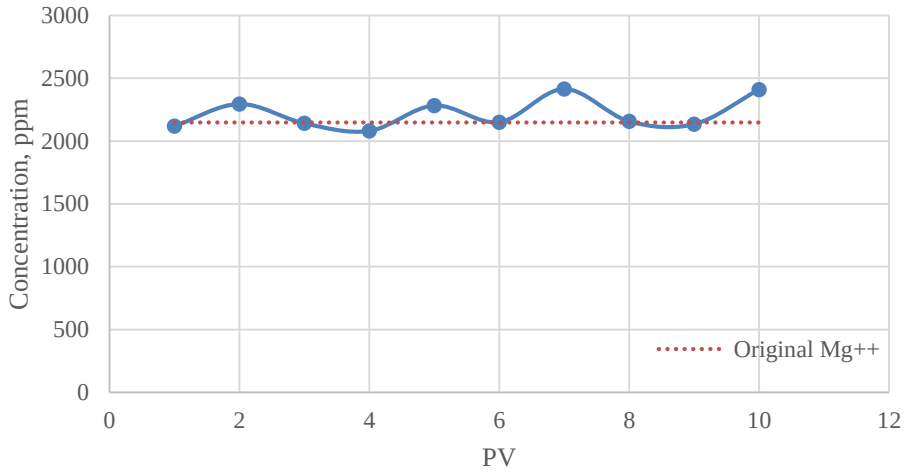

Figure 114: Magnesium concentration for SW-S-SW-P SW sequence experiment (CF-9)

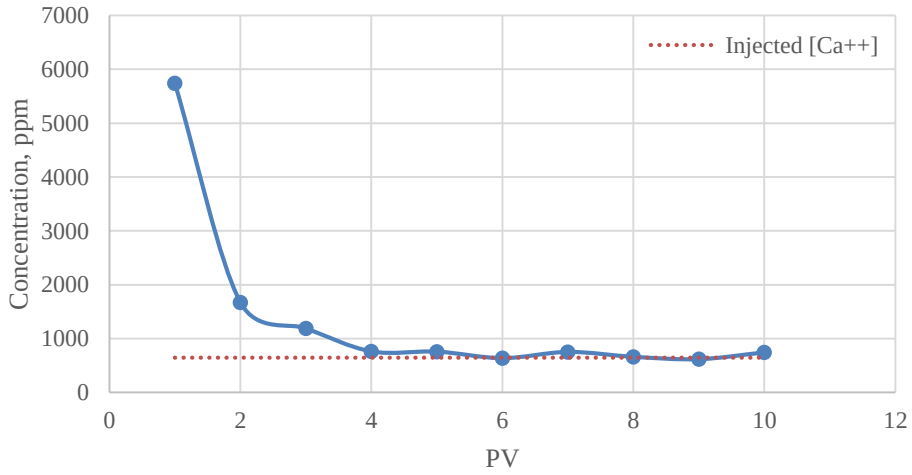

Figure 115: Calcium concentration for SW-S-SW-P SW sequence experiment (CF-9)

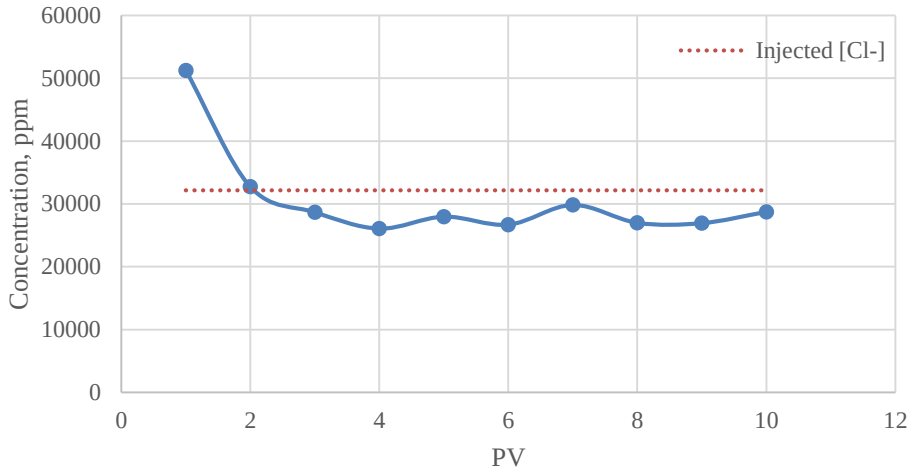

Figure 116: Chloride concentration for SW-S-SW-P SW sequence experiment (CF-9)

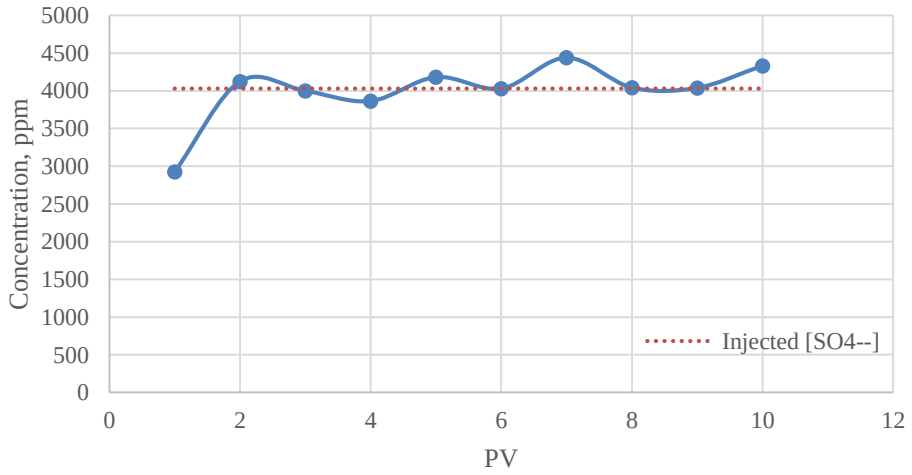

Figure 117: Sulfate concentration for SW-S-SW-P SW sequence experiment (CF-9)

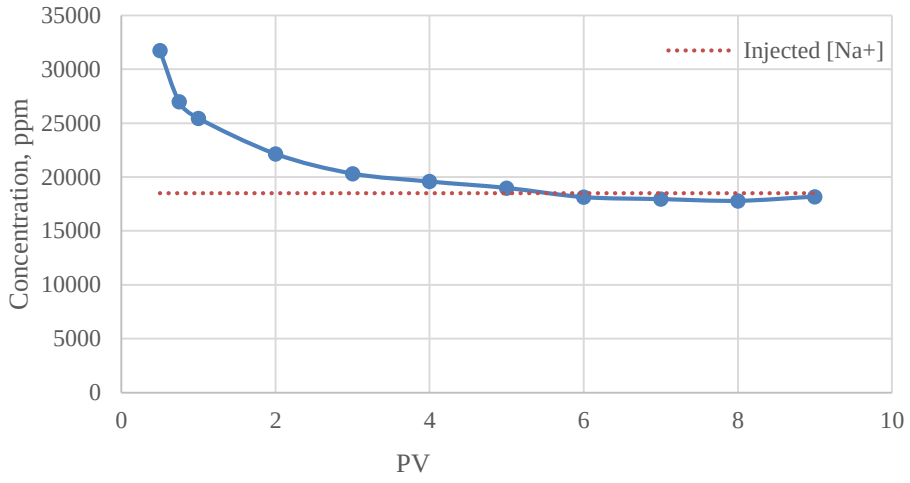

Figure 118: Sodium concentration for SW-P-SW-S-SW sequence experiment (DF-4)

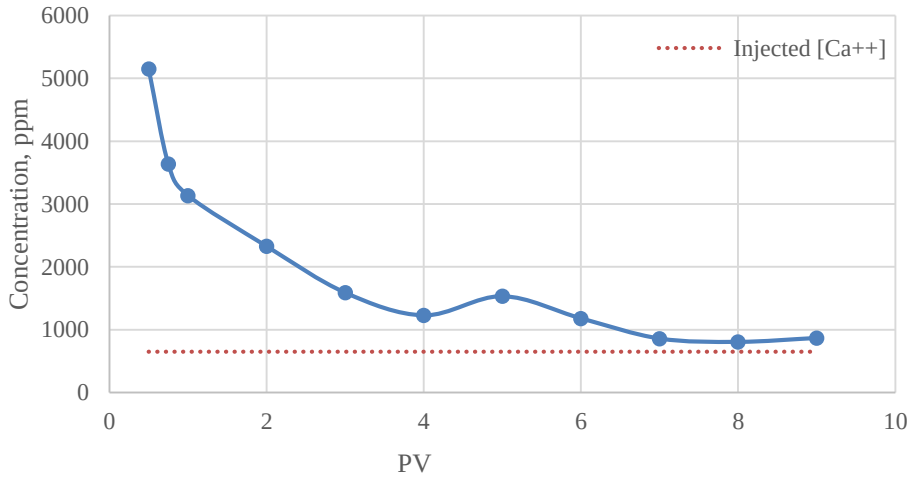

Figure 119: Calcium concentration for SW-P-SW-S-SW sequence experiment (DF-4)

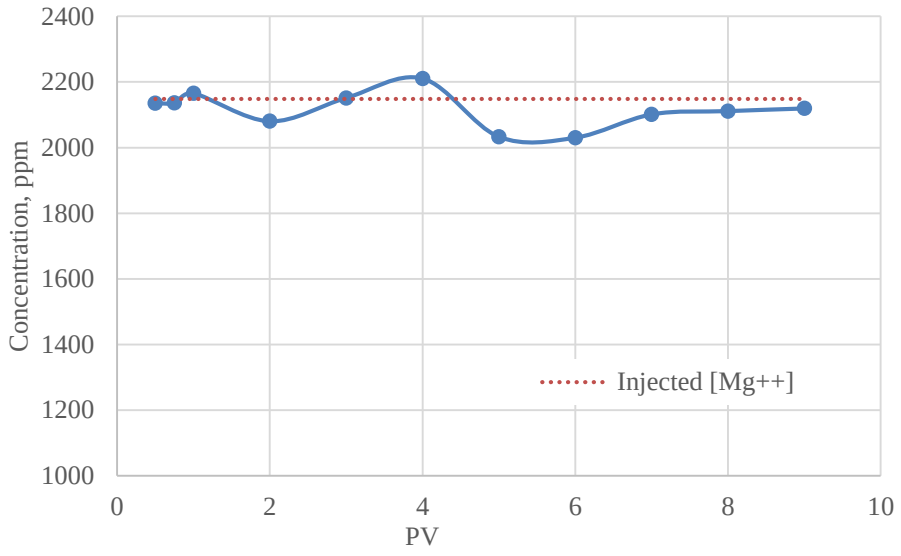

Figure 120: Magnesium concentration for SW-P-SW-S-SW sequence experiment (DF-4)

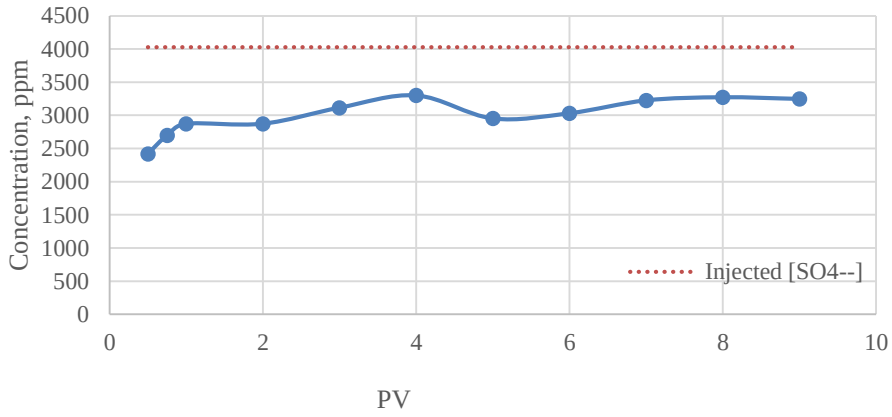

Figure 121: Sulfate concentration for SW-P-SW-S-SW sequence experiment (DF-4)

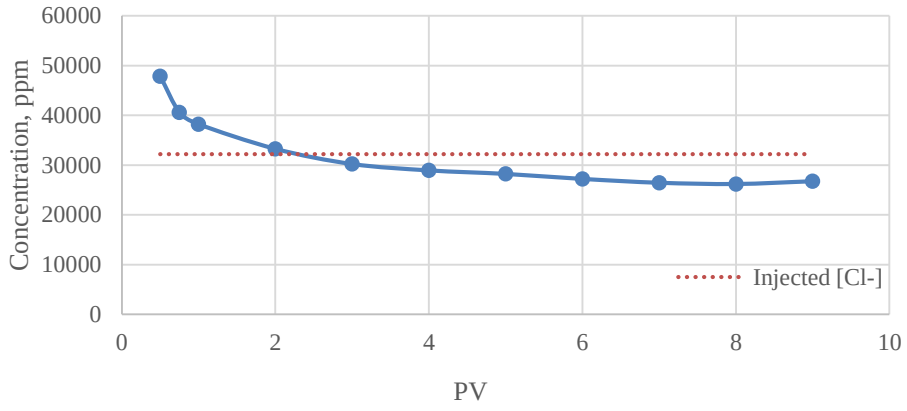

Figure 122: Chloride concentration for SW-P-SW-S-SW sequence experiment (DF-4)

Vitae

Name	:Mohamed Elmuzafar Ahmed Eltahir Ahmed
Nationality	:Sudanese
Date of Birth	:1/1/1991
Email	:momuah@gmail.com
Address	:Al-Thugba - Al-Khobar – Saudi Arabia
Academic Background	: M.Sc. in Petroleum Engineering (December 2017)
	King Fahd University of Petroleum & Minerals
	Dhahran, Saudi Arabia
	B.Sc. in Petroleum Engineering (October 2012)
	University of Khartoum
	Khartoum, Sudan
Research interest	: Chemical EOR, Micro-scale imaging, Adsorption,
	Reservoir simulation, Colloids, Well testing.